PETROGENESIS OF NEPHELINE SYENITES AND PHONOLITES

FROM THE LOFDAL INTRUSIVE COMPLEX, KUNENE REGION, NAMIBIA

Darragh E. O'Connor

Submitted in Partial Fulfillment of the Requirements

for the Degree of Bachelor of Science, Honours

Department of Earth Sciences

Dalhousie University, Halifax, Nova Scotia

April 2011

Distribution License

DalSpace requires agreement to this non-exclusive distribution license before your item can appear on DalSpace.

NON-EXCLUSIVE DISTRIBUTION LICENSE

You (the author(s) or copyright owner) grant to Dalhousie University the non-exclusive right to reproduce and distribute your submission worldwide in any medium.

You agree that Dalhousie University may, without changing the content, reformat the submission for the purpose of preservation.

You also agree that Dalhousie University may keep more than one copy of this submission for purposes of security, back-up and preservation.

You agree that the submission is your original work, and that you have the right to grant the rights contained in this license. You also agree that your submission does not, to the best of your knowledge, infringe upon anyone's copyright.

If the submission contains material for which you do not hold copyright, you agree that you have obtained the unrestricted permission of the copyright owner to grant Dalhousie University the rights required by this license, and that such third-party owned material is clearly identified and acknowledged within the text or content of the submission.

If the submission is based upon work that has been sponsored or supported by an agency or organization other than Dalhousie University, you assert that you have fulfilled any right of review or other obligations required by such contract or agreement.

Dalhousie University will clearly identify your name(s) as the author(s) or owner(s) of the submission, and will not make any alteration to the content of the files that you have submitted.

If you have questions regarding this license please contact the repository manager at dalspace@dal.ca.

Grant the distribution license by signing and dating below.

_____ _____

Name of signatory Date

ABSTRACT

Petrographic descriptions and mineral chemistry analyses of the nepheline syenite plugs and phonolite dykes of the Lofdal intrusive complex, northwestern Namibia, reveal primary insights into the sequence of magma crystallization with implications for nepheline syenite and phonolite association, for determining the nature of accessory mineral phases, and for any information on the nature of rare earth elements (REEs) associated with accessory mineral phases. The Lofdal intrusive complex is a 750 m.y. old set of intrusive bodies composed of syenite, nepheline syenite, phonolite, diatreme breccias, and carbonaite. These are found intruded through the Welwitschia inlier of the 2.0 b.y. old Huab Metamorphic Complex (HMC) in northwestern Namibia. Field relations indicate an early intrusive silicate assemblage of dominantly nepheline syenite followed by intrusive dykes of phonolite and then carbonatite. The Lofdal intrusive complex comprises a central set of intrusive plugs of nepheline syenite and carbonatite with early diatreme breccias, all surrounded by a 200 km^2 hydrothermal alteration zone with associated southwest to northeast striking dykes of phonolite and carbonatite.

Rare earth element mineralization and enrichment is currently being explored within the carbonatite dykes and related hydrothermal alteration of the Lofdal intrusive complex. The REE-mineralization is variable throughout the complex and includes both light-REE and heavy-REE mineralization. Current exploration has suggested that the two enrichments occur separately from one another. The heavy-REE enrichment is evident to have occurred during late stage hydrothermal activity and is dominanted by the mineral xenotime.

Twenty one samples of nepheline syenite and phonolite of the Lofdal intrusive complex underwent complete analysis to understand the mineral assemblages and crystallization sequence of these assemblages. These descriptions show an overall similar mineralogical assemblage in the nepheline syenites and phonolites with both major-rock forming minerals and accessory and light-REE mineralization. EMP analyses of feldspars and biotites from nepheline syenite and phonolite suggest a co-magmatic relationship between the two rock units, strengthening the current model for silicate-carbonate (nepheline syenite-phonolite-carbonatite) magmatic intrusive rocks. Future work should continue with exploring the relationship of REE-mineralization of nepheline syenites and phonolites and try to relate this to the later enrichment of heavy-REE mineralization with the carbonatite plugs and dykes.

TABLE OF CONTENTS

List of Figures

List of Tables

Acknowledgements

Thanks and praise to my supervisors, Yana Fedortchouk & Scott Swinden, for giving me the opportunity to do this project.

Many thanks to Luke Hilchie for helping with this project. Your intriguing geological sense allowed me to view the project from directions I would have otherwise thought.

Lastly, I would like to thank Zhihai Zhang for his insight and explanations when needed most.

CHAPTER 1.0 INTRODUCTION

1.1 *General Statement*

This is a petrogenetic study of nepheline syenite plugs and phonolite dykes within the Lofdal intrusive complex, north-western Namibia, Africa. The Lofdal Intrusive Complex is a ca 750 Ma silicate-carbonate complex in north central Namibia. Alkalic syenites of the complex have been known for many years (Frets , 1969) but it has only recently been recognized that there is also widespread phonolitic dyking and a later phase of carbonatite intrusion. The carbonatites are currently the target of a rare earth element exploration program.

Although some detailed petrological investigations have been carried out on the carbonatites in the complex (Kaul, 2010; Ndululilwa, 2009), to date there have been no detailed studies of the early alkali silicate phases. Understanding of this early magmatism is critical to further our understanding of the magmatic history of the complex as a whole.

This study is the first detailed petrographic and mineralogic study of the nepheline syenites in the Lofdal Complex with the overall objective of documenting the nature of the magmatic rocks, investigating the relationship between the plutonic nepheline syenites and the phonolite dykes, and determining whether any evidence of the carbonatite-associated rare earth element mineralization is present in the earlier-crystallizing silicate rocks.

The purpose of the study is to describe the mineralogy of the two rock types, to investigate their possible genetic relationship, and to determine a possible source of rare earth element (REE) mineralization.

1.2 *Definition and Occurrences of Nepheline Syenite*

Syenites are defined as intrusive igneous rocks that contain alkali feldspar as the dominant felsic mineral. *Nepheline syenites* are syenites formed from silica-undersaturated magmas that do not crystallize quartz; they consist dominantly of alkali feldspar and nepheline phenocrysts and a groundmass with minor amounts of mafic minerals, namely alkali amphiboles, pyroxenes, or both. *Phonolite* is used at Lofdal as a field term for intrusive nepheline-bearing dykes and so although not strictly accurate, the term is used herein for consistency with other workers. Minor amounts of alkali amphiboles and alkali pyroxenes may occur both as phenocrysts and in the groundmass (MacKenzie et al., 1982). Replacement products of nepheline may include cancrinite, sodalite, analcime, and other feldspathoids. Classification of nepheline syenites (Table 1.1) is based on the modal proportions of nepheline with associated feldspar, pyroxenes, and sodalite (Mitchell & Jambor, 1996).

Nepheline syenites are a common component of relatively shallow intrusions of subvolcanic origin that occur in rift-related continental provinces. The complexes associate with volcanic sequences and dykes, and can also contain carbonatite intrusions. (Mitchell & Jambor, 1996).

The formation of rift-related nepheline syenititic magma by low-pressure fractionation of olivine alkali basalt or basanite magma was demonstrated experimentally. However, the presence of high-pressure nodules in phonolites and trachytes, as well as the presence of silica-undersaturated glass found in mantle xenoliths, show that the melts may form at much greater depths (i.e. plume related magmatism). No direct evidence of the mantle processes responsible for differentiation and depth of formation of these melts were observed in these magmas, although it is still a possibility (Mitchell & Jambor, 1996).

Mineral Assemblage	Current Name	Alternative Name
Neph + <perthitic feldspar	foyaite	hypersolvus nepheline syenite
Neph + < Ab + Kspar	litchfieldite	subsolvus nepheline syenite
Neph + < Ab	mariupolite	Mariupolite
Ab + < Neph	monmouthite	Mariupolite
Px(<30%) + < Neph	urtite	leuco-ijolite
Px(30-70%) + Neph	ijolite	Ijolite
Px(>70%) + >Neph	melteigite	mela-ijolite
Sod + Neph + perthite	Ditroite	hypersolvus sodalite nepheline

Table 1.1: Nomenclature of alkali-rich intrusive rocks based on mineral assemblage (Mitchell & Jambor, 1996)

1.3 *Definition of Carbonatites*

A plutonic or volcanic igneous rock containing greater than 50% modal carbonate minerals is classified as a *carbonatite.* Further subdivisions are based on modal mineral abundance of specific carbonate minerals (e.g. calcite, dolomite), and include calcio-, magnesio-, and ferrocarbonatites (Le Maitre, 2002). Interest in carbonatites revolves around the scientific issues of petrogenesis and economic potential due to incompatible element enrichment, mainly REE. Relative to the already enriched continental crust, carbonatites are enriched in Pb, Th, U, Sr, Ba, Y, Nb, and light REEs giving possible economic value (Mitchell & Jambor, 1996 & Bell, 1989).

Although most REEs are currently mined and processed in China (95 to 97%), little to no information is disclosed, either on the reserves remaining or on the amount of current production. China has also begun to restrict the export of these elements to the Western World (Bradsher, 2010; BBC, 2010). This has led to exploration effot for new REE deposits to compensate for the lack of available REEs. The only past producer in North America, at Mountain Pass, California, closed in 2004

due to the high extraction labour costs but is currently being reopened for the mining of bastnäsite (See section 3.2). The aim is to have Mountain Pass producing one sixth of the global REE supply by 2012 (Lang, 2010; Molycorp Minerals, 2009).

Based on 527 global occurrences of carbonatite complexes, 90% are stated to have either a magmatic or hydrothermal origin (Woolley & Kjarsgaard, 2008) and dominantly occur in intra-continental settings (Ndalulilwa, 2009). Carbonatites are believed to represent either primary magmas derived from partial melting of the mantle, or magmas produced by immiscible separation from, or fractional crystallization of a primary silicate melt. Lee and Wyllie (2005) and Mitchell and Jambor (1996), state that despite the possibility of primary carbonatite magmas, petrological evidence suggests that carbonatite complexes are derived from alkaline carbonated silicate magmas. Thus the concept of primary carbonatite melts in the mantle is not necessary to explain the occurrence of carbonatites in the crustal regime.

1.4 *Nepheline Syenite and Carbonatite Association*

Of the 527 known carbonatite complexes, 477 (90%) are associated with at least one type of igneous rock. Of the 477 carbonatite complexes, 84% are magmatic in origin while 16% are carbohydrothermal in origin. The carbohydrothermal carbonatites are all associated with at least one type of silicate igneous rock, with a common association with nepheline syenites and syenites. Of the magmatic carbonatites, 76% have a diverse range of silicate rock associations. In total, 68 or the 477 carbonatite complexes are associated with phonolite and/or nepheline syenite rocks (Woolley & Kjarsgaard, 2008). It is safe to infer that most, but not all, carbonatite magmas are genetically related to carbonated silicate parental magmas.

Lee and Wyllie (1998) used silicate-carbonate-H_2O phase diagrams to show two possible processes of carbonatite formation. They describe a parental carbonated silicate magma following an

evolutionary path of fractional crystallization, which enriches incompatible carbonate components, and results in a carbonate-rich melt at the silicate-carbonate liquidus boundary. They also show that the same parental magma may reach a silicate-carbonate liquid miscibility gap during evolution, resulting in exsolution of an immiscible carbonate-rich liquid from the silicate magma (Fig 1.1).

While the spatial and temporal coincidence of alkaline igneous rocks with carbonatites suggests the two have a consanguineous relationship (Woolley A. R., 2003), the two genetic theories both have faults. Fractional crystallization processes would be a more viable theory if gradational relationships and intermediate compositions were found. Even though rocks of intermediate composition, known as bergalites, do occur sparsely within carbonatite complexes, their rarity does not fully support the concept of fractional crystallization. Similar problems arise with the liquid immiscibility model. Although globules of silicate glass in carbonatite and globules of carbonatite in silicate glass have been found, these observations do not necessarily indicate that immiscibility of a single homogeneous liquid into two liquids occurred in thermodynamic equilibrium (Mitchell & Jambor, 1996).

1.5 *Rare Earth Elements in Carbonatites*

The rare earth elements (REEs) comprise a total of 16 elements which include yttrium (Y, atomic number 39), and the lanthanide series, consisting of lanthanum (La, 57) through lutetium (Lu, 71). The large group is divided into two groups known as light rare earth elements (LREEs) and heavy rare earth elements (HREEs) (Winter, 2010). LREEs are generally considered to consist of yttrium, lanthanum, cerium (Ce), praseodymium (Pr), neodymium (Nd), and samarium (Sm). HREEs are the remaining lanthanide series which includes europium (Eu), gadolinium (Gd), terbium (Tb), dysprosium (Dy), holmium (Ho), erbium (Er), thulium (Tm), ytterbium (Yb), and lutetium (Lu). Promethium (Pm, 61) is not included in either division as it neither stable nor long-lived upon formation (Jones et al.,1996).

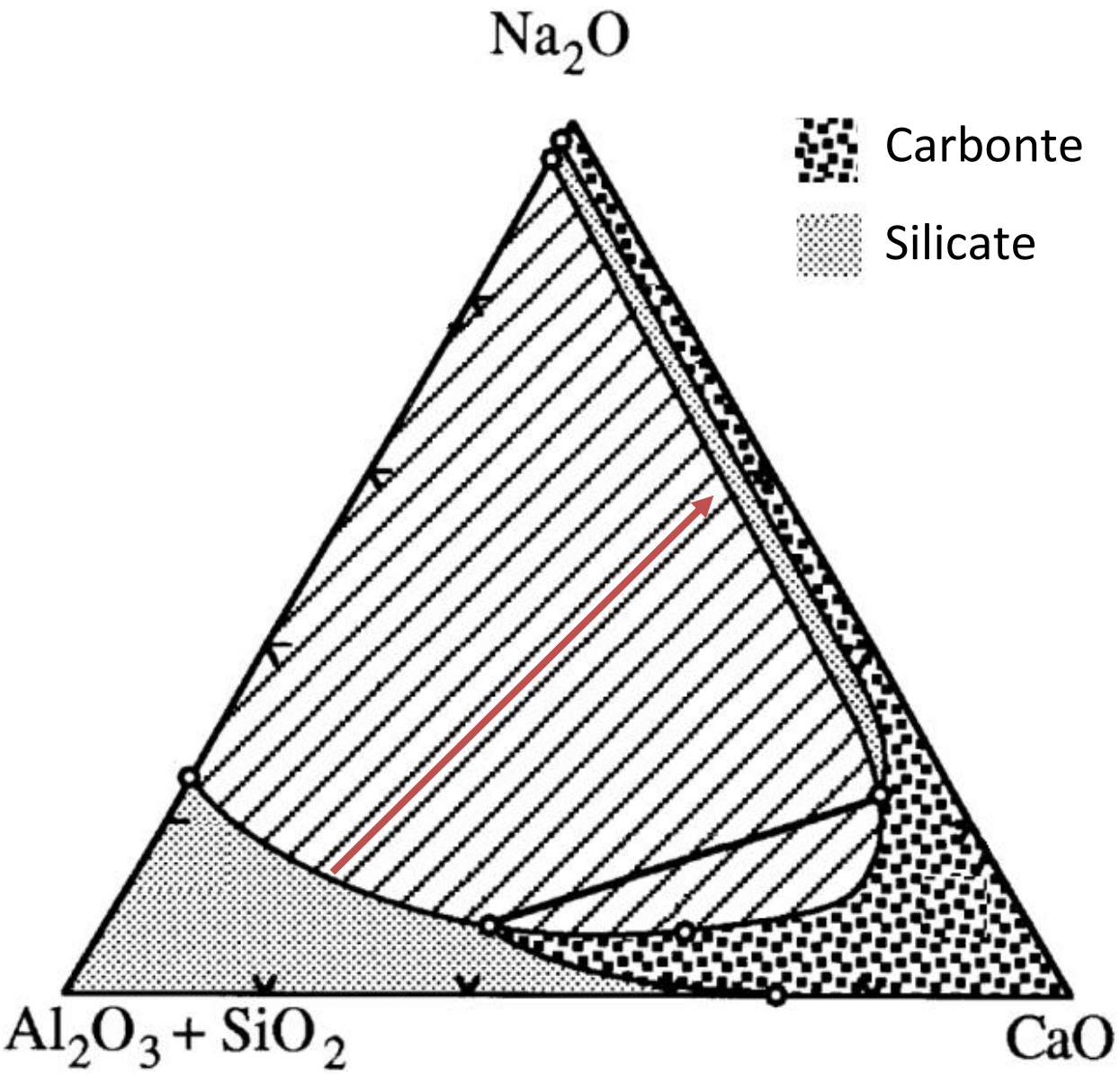

Figure 1.1: Silicate-carbonate-H2O phase diagram exhibiting both fractional crystallization and liquid immiscibility formation of carbonatite. The liquid immiscibility gap is shown to occur at the red arrow. Fractional crystallization would cause enrichment of CaO along the bottom of the diagram, leading to the eventual change of silicate to carbonate (nepheline syenite to carbonatite).

Carbonatites are enriched in a variety of elements, including both light and heavy REEs. Fractionation of light REE and heavy REE occurs due to the progressive decrease in ionic radius from light to heavy elements. However, differing crystal lattice arrangements cause preferential partitioning of LREEs or HREEs into certain minerals. Garnet, for example, strongly favours HREEs; consequently, magmas derived from garnet-bearing sources are relatively depleted in HREEs if garnet was refractory during melting. Thus, specific minerals can be valuable tools for understanding REE concentrations in igneous rocks, and can provide information about magma source region mineralogy. Although both REE groups are enriched in carbonatites, most carbonatite complexes have high LREE:HREE ratios (Winter, 2010; Bell, 1989). The rare earth (RE)-minerals of these elements are broken into three main groups: oxides (e.g. pyrochlore [$(Na,Ca)_2Nb_2O_6(OH,F)$] & perovskite [$CaTiO_3$]), phosphates (e.g. apatite [$Ca_5(PO_4)_3(F,Cl,OH)$] and monazite [$(Ce,La)PO_4$]), and fluorocarbonates (bastnäsite [$(Ce,La,Y)CO_3F$], parisite [$\underline{Ca}(\underline{Ce},\underline{La})_2(\underline{CO_3})_3\underline{F_2}$], and synchysite [Ca(Ce, La, Nd, Y)(CO3)2F]) (Jones, Wall, & Williams, 1996; Wall & Mariano, 1996). These minerals are petrogenetically important because as the hosts of REEs, they directly reflect the distribution of these elements during magmatic or carbohydrothermal crystallization. Thus, understanding the formation and distribution of these REE minerals may elucidate the processes of formation and genetic relationships within surrounding rocks (e.g. nepheline syenites).

The Mountain Pass mine, California, and Kangankunde Mine, Malawi, are two carbonatite complexes which are generally interpreted to contain RE-minerals that crystallized from a magma. At Mountain Pass, the carbonatite contains bastnäsite and parisite within the calcitic and dolomitic magmatic units. Other RE-minerals, including synchysite, sahamalite (an oxide), and monazite, are found in association with quartz, fluorite, baryte, and strontianite, which have apparently been deposited from hydrothermal solutions . The Kangankunde Carbonatite Complex is a ferroan dolomite and ankerite carbonatite and a rich REE deposit. Although the complex does not have a strong association with alkali silicate rocks, as compared to the Lofdal intrusive complex (see section 1.5), the Kangankunde Complex

still indicates the enrichment of RE-minerals in association with carbonatite magmatism (Wall & Mariano, 1996). These two systems show two well known occurences or REE-mineralization associated with carbonatites. This gives indication that Lofdal may have similar REE enrichment.

1.6 *Nepheline Syenite and Carbonatite Occurrence at Lofda intrusive complexe*

The Lofdal intrusive complex is centered on the Lofdal 491 farm, 35km northwest of the town of Khorixas in Damaraland, northern Namibia (Fig 1.2). The complex consists of a number of discrete intrusions of syenite, nepheline syenite, phonolite, and carbonatite. The Lofdal nepheline syenites occur in a series of genetically and geographically related satellite plugs, with a main 2 km^2 plug located in the south-eastern part of the complex (Frets, 1969).

Frets (1969) describes a great number of east-west striking dykes, which vary in composition, and which intrude both the nepheline syenite plugs and the Precambrian basement. Later referred to as the Bergville Dyke Swarm (Miller, 2008), the dykes are roughly parallel trending NNE to NE, range from 20 cm to 8 m in width, and cover an area of 20 km by 6 km. Rock types include tinguaite (dyke section of phonolite), phonolite, trachyte, lamprophyre, and carbonatite (Miller, 2008). The carbonatite dykes intrude through silicate dykes, indicating the carbonatite dykes are the youngest intrusion in the immediate area (Wall et al., 2008).

Previous studies (Kaul, 2010 and Ndalulilwa, 2009) of the nepheline syenites, phonolites, and carbonatites at the Lofdal intrusive complex have suggested that most of the REE-mineral crystallization resulted from metasomatic activity following the emplacement of carbonatite dykes within the phonolites and nepheline syenites. Kaul (2010) identifies a more moderate LREE:HREE ratio in these dykes suggesting that late stage hydrothermal activity may have caused a HREE enrichment.

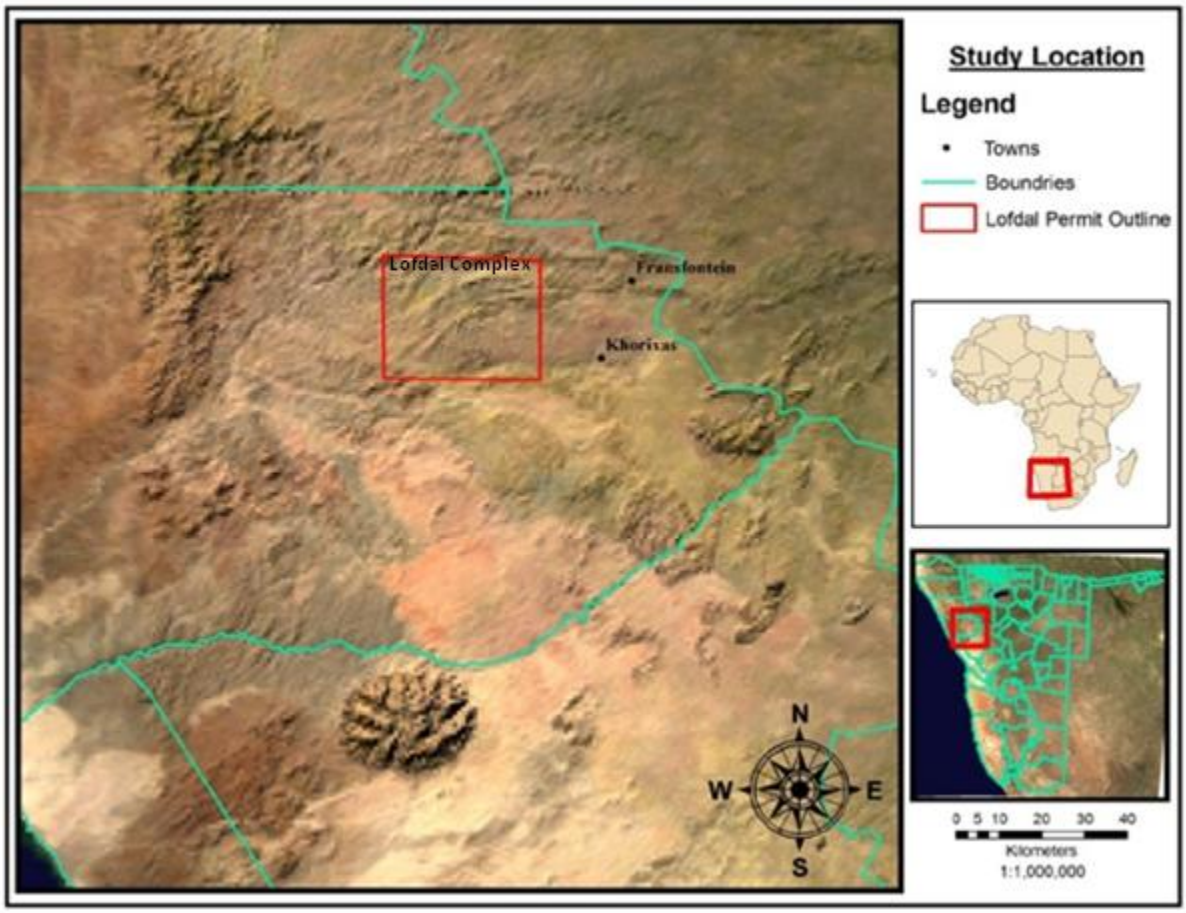

Figure 1.2: Arial map of the Lofdal alkaline intrusive complex exploration permit. Located 35 km northwest of Khorixaz, Damaraland, Namibia, indicated by the red box (After Kual, 2010)

1.7 *Sample Collection and Preparation*

Samples of nepheline syenite were taken from an intrusive plug near the southwestern end of the complex (Fig 1.3). The plug, which measures roughly 700 m by 500 m in surface exposure, was traversed and sampled systematically throughout its exposed extent. In addition, samples of phonolite dykes were taken from the north-eastern part of the complex for comparison. Sampling was carried out by Scott Swinden, Swinden Geoscience Consultants Ltd. Twenty one hand samples, ranging from 10 to 15 cm in size, were taken from the study area, consisting of fourteen samples from the nepheline syenite plugs and seven samples from the phonolite dykes (Fig. 1.4). The main goal of the sampling was to assemble a collection which was representative of the nepheline syenites and phonolites from the Lofdal Complex, that exhibited a variety of characteristics from the same rock unit, and would allow conclusions to be drawn regarding the overall nature of silicate magmatism in the complex and in particular the relationship between nepheline syenite and phonolite.

Sample preparation involved making mounted thin sections. Two types of thin sections were prepared for two different uses. The first were normal, glass plated thin sections. The intended use was for mineral identification using a petrographic microscope (Nikon Eclipse 50iPOL). The second were polished thin sections. The intended use was for Electron Microprobe (EMP) analyses as well as reflective light microscopy.

1.8 *Study Scope*

The study was completed by analyzing 7 phonolite and 14 nepheline syenite samples collected from the Lofdal instrusive complex. The study objectives were:

- To document the mineralogy and petrography of the Lofdal nepheline syenites and phonolites through detailed thin section microscopy.
- To determine the composition of major mineral phases

- To determine the nature of accessory phases and interpret their mineralogy
- To use the petrographic and mineral composition data to investigate the petrogenesis of the silicate rocks and in particular, to investigate the relationship between the nepheline syenites and the phonolites
- To see if accessory phases provide any information on the nature of RE elements in the rock, and in particular, whether RE elements were crystallizing as a liquidous phase in the silicate magmas

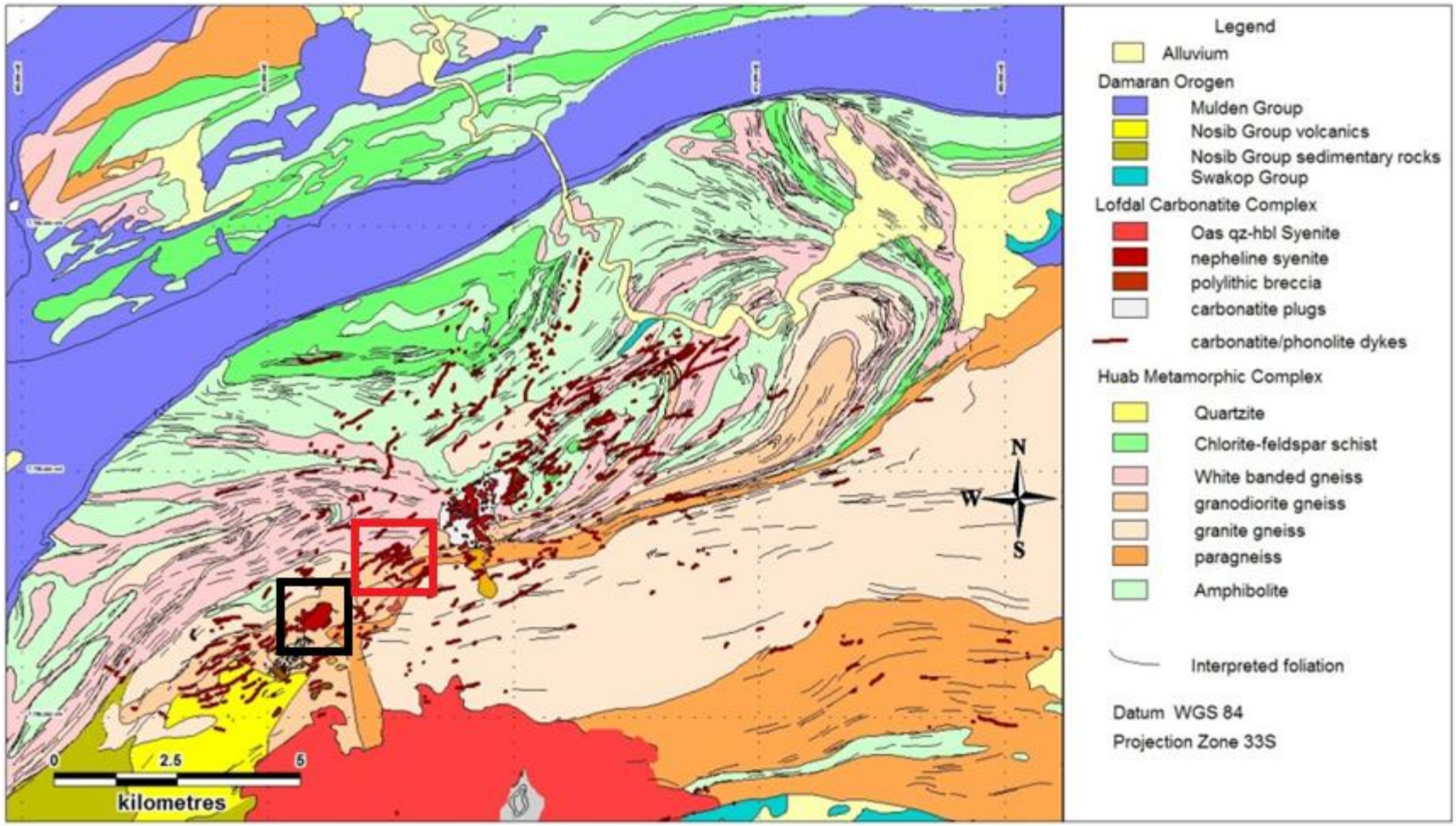

Figure 1.3: Geological map of Lofdal nepheline intrusive complex. The rocks related to the syenite complex are indicated by the square (samples collected: ESY-1-14 and PH-3-5). The phonolite samples found outside of this area are indicated by the red square (samples collected: PH-1,2,6,7).

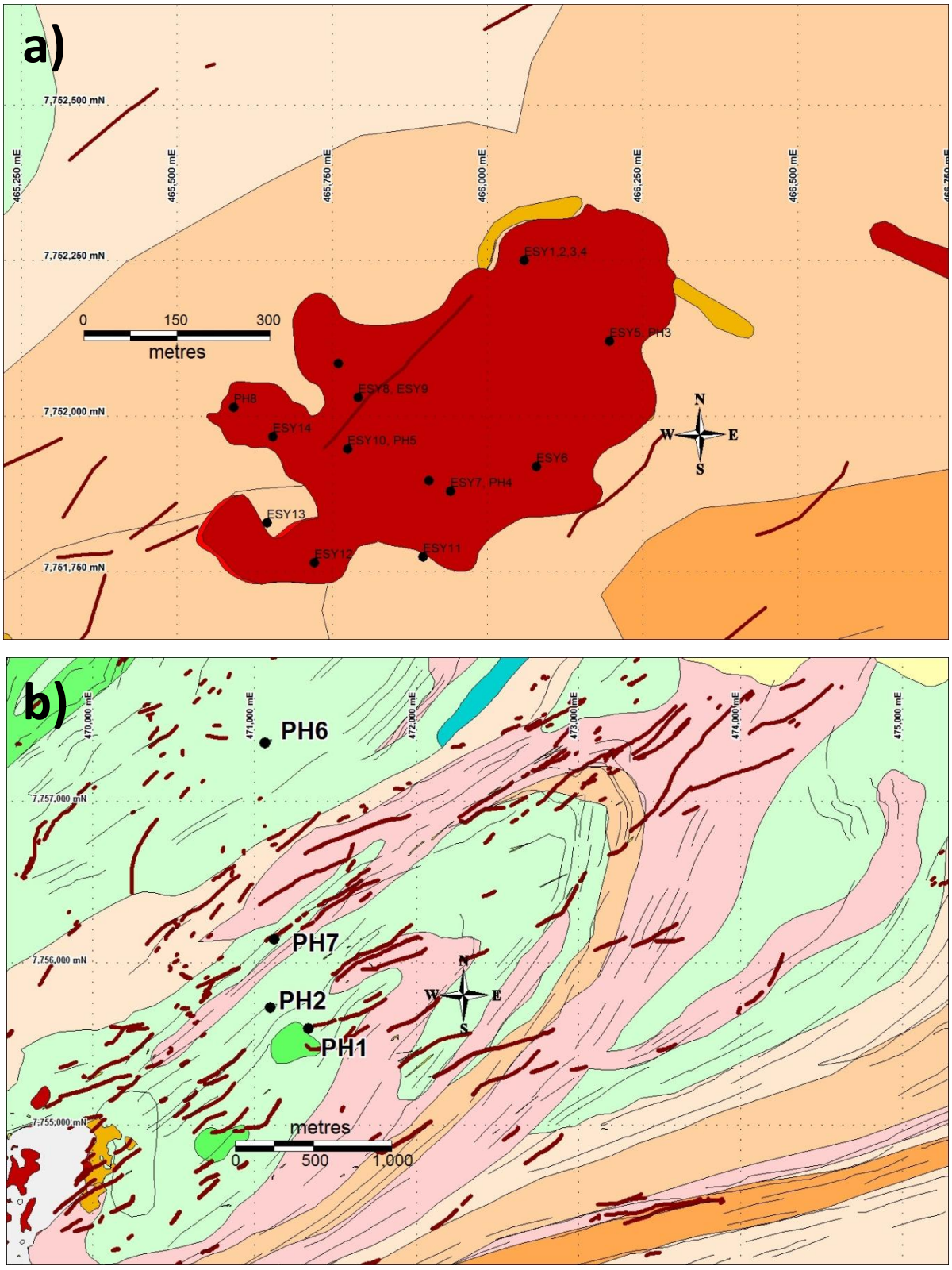

Figure 1.4: An enlarged view of the sampling areas. (a) The main nepheline syenite plug showing the location sampling areas. (b) The main area in which the phonolite samples were taken. (Note: the legend from figure 1.3 applies to this map)

CHAPTER 2.0 GEOLOGICAL SETTING

2.1 *Geological History of southern Africa*

The regional geology of north-western Namibia is best understood by looking at the overall geological evolution of southern Africa which encompasses rocks from the Archean to the Quaternary. The formation of stable Archean cratons surrounded by mobile belts of tectonically active areas gave rise to early Earth. Over long periods of time these mobile belts stabilized and resulted in the amalgamation of large cratons. Today, four cratons are identified in southern Africa. The eastern side of southern Africa is composed of the older Archean Zimbabwe Craton and Kaapvaal Craton. The western side of southern Africa is composed of the Congo Craton and the Kalahari Craton (Fig. 2.1). Altogether these became accreted during the Proterozoic time period.

Following this accretion was a large scale rifting event throughout most of the African continent about 750 MA to produce a series of late Proterozoic orogens that are collectively referred to as the "Pan African" orogens. The event caused much of the Precambrian sedimentary sequences and older rocks to become highly deformed, producing metamorphosed and deformed metasedimentary gneiss and schist. One of these was the Damara Orogen, formed by rifting between the Congo and Kalahari cratons.

This was followed by a Wilson cycle of opening of Pan African basins (incliuding the Damara) producing thick sequences of late Proterozoic sedimentary and volcanic rocks. Subsequent closure of the pan African basins resulted in accretion of pan African rocks to the older cratons, metamorphism and deformation.

This was followed by a lengthy period of sediment deposition. The Karoo Sequence covers large areas of southern Africa and dates from the Carboniferous to Jurassic (300 to 180Ma). These sediments

consist of glacial till as well as later Permian to Triassic fluvial sands. In the early Cretaceous Africa began to emerge as a separate tectonic plate. As separation occurred, large volumes of volcanic melt were erupted to the surface as flows and intruded to form dykes. To recent, much of southwest Africa is arid and still deeply undergoing erosional activity.

2.2 *Regional Geology*

The Lofdal nepheline syenite plugs and phonolite dykes currently being explored are situated in inliers of the Congo Craton within the Damara Orogen. In north-central Namibia, there are three exposed inliers known as Kamenjab, Braklaagte, and Welwitschia (Fig 2.2). These inliers are surrounded by younger volcanic and sedimentary rocks of the Damara Orogen. The Welwitschia inlier is underlain mainly by the Huab Metamorphic Complex (HMC), which is Mokolian in age (~2000 Ma) (Table 2.1) This unit was intruded by both the Oas Quartz Syenite and Lofdal intrusive complex at about 750 Ma.

Stratigraphic Subdivision	**Stratigraphic Unit**
< 135 Ma	Post Karoo cover
135 – 300 Ma	Karoo Sequences and Intrusions
460 – 540 Ma (Ordovician – Cambrian)	Damara Granites
540 – 1000 Ma (Namibian)	Damara Sequence, Naauwpoort Formation
1000 – 1800 Ma(Middle to Late Mokolian)	Fransfontein Granite Suite
1800 – 2000 Ma (Early Molokian)	Huab Metamorphic Complex

Table 2.1: General stratigraphy of the lithological units within the study area (after Ndalulilwa, 2009)

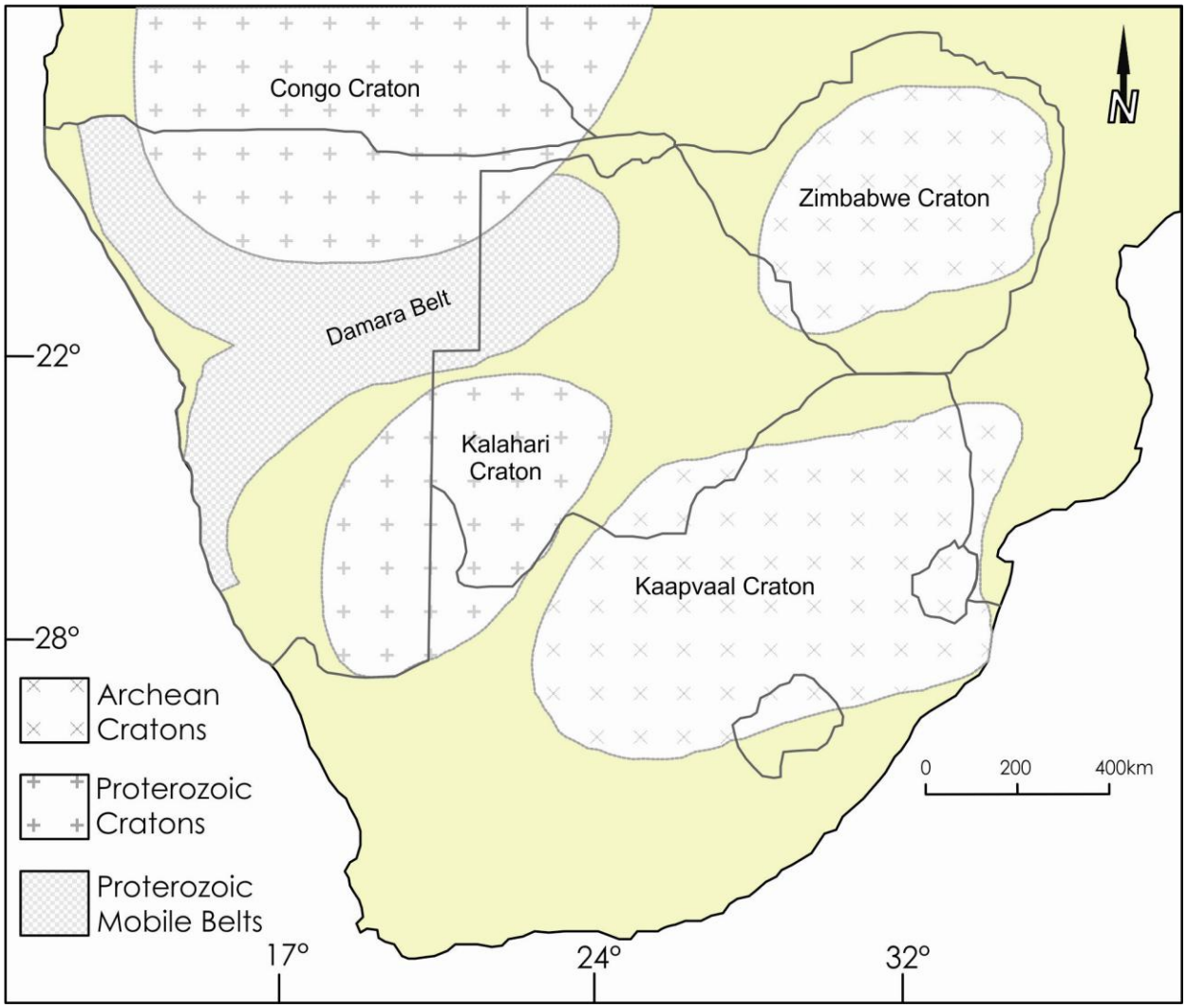

Figure 2.1: Cratons and mobile belts of southern Africa. The study area is located between the Congo Craton to the north and the Kalahari to the south-east (after Schneider, 2008).

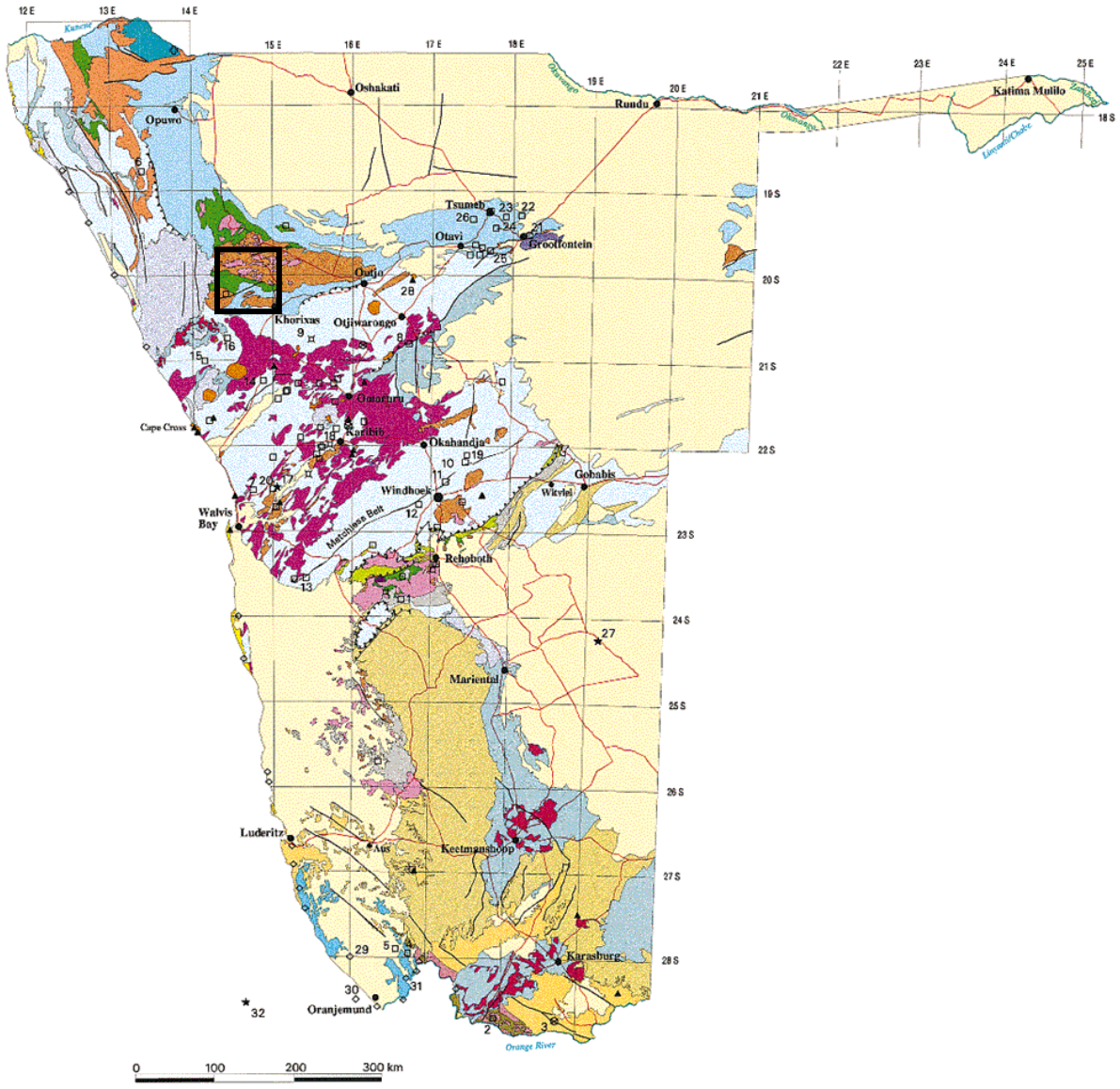

Figure 2.2: An overall geological map of Namibia. The black box in the northwestern corner of the map represents the area of the Kamenjab, Braklaagte, and Welwitschia inliers. The Welwitschia inlier is found to host the Lofdal intrusive complex.

2.2.1 *The Huab Metamorphic Complex (HMC)*

Originally described by Frets (1969), the HMC is composed dominantly of leucocratic geniesses and contains layers of quartzite, mica schist, and amphibolites. The complex here is considered to be between 1800 – 2000 Ma. on the basis of the age of the intruding Fransfontein granite, which is dated at approximately 1700 Ma (Frets, 1969). It was metamorphosed to amphibolites grade and intensely deformed prior to intrusion of the Fransfontein Granite.

2.2.2 *The Fransfontein Granitic*

The Fransfontein granite (FGS) is exposed as an intrusion in the northern section of the Welwitschia inlier. The Fransfontein granite is composed of a uniform and coarsely-grained texture mineralogically dominanted by quartz, albite, and microcline with minor biotite, chlorite, magnetite, and other accessories. The granite is seen in contact with schistose and foliated gneisses and metasediments of the older HMC. The gneisses of the HMC show macro-and microscopic deformation. This deformation is not seen within the Fransfontein granite, indicating that the Fransfontein granite is a late-to post-tectonic intrusion. Through U/Pb dating methods the FGS was imprecisely dated with two discordia, giving ages of 1871±30Ma and 1730±30Ma (Frets, 1969; Burger et al., 1976) and allowed for the relative dating of the HMC.

2.2.3 *The Naauwpoort Formation and Damara Orogen*

The Naauwpoort Formation is the basal volcanic sequence within the Naauwpoort volcanic series. These volcanics rests unconformably atop and cut through as intrusions within the deformed basement gneisses of the HMC (Frets, 1969). These volcanics were extruded during intracontinental rifting, producing K-rich and Na-rich lavas (Miller, 2008). Through U/Pb dating, the age of the Naauwpoort Formation was calculated to be between 820 to 730 Ma. Because these volcanics represent

the same episode of magmatism as the Lofdal intrusive complex, a date of approximately 750 Ma is given to the intrusive Lofdal rock units.

The Neoproterozoic Damara Orogen (Damara Belt, Damara mountain belt) represents the formation of the Pan-African orogney, located south of the Congo Craton and north of the Kalahari Craton. The Damara Belt formed during a complete tectonic sequence involving continental rifting, spreading, passive continental margin formation, mid-ocean ridge formation, oceanic seafloor subduction, and continental collision of the two previously mention cratons.

The closing of the Damara basin in the latest Proterozoic by subduction beneath the Congo Craton led to the metamorphism and deformation of the Damara stratified rocks, described by Frets (1969) and Miller (2008).

2.3 *Local Geology of the Lofdal intrusive complex*

The Lofdal intrusive complex is composed of a suite of alkali silicate rock and carbonatites emplaced as intrusions through the HMC nearly 750 Ma (Fig 1.3). The Oas Syenite is the largest body of alkali silicate rock and was first described by Frets (1969) and was dated at 757 ± 2 Ma (Swinden, 2011). Later, Frets (1969) mapped and described the southern area of the Lofdal complex as an intrusive rock into the HMC. More recent works have described this unit as the Lofdal intrusive complex composed of nepheline syenites, phonolites, diatreme breccias, and carbonatites (Swinden, 2011).

The Lofdal nepheline syenites have been described as medium to coarse grained feldspar- and nepheline-porphyritic syenites showing some phases of very-coarse grained pegmatitic syenite. The nepheline syenites are cut by the late forming phonolites and are also incorporated into the later volcanic breccias. The syenites have been dated using Rb-Sr whole rock at 764 ±60 Ma (Swinden, 2011).

The Lofdal phonolites are mineralogically described as being alkali feldspar and nepheline rich which form SW to NE striking dykes. The dykes are observed to cut the syenites and are geographically related to the carbonatite dykes.

A widespread occurrence of nepheline syenite and HMC related breccias occur throughout the Lofdal intrusive complex. These were originally described by Frets (1969) as 1 to 50 cm angular fragments held in a fine-grained matrix. It is now observed that both HMC breccias and nepheline syenite breccias occur and are angular and chaotic. The late stage carbonatite dykes are observed to cut the breccias indicating that the nepheline syenites and breccias both predate the carbonatites.

The carbonatite of the Lofdal intrusive complex occur as parallel striking dykes to the phonolites and as larger plugs, comparable to the nepheline syenites. The carbonatite dykes intrude through or adjacent to the younger phonolite dykes and cover an area exceeding 200 km^2. The carbonatite plugs exist as two dominant bodies noted as the “Main” intrusion and the “Emanya” intrusion (Fig 2.3). These plugs intrude nepheline syenite, which form an outcrop carapace on top of the carbonatite at the current exposure level.

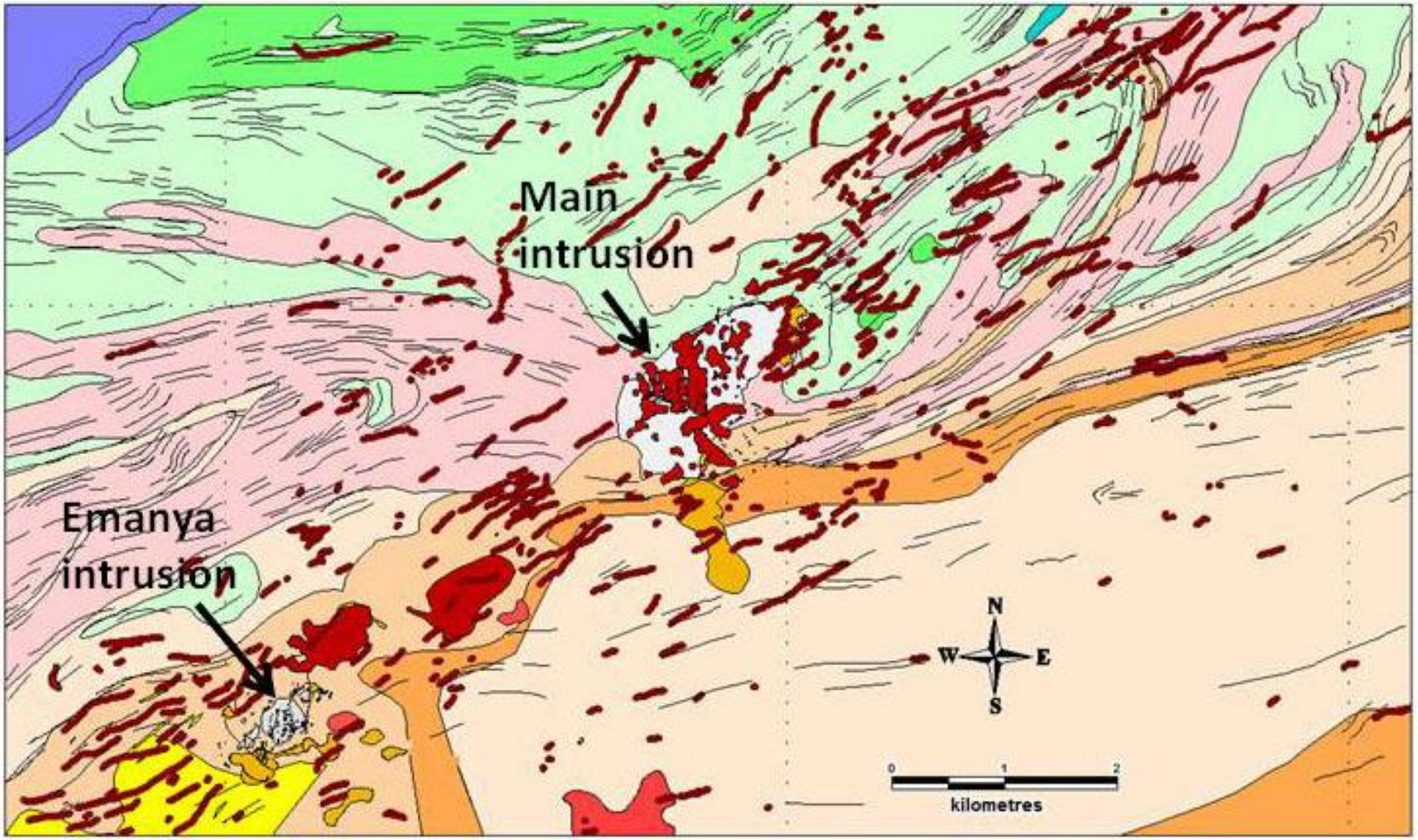

Figure 2.3: Detailed geological map of the central Lofdal intrusive complex. The Main intrusion and Emanya intrusion are shown to indicate the area of carbonatite plugs. (See Figure 1.3 for legend)

CHAPTER 3.0 RESULTS

3.0 *General Statement*

Samples of phonolites and nepheline syenites from the Lofdal intrusive complex were investigated and described using petrographic microscope and the detailed petrographic descriptions are reported below in Section 3.2. Minerals were identified using their optical properties and in some cases using the EDS spectra. Composition of the minerals was determined by EMP analyses (see Appendix A).

3.1 *Petrographic Descriptions*

3.1.1 *Nepheline Syenites*

ESY-1

General Information

Sample ESY-1 is a coarse-grained, slightly altered, inequigranular nepheline syenite. The grains in this sample are between 5 and 10 mm in size with interstitial material in the 0.1 to 1 mm size range. The sample is dominated by 10 mm, perthitic, poikilitic, subhedral alkali feldspar which composes nearly half of the mineral assemblage. Inclusions include thin parallel veins of sericite, fine grained sericite, and rare carbonates. Similarly sized subhedral, altered plagioclase constitutes ~15% of the mineral assemblage. These grains often appear as long laths with euhedral cores and altered rims. Anhedral, 3 to 5 mm grains of biotite are juxtaposed to the two feldspar grains and make up an additional ~10% of the mineral assemblage. Prismatic pseudomorphs of 5 to 10 mm compose 20% of the mineral assemblage of this sample. Sericite aggregates compose the majority of these pseudomorphs with lesser amounts of 0.05 to 1 mm biotite, rare 0.5 mm calcite, and 0.5 to 1 mm, cancrinite (?) (Fig. 3.1). All of the previously mentioned material with the addition of euhedral magnetite with ilmenite/hematite exsolution lamellae

and apatite make up the fine grained, 0.1 to 1 mm interstitial material found between the coarse grained minerals. In hand sample the weathered surface is stained light brown. Two distinctive grains appear on the surface: 1) elongate to stubby, brown stained prisms and 2) anhedral mafics. Small 5 mm pits are also found on the weathered surface. Fresh surfaces show a coarse crystalline texture with many different 0.5 to 3 cm grains. Alkali feldspar, plagioclase, and biotite are present with an unknown mineral of 1 cm laths which have milky white cores with rose-coloured rims.

Mineralogy

Coarse-Grained Material (95%)

- Prismatic Pseudomorphs: Prismatic pseudomorphs are 1 to 5 mm in size and compose nearly 20% of the mineral assemblage. The aggregate material is composed of fine grained sericite, subhedral to anhedral biotite, and relatively small prismatic ilmenite.
- Alkali feldspar: Composing most of the sample, 5 to 10 mm, perthitic alkali feldspar is the dominant phase. All grains appear dirty and colourless in plane polarized light (PPL). In cross polarized light the grains contain abundant perthitic lamellae. Parallel, thin veins of sericite cut through most samples.
- Plagioclase: Laths of plagioclase range from 5 to 10 mm and constitute nearly 15% of the mineral assemblage. The laths are sub- to anhedral and have irregular grain boundaries. Alteration occurs predominantly near the grain rim but occasionally within the core. Sub-parallel fractures, in-filled by sericite and carbonate, are found within both feldspars and are continuous through neighbouring grains.
- Anhedral biotite: Extremely anhedral, 3 to 5 mm grains of biotite compose ~10% of the mineral assemblage. The biotite usually has irregular grain boundaries. Many of the grains have a

circular grain shape, unlike typical platy biotite grains. Prismatic, 0.1 mm opaques are randomly distributed within the biotite grains.

Interstitial Material (5%)

An interstitial matrix constitutes ~5% of the mineral assemblage. The material consists of alkali feldspar (20%), biotite (20%), sericite (30%), nepheline (10%), carbonate (20%), and very few prismatic opaques. The grains vary in size between 0.1 to 1 mm. Although many of the grains are euhedral with sharp crystal boundaries, some are anhedral, appearing as thought they grew in vacant space during the end of crystallization.

ESY-2

General Information

Sample ESY-2 is a coarse-grained, inequigranular nepheline syenite. On the basis of size, two discrete mineral assemblages exist. Larger phenocrysts range in size between 1 to 10 mm, embedded in a finer grained interstitial material with a size range of 0.05 to 0.5 mm. There are four types of phenocrysts that include: 1) Highly altered prismatic nepheline with cancrinite rims (Fig. 3.2), 2) prismatic euhedral to rounded subhedral alkali feldspar, 3) subhedral to anhedral, altered laths and stubby crystals of aegirine, and 4) euhedral prismatic titanite. Many of the colourless phenocrysts appear dirty due to alteration products. The interstitial material comprises a variety of subhedral to anhedral crystals of alkali feldspar (70%), amphibole (23%), prismatic opaques (5%), and fluorite (1-2%). Many alteration products are present in the alkali feldspar but they are too small to identify. In hand

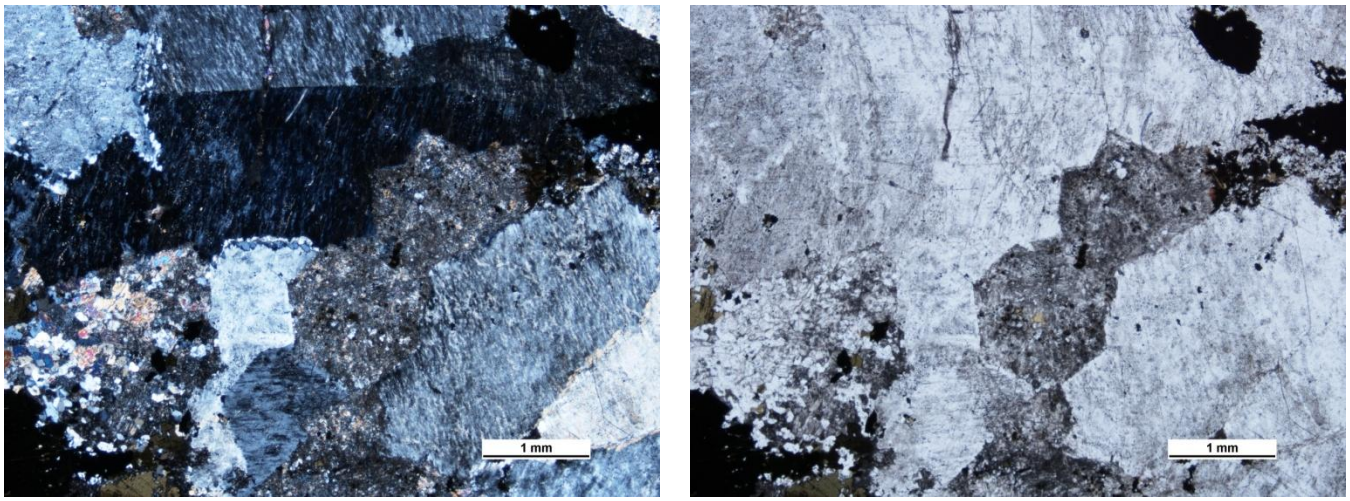

Figure 3.1: Prismatic, 1 to 2 mm nepheline pseudomorphs are enclosed by perthitic alkali feldspar found in sample ESY-1. The prismatic pseudomorphs to the right in both panels have been completely replaced by fine-grained cancrinite and sericite. The pseudomorph grain to the left is composed of larger grained cancrinite in association with fine-grained sericite.

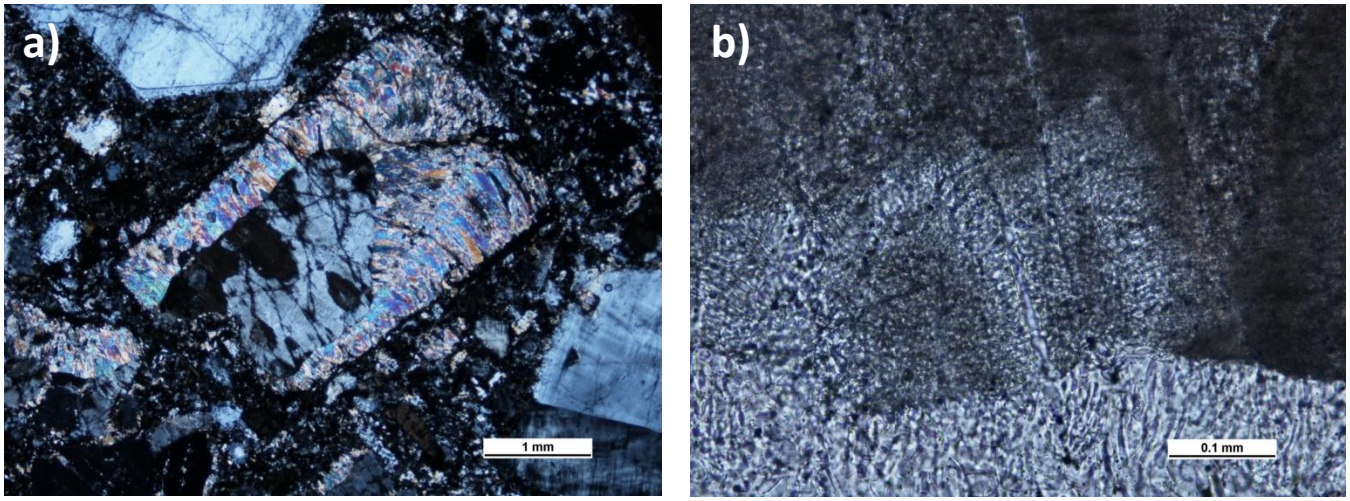

Figure 3.2: From sample ESY-2 showing alteration and replacement textures of nepheline. **a)** A 3 mm, prismatic pseudomorph containing nepheline at its core with replacement of the rim by cancrinite and alteration of the core to fine-grained material. Taken in XPL. **b)** Alteration products within the nepheline core showing resemblance to myrmekitic texture in PPL. The products of this replacement are fluorite and a fine-grained unknown felsic mineral.

sample the weathered surface is gray to brown in colour. Pits ranging from 1 to 10 mm scour this surface. White phenocrysts with smaller black inclusions are present at the bottom of these pits. Prismatic alkali feldspars ranging from 0.1 to 2 cm slightly protrude from the surface. Black, prismatic 0.5 to 1 cm phenocrysts are rare on this surface. These appear heavily weathered and are possibly composed of fine-grained, mafic aggregates. The fresh surface complements the weathered surface by containing the same phenocrysts in a mild gray matrix with addition of 1 to 5 mm, elongate, red phenocrysts which are present in low abundances.

Mineralogy

Phenocrysts (80%)

- Altered nepheline: Prismatic, altered nepheline, ranging from 1 to 8 mm in size, composes 45-50% of the phenocryst assemblage. Typically there is a nepheline core, often half the size of the original grain, with radiating branches of near-fibrous cancrinite that extend to the original euhedral grain boundary. The core nepheline is colourless but dirty due to the abundance of alteration products. The core also shows abundant fractures, making the grains appear shattered. Some areas are completely altered to a brown, fine grained, aggregate mass. An irregular intergrowth texture, resembling myrmekite, of fluorite and an unidentifiable mineral is present between the contact of nepheline and cancrinite (Fig. 3.2).
- Alkali feldspar: Both euhedral prismatic and subhedral rounded 1 to 10 mm alkali feldspar compose 30-35% of the phenocryst assemblage. Grains usually appear dirty due to alteration products (sericite) and have irregular grain boundaries. Most grains contain either simple Carlsbad twins, tartan twins, or both.

- Altered aegirine: Subhedral laths and round 0.5 to 5 mm aegirine composes 15-20% of the phenocryst assemblage. The grains consist either of fresh aegirine cores with altered rims or are completely altered to fine grained aggregates.
- Titanite: Euhedral titanite ranging from 0.5 to 2 mm composes 5% of the phenocryst assemblage. The grains are diamond shaped and sometimes are cracked into many, closely separated pieces.

Interstitial Matrix (20%)

The matrix consists of subhedral to anhedral crystals of alkali feldspar (70%), amphibole (23%), prismatic opaques (5%), and fluorite (1-2%). Alkali feldspar and amphibole grains have irregular boundaries. The euhedral opaques and fluorite-containing grains have sharp boundaries and appear to overprint surrounding material.

Specific Features

Fluorite appears in two forms. First, it is present as an inclusion in a very fine-grained, euhedral matrix felsic crystal. It is also one of the alteration products of nepheline, often found between nepheline and cancrinite in a texture resembling myrmekite.

ESY-3

General Information

Sample ESY-3 is a coarse-grained, slightly altered, inequigranular nepheline syenite. The sample is identical to sample ESY-1. The coarse grained material is between 5 to 10 mm with interstitial material that ranges from 0.1 to 1 mm. The slide is dominated by 5 to >20 mm, perthitic, euhedral alkali feldspar, composing ~60% of the mineral assemblage. Prismatic pseudomorphs (at one time nepheline) of 5 to 10

mm compose 20% of the mineral assemblage. The pseudomorphs contain fine-grained white mica as the dominant mineral with minor amounts of biotite, calcite, and some feldspar. Anhedral, 1 to 5 mm biotite makes 10% of the mineral assemblage. The grain boundaries are highly irregular. Areas within the core of the biotite grains variably contain fine grained biotite aggregate. A single 5 mm, kinked plagioclase grain makes up 1-2% of the mineral assemblage. The grain appears euhedral with an irregular grain boundary. The interstitial material makes up 5% of the mineral assemblage. This material is composed of the same mineralogy as the coarse grains, except that it is only 0.1 to 1 mm in size, and it contains similarly sized prismatic opaques. Along the weathered surface, the hand sample has jagged looking pits that vary in size from 5 to 20 mm. Prismatic, coarse grains are stained red-brown and blend in with the finer-grained red-brown interstitial material. Fresh surfaces show an assemblage of coarse-grained leucocratic material (alkali feldspar and probably fibrous sericite pseudomorphs and plagioclase) ranging in size from 5 to 35 mm. Anhedral biotite grains range from 3 to 10 mm but consume a considerably lesser percentage of the mineral assemblage.

Mineralogy

Coarse-Grained Material (95%)

- Prismatic Pseudomorphs: Prismatic pseudomorphs are 3 to 7 mm in size and compose nearly 20% of the mineral assemblage. The aggregate material consists of fine grained sericite, subhedral to anhedral biotite, rare carbonate, and relatively small prismatic ilmenite (Fig 3.3).
- Alkali feldspar: Composing nearly 60% of the sample, 5 to 10 mm, perthitic alkali feldspar is the dominant mineral in this assemblage. All grains appear dirty and colourless in PPL due to the presence of alteration products. Parallel fractures in-filled with sericite run though most grains. Some intergrowth of carbonate minerals with sericite is visible where the fractures thicken.

- Anhedral biotite: Extremely anhedral, 1 to 5 mm grains of biotite compose ~10% of the mineral assemblage. The biotite grains have irregular grain boundaries and are circular in shape. Prismatic, 0.1 mm opaques are randomly distributed within the biotite grains.
- Plagioclase: A single plagioclase grain is found in this sample. It composes at most 2% of the mineral assemblage. The grain is oddly shaped in that it is kinked, making a subtle U-shape (Fig. 3.3).

Interstitial Material (5%)

The interstitial material is identical to that of sample ESY-1. It is again found between the coarse grained material and composes ~5% of the mineral assemblage. The material is made of alkali feldspar (20%), biotite (20%), sericite (30%), nepheline (10%), carbonate (20%), and very few prismatic opaques. The grains vary in size between 0.1 to 1 mm. Although many of the grains are euhedral with sharp crystal boundaries, some appear anhedral.

Specific Features

A thin leucocratic vein (composed mostly of aggregated alkali feldspar with minor plagioclase and possibly nepheline) cuts though all coarse grained material in this sample. The vein may also carry prismatic opaques and broken pieces of the fine grained sericite pseudomorph.

ESY-4

General Information

Sample ESY-4 is a coarse-grained, inequigranular, highly altered nepheline syenite. The sample is composed of coarse grained, euhedral, perthitic alkali feldspar, subhedral plagioclase, and anhedral biotite surrounded by an interstitial matrix of fine-grained, subhedral sericite with possible cancrinite

and minor amounts of alkali feldspar, plagioclase, nepheline, biotite, and prismatic opaques (Fig. 3.4). The coarse-grained alkali feldspar and plagioclase are 5 to 10 mm in size and have rough grain boundaries. Both contain parallel fractures which have been in-filled by fibrous sericite. Coarse grained, anhedral biotite (0.5 to 2 mm) only appears along the grain boundary of large alkali feldspars. The fine-grained, interstitial material dominantly comprises <0.01 to 0.2 mm anhedral sericite. The remaining material ranges from 0.01 to 0.1 mm in size. The weathered surface of the hand sample is yellow to brown in colour. Besides a few 0.5 to 1 cm feldspar grains, this surface is featureless. The fresh surface of this sample shows 0.5 to 2 cm, milky-white to rose coloured feldspar grains hosted in an aphanitic, dark gray to green matrix.

Mineralogy

Coarse-Grained Material (65%)

- Alkali feldspar: Highly perthitic, 3 to 15 mm, euhedral alkali feldspar composes 80% of the coarse grained mineral assemblage. Many nearly parallel fractures run though this sample and have been in-filled by sericite. Most crystals feature simple twinning, while few have tartan twinning. Very small (<0.01 mm) inclusions, most likely sericite, are found unsystematically distributed throughout the grains.
- Plagioclase: Anhedral, 5 mm, elongate coarse grains of plagioclase compose 15% of the coarse grained mineral assemblage. Although heavily altered along the rims, the grains contain many polysynthetic twins. Small sericite inclusions, much the same as in alkali feldspar, are found throughout these plagioclase grains.
- Anhedral biotite: Extremely anhedral, 1 to 2 mm biotite with jagged grain boundaries composes 5% of the coarse grained mineral assemblage. The biotite has no specific habit. It is often found along the grain boundaries of alkali feldspar in association with 0.5 mm ilmenite.

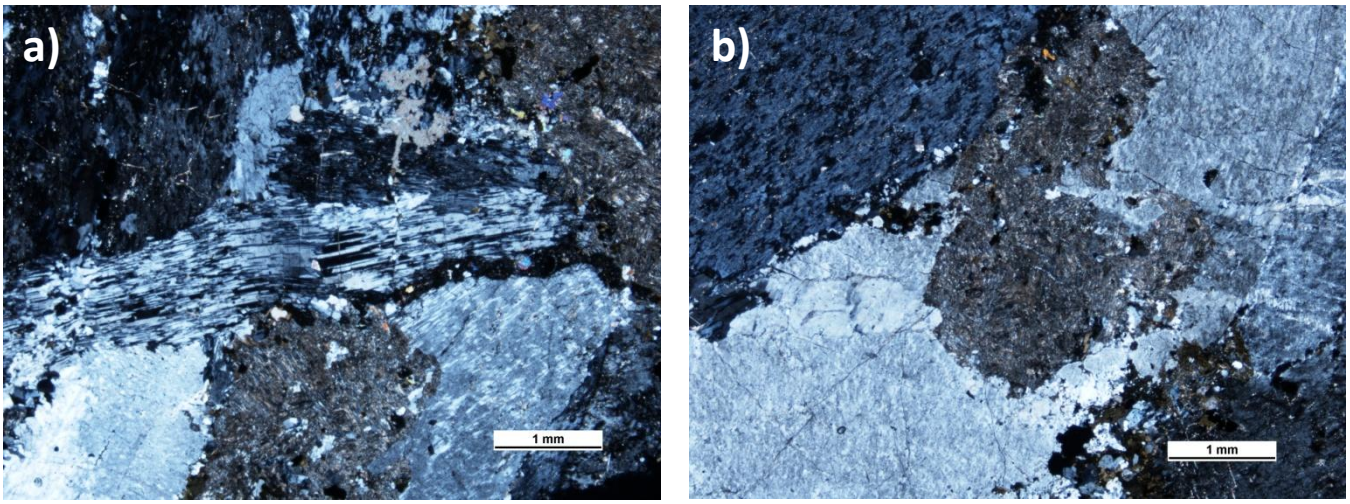

Figure 3.3: Microphotograph (both XPL) from sample ESY-3. **a)** Coarse-grained plagioclase, alkali feldspar, nepheline pseudomorphs with interstitial calcite. The plagioclase grain has continuous polysynthetic twinning but is bent at the midpoint of the grain. **b)** Euhedral nepheline pseudomorphs of fine-grained sericite and cancrinite surrounded by perthitic alkali feldspar and anhedral biotite.

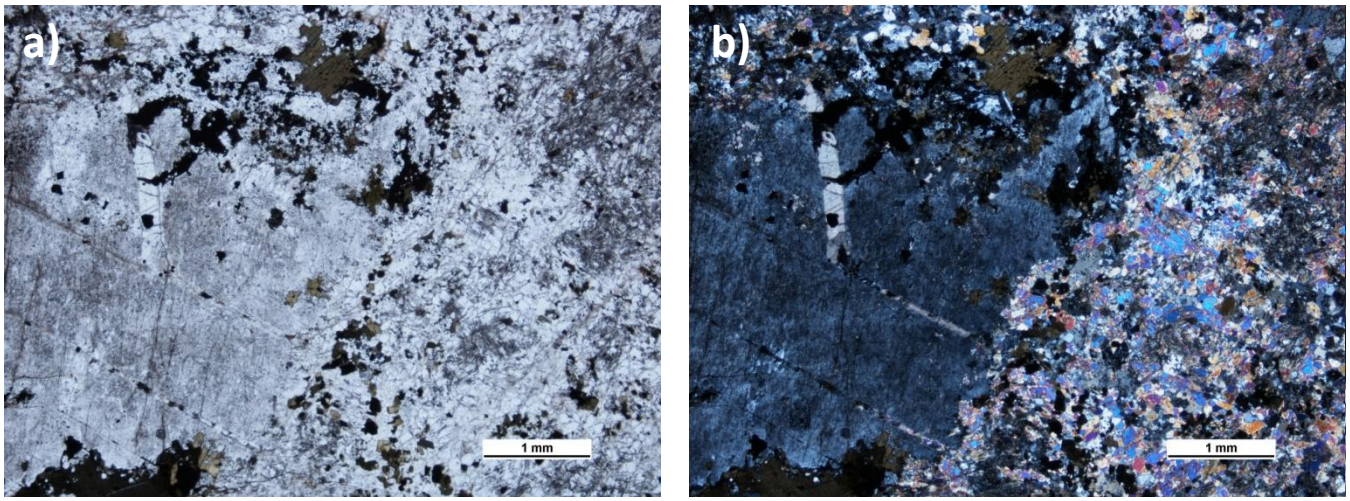

Figure 3.4: The same microphotograph from sample ESY-4 (the left panel (a) is taken in PPL with the right panel (b) taken in XPL). Anhedral alkali feldspar and biotite are surrounded by fine-grained replacement products of cancrinite, euhedral magnetite/hematite, and fragmented biotite. Two fractures, filled by sericite, are running parallel within the alkali feldspar grain. A single vein of calcite runs from the grain boundary and stops when in contact with the in-filled fractures.

Interstitial Material (35%)

The interstitial material is found in the space between the coarse-grained phenocrysts. It is dominantly composed of (75%) very fine-grained aggregate sericite possibly with some cancrinite. The remaining 25% of the interstitial material is equally composed of anhedral alkali feldspar, anhedral biotite, and prismatic opaques with possibly a minor amount of nepheline. The alkali feldspar appears dirty in PPL due to the high number of small alteration products found in the crystal structure.

Specific Features

Carbonate veins are present within the coarse-grained alkali feldspar. The veins resemble the shape of a carrot, being 0.25 mm near the grain boundary and thinning to an end near the core of the grain. These veins do not persist through the rest of the coarse-grained nor interstitial material (Fig. 3.4).

ESY-5

General Information

Sample ESY-5 is an inequigranular, slightly altered nepheline syenite. Two discrete mineral assemblages exist based on grain size. Larger phenocrysts range in size between 1 to 20 mm. There are four types of phenocrysts: 1) Coarse-grained, perthitic alkali feldspar ranging from 2 to 20 mm, 2) anhedral, highly altered laths of aegirine, 3) prismatic, 2 to 5 mm nepheline, and 4) prismatic, diamond shaped titanite. These grains are hosted in a fine-grained, dominantly leucocratic matrix. Subhedral grains of alkali feldspar, plagioclase, and nepheline compose ~85% of the interstitial matrix assemblage. Very fine grained, anhedral amphibole, prismatic opaques, and aegirine compose the remaining 15% of the matrix assemblage. Rare areas within the matrix contain a distinctive fluorite-purple-colouring. In hand sample the light-brown weathered surface is featureless. Fresh surfaces have a variety of phenocrysts within a dark gray to green matrix. Three phenocrysts can be seen on this surface: 1)

colourless, 2 to 10 mm alkali feldspar, 2) prismatic melanocratic grains with altered rims (aegirine?), and 3) pink to red, subhedral, 1 to 5 mm grains.

Mineralogy

Coarse-Grained Material (55%)

- Alkali feldspar: Dominantly prismatic, euhedral, 1 to 20 mm, perthitic alkali feldspar composes 45% of the phenocryst assemblage. The larger the grain the more likely it is to contain a zoning pattern. The grains that are 15 to 20 mm often contain a central phenocryst with tartan twinning while the rim material is featureless (Fig. 3.5). Very few alteration products are present. Those that are present are extremely small and resemble sericite. Simple Carlsbad twinning is present in many grains, regardless of size.
- Prismatic nepheline: Prismatic, 2 to 5 mm, often fractured nepheline composes 25% of the phenocryst assemblage (3.2.1.5). The grains contain initial alteration products of fluorite and an unknown mineral, identical to the myrmekite-like texture seen in sample ESY-2.
- Anhedral aegirine: Often altered, 0.5 to 5 mm aegirine composes approximately 25% of the phenocryst assemblage. The grains form either large laths or rounded, stubby crystals. Both have a common alteration product; a high relief, low birefringent aggregate material. Aegirine is usually found in association with 0.1 mm prismatic opaques and also with prismatic titanite.
- Prismatic titanite: Prismatic to subhedral, 0.1 to 1 mm titanite composes 5% of the phenocryst assemblage. Nearly half of the phenocrysts have alteration along the rims, causing the grains to have an irregular subhedral shape. Fractures are common throughout the grains but are not a distinguishing feature.

Interstitial Material (45%)

The matrix material is composed of both felsic and mafic grains that range in size between 0.05 to 0.1 mm. The mineralogy of the matrix is: 70% anhedral alkali feldspar and nepheline, 15% plagioclase, 10% anhedral aegirine, 4% anhedral amphibole, and 1% prismatic magnetite/ilmenite. A slight purple-fluorite-coloured staining occurs throughout the matrix. Microphenocrysts of alkali feldspar and nepheline, ranging in size from 0.1 to 0.4 mm, are rare but usually appear in the matrix farthest from any phenocrysts.

Specific Features

A single, large (4 mm), prismatic apatite grain is present. This was distinguished from nepheline using two properties: the relatively high relief of apatite and the early alteration products of nepheline, which are not associated with the apatite. These early alteration products, as well as most of the groundmass, contain an abundance of fluorite which is identifiable due to purple staining in PPL.

ESY-6

General Information

Sample ESY-6 is an inequigranular, highly altered nepheline syenite. Phenocrysts ranging in size from 1 to 15 mm sit in a 0.05 to 0.3 mm groundmass. There are five types of phenocrysts present within the sample: 1) prismatic, perthitic, 2 to 15 mm alkali feldspar, 2) prismatic, highly altered, 1 to 5 mm nepheline, 3) highly altered, 1 to 4 mm, prismatic to stubby grains of aegirine, 4) 2 to 4 mm, subhedral apatite, and 5) prismatic, 0.5 to 2 mm titanite. The matrix consists of a variety of felsic and mafic minerals. The felsic minerals (alkali feldspar, nepheline, plagioclase, and possibly fine grained sericite) compose 80% of the matrix. The mafic minerals (anhedral amphibole and aegirine) compose the final 20%

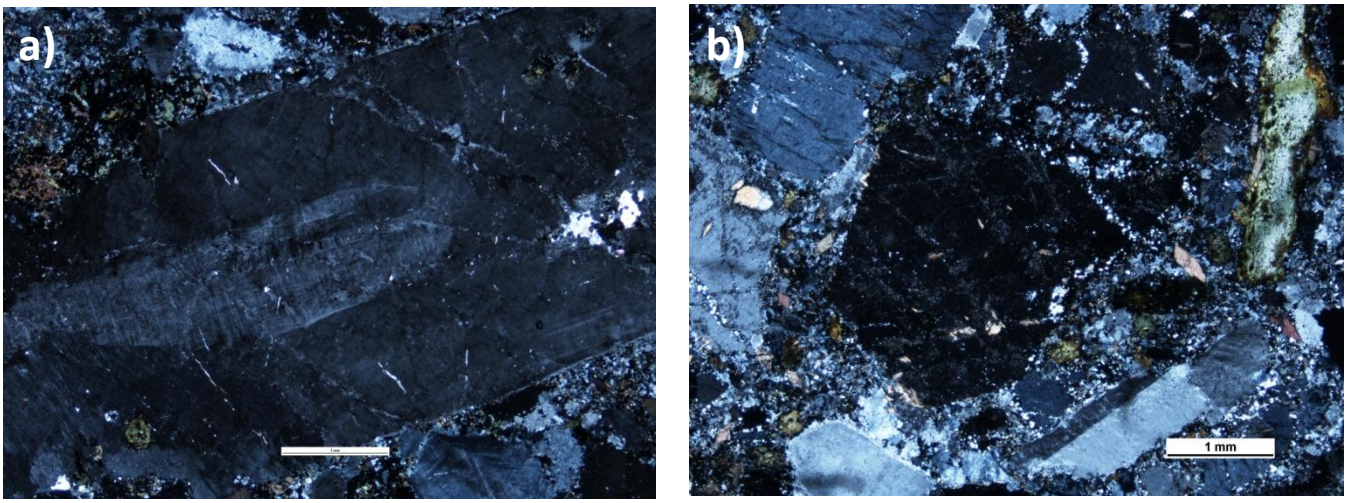

Figure 3.5: Microphotographs showing zoning and veining in sample ESY-5 in XPL. **a)** Zoned alkali feldspar with simple twinning intergrown with another alkali feldspar . **b)** Near-fresh nepheline cut by leucocratic veins at the top with some yellow-white alteration products near the bottom.

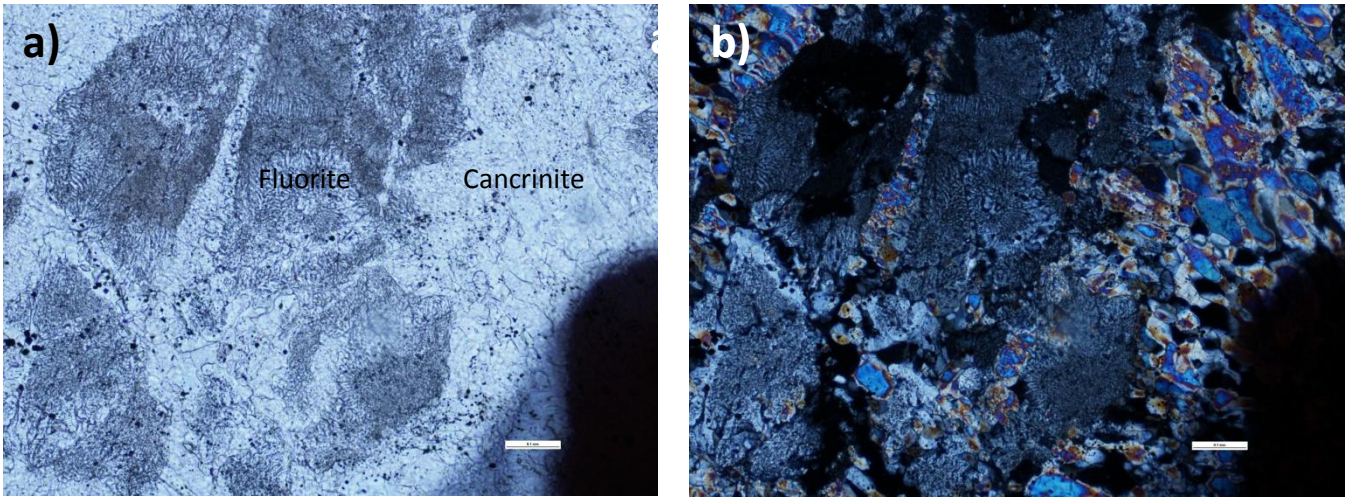

Figure 3.6: Microphotograph of sample ESY-6 showing the replacement and alteration products of nepheline in PPL (a) and in XPL (b). The symplectitic texture of anhedral cancrinite surrounds an alteration of product of fluorite and an unknown leucocratic mineral.

of the matrix material. Purple staining occurs in the matrix and within the alteration products of nepheline. In hand sample the weathered surface is highly irregular. Pits (~5 mm) cover most of the area with 1 cm, prismatic, dirty-white phenocrysts covering the remainder of the surface. Fresh surfaces expose four well developed phenocrysts which are: 1) a colourless, ~1 cm, prismatic feldspar, 2) a prismatic, milky-white unknown mineral, 3) a pink-to-red, anhedral feldspar, and 4) 2 to 10 mm, prismatic opaques. These sit in a dark green-to-gray, very fine grained matrix.

Mineralogy

Coarse-Grained Material (50%)

- Alkali feldspar: Perthitic, 1 to 15 mm, subhedral alkali feldspar composes 40% of the phenocryst assemblage. The grains appear dirty in PPL due to the high number of alteration products. Simple Carlsbad twinning is present in most of the grains with small amounts of tartan twinning in the less altered material. Zoning is present in the single 15 mm grain.
- Nepheline: Highly altered, subhedral, 0.5 to 5 mm nepheline composes 20% of the phenocryst assemblage. The grains appear in two stages of alteration. The first is a nepheline core with fibrous cancrinite branching outward to the grain boundary. This inner core also contains an alteration product of fluorite and an unknown low birefringence, high relief mineral. This material resembles myrmekite texturally (Fig. 3.6). The second is a more pervasive degree of alteration as the entire grain is a prismatic pseudomorph composed of ~0.5 mm cancrinite aggregate.
- Aegirine: 0.5 to 3 mm, extremely altered, laths to stubby grains of aegirine compose 30% of the phenocryst assemblage. These grains are severely anhedral and produce an alteration product of fine grained, dirty looking aggregate.

- Apatite: Prismatic, 0.5 to 2 mm apatite composes 5% of the phenocryst assemblage. Small alteration products are distributed evenly throughout the grains but are too small for identification.
- Titanite: Prismatic, subhedral, 0.5 to 1.5 mm titanite composes 5% of the phenocryst assemblage. These grains are diamond-shaped prisms or subhedral, nearly round grains with irregular grain boundaries.

Interstitial Material (50%)

The interstitial matrix is composed of 80% felsic and 20% mafic minerals (0.01 to 0.1 mm). The felsic mineral assemblage is dominantly made up of subhedral alkali feldspar with lesser nepheline and rare plagioclase. The mafic mineral assemblage is equally made up of anhedral aegirine and anhedral laths of amphibole. Rare microphenocrysts (0.1 to 0.5 mm) of alkali feldspar with tartan twinning are distributed homogeneously within the groundmass. Purple staining, indicating the presence of fluorite, is shown throughout the matrix.

Specific Features

Thin (~0.1 mm) leucocratic veins of low relief, low birefringence minerals (quartz or nepheline) run in multiple directions throughout the section. These veins cut both the matrix and phenocrysts. Fluorite is again present as a purple staining with the entirety of the matrix and within alteration products of nepheline.

ESY-7

General Information

Sample ESY-7 is a coarse- to medium-grained, inequigranular, highly altered, carbonate-rich nepheline syenite. Coarse grains (0.5 to 4 mm) are composed of extremely anhedral biotite, alkali

feldspar, plagioclase, and pseudomorphs comprising fine grained, fibrous aggregates of unknown low relief, colourless, low birefringent mineral. The medium to fine grains (0.05 to 0.5 mm) are dominantly (90%) leucocratic minerals (subhedral calcite, alkali feldspar, plagioclase, and nepheline) with minor (10%) subhedral to anhedral biotite. Prismatic, subhedral opaque grains, often containing inclusions of calcite, are evenly distributed and compose 1 to 2 % of the mineral assemblage. A single leucocratic vein runs through the entirety of this section. In hand sample the weathered surface is light to dark brown in colour, unevenly rough, and otherwise featureless. The fresh surface contains two identifiable phenocrysts which are: 1) subhedral, milky white, 1 to 10 mm plagioclase and 2) subhedral, colourless but dirty looking, 2 to 5 mm, highly altered alkali feldspar. The surrounding material is a mild gray to dark green.

Mineralogy

Coarse-Grained Material (25%)

- Subhedral plagioclase: Anhedral, 1 to 3 mm plagioclase with irregular grain boundaries composes 70% of the coarse-grained mineral assemblage. Most contain obvious polysynthetic twinning. The grains are often pairs or larger glomerophyritic groups. Very fine-grained alteration products are probably sericite. Some larger inclusions of calcite are present.
- Subhedral alkali feldspar: Retaining very little original shape, these anhedral to subhedral, ~2 mm grains of alkali feldspar compose 5 to 10 % of the coarse-grained mineral assemblage. Carlsbad twinning is present in most grains. Small alteration products give the colourless minerals a dirty appearance in PPL. These alteration products consist mostly of sericite within the grain and calcite along the grain boundary.
- Anhedral biotite: Most of the biotite is medium- to fine-grained, subhedral grains. The coarser-grained biotite is extremely anhedral, with jagged grain boundaries, and composes 5 to 10% of

the coarse grained mineral assemblage. Inclusions of 0.1 mm calcite, prismatic opaque minerals, and felsic minerals (plagioclase and alkali feldspar) are present within biotite grains.

- Anhedral pseudomorphs: Highly altered, 2 to 5 mm pseudomorphs compose 5 to 10% of the coarse grained mineral assemblage. The pseudomorphs are colourless but dirty looking in PPL due to the high degree of alteration. The pseudomorph is a fine grained, anhedral aggregate of calcite, plagioclase, and possibly alkali feldspar.

Medium- to Fine-Grained Material (75%)

The medium to fine grained material is composed of (45%) subhedral calcite, (30%) subhedral biotite, and (25%) of plagioclase, alkali feldspar, and possibly nepheline. Small amounts of calcite are present within the feldspars. This may be the same alteration occurring in the coarse grained material in which calcite is substituting for both types of feldspars. Purple staining is present within the calcite, reflecting the presence of fluorite. Isotropic material, which is colourless, persists within the matrix and is indicative of sodalite (Fig. 3.7). This is another known alteration of cancrinite within the Lofdal intrusive complex.

Specific Features

A single, 0.5 mm wide vein composed of leucocratic material runs though both finer and larger grained material. The vein consists of colourless, fibrous material that has partially altered to carbonate. This may indicate that the vein material is the same fine- and coarse-grained feldspar present in the rest of the section. Fluorite is found within all of the secondary calcite.

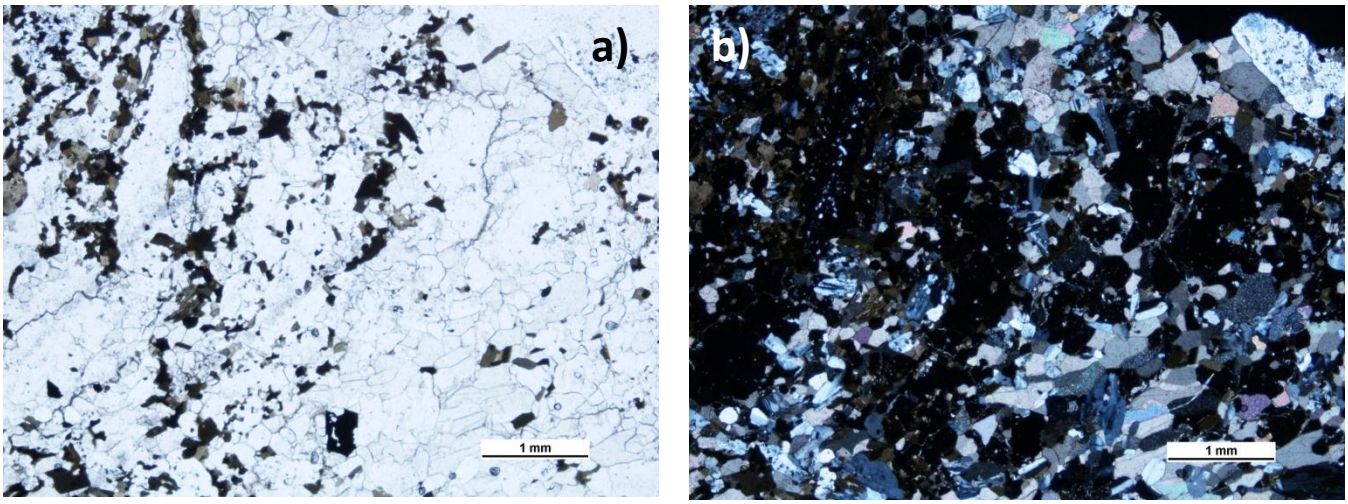

Figure 3.7: Microphotograph of sample ESY-7. Both panels contain the same image but panel a) is in PPL and panel b) is in XPL. The panels together show an assortment of fragmented biotite, euhedral to subhedral magnetite, and large portions of colourless minerals. The colourless minerals are in fact feldspars and carbonates as well as can be seen in panel b) an isotropic mineral. This mineral is sodalite, a known alteration products of nepheline within the Lofdal intrusive syenite complex.

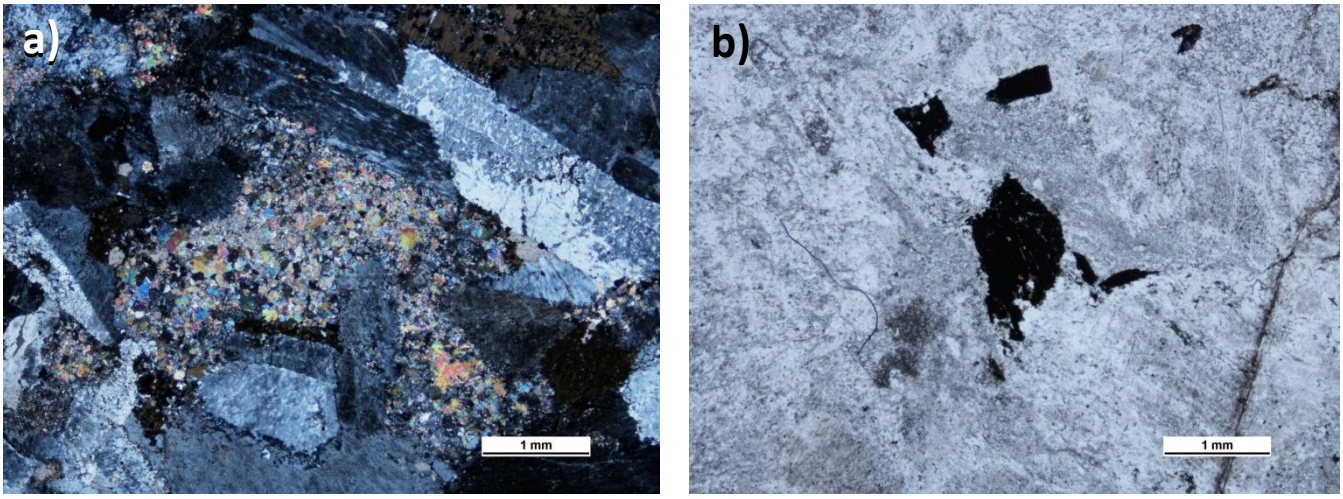

Figure 3.8: Microphotograph of sample ESY-8 showing sample mineralogy. **a)** Fine-grained cancrinite and very fine-grained sericite composed anhedral pseudomorphs of nepheline, surrounded by prismatic alkali feldspars. **b)** Three 0.5 to 1 mm, subhedral opaque grains. The top two grains are magnetite with exsolution lamellae of hematite and/or ilmenite. The bottom most grain has the same mineralogy but contains inclusions and grain boundaries which are biotite rich.

ESY-8

General Information

Sample ESY-8 is a coarse gained, highly altered nepheline syenite. It contains 1 to 10 mm grains, subhedral to euhedral prismatic (50%) alkali feldspar, (15%) plagioclase, (5-10%) biotite, and (20-30%) highly altered nepheline. Few ~1 mm sized opaque minerals exist and are grouped in a single area. A high number of internal alteration products are noted within the alkali feldspar as well as the plagioclase. In hand sample the weathered surface is light brown in colour. There are a number of 5 to 10 mm, rounded pits as well as 1 to 2 cm, euhedral feldspar grains cover this surface. On fresh surfaces three coarse-grained minerals can be identified based on colour: 1) milky-white, subhedral, 3 to 10 mm grains (alkali feldspar or plagioclase), 2) euhedral mafic laths (biotite), and 3) red to pink coloured, anhedral grains (alkali feldspar?).

Mineralogy

Coarse-Grained Material

- Altered nepheline: Completely altered, 2 to 5 mm nepheline composes 20-30% of the mineral assemblage. The grains are now complete pseudomorphs which contain 0.01 to 0.5 mm 50% cancrinite, 45% calcite, and 5% fluorite. The grain boundaries are richer in calcite than the core. This calcite may be an alteration of the surrounding feldspar as it appears to have been propagating into adjacent grains (Fig. 3.8).
- Alkali feldspar: Partially altered, 1 to 10 mm, perthitic alkali feldspar composes half of the mineral assemblage. Large groups of sericite, cancrinite, and calcite are found as alteration products within the cores of the grains. These are all associated with in-filled fractures of the same material. The grain boundaries are irregular in areas and are replaced by calcite.

- Plagioclase: Irregular, subhedral to anhedral, 1 to 5 mm grains of plagioclase compose 5-10% of the mineral assemblage. These grains contain polysynthetic twins. Along the grain boundary there is a replacement texture in which fine grained calcite is forming.
- Anhedral biotite: Anhedral, irregular, 0.5 to 2 mm biotite composes 5-10% of the mineral assemblage. The grains are commonly highly altered and usually composed of finer aggregate. However, this aggregate material is usually adjacent to one or more 0.5 mm or larger opaque magnetite grains (Fig. 3.8).

Specific Features

The nepheline has been completely altered to 0.1 to 0.5 mm cancrinite and associated calcite. The alteration products fill fractures in adjacent alkali feldspar grains and propagate into the grain boundaries of alkali feldspar and plagioclase. Fluorite is associated with the calcite and cancrinite alteration and can be seen in both the nepheline pseudomorphs and in the veins within alkali feldspar.

ESY-9

General Information

Sample ESY-9 is a highly altered, coarse-grained nepheline syenite. There are four distinct mineral types in this sample including: 1) euhedral to subhedral alkali feldspar, 2) pseudomorphed, prismatic nepheline, 3) anhedral biotite, and 4) anhedral, irregular opaques. The grains range in size from 1 to 5 mm. Most are highly altered with nepheline being completely substituted to cancrinite with fluorite. The feldspars appear extremely dirty in PPL due to the alteration products. In hand sample the weathered surface is identical to sample ESY-8. Pits, ranging from 5 to 10 mm, as well as prismatic, 1 cm alkali feldspar cover the entirety of the surface. Fresh surfaces show two felsic minerals and one mafic mineral. The felsic minerals are both prismatic and range in size from 5 mm to 15 mm. They can be

distinguished by colour; one is colourless while the other is milky white (feldspars?). The mafic mineral is nearly prismatic and ranges in size from 2 to 10 mm (biotite) (Fig. 3.9).

Mineralogy

Coarse-Grained Material

- Pseudomorphed nepheline: Prismatic pseudomorphs after nepheline compose 30-35% of the mineral assemblage. These grains have been completely altered to 0.1 to 0.5 mm cancrinite with associated calcite and fluorite.
- Alkali feldspar: Prismatic, euhedral to subhedral, 2 to 5 mm alkali feldspar composes 35-40% of the mineral assemblage. A high degree of alteration has occurred as evinced by the dirty appearance in PPL. The grain boundaries are irregular and appear to have been replaced by carbonate.
- Anhedral biotite: Anhedral, 0.5 to 2 mm biotite composes 15-20% of the mineral assemblage. Biotite in this sample contains the same properties as in sample ESY-8. They are associated with 0.1 to 0.5 mm opaque grains and are often formed from fine grained aggregate biotite.
- Anhedral opaques: Highly anhedral, 0.5 to 2 mm opaque grains (magnetite?) compose 5-10% of the mineral assemblage. These grains often appear in association with biotite. Most opaque crystals have irregular grain boundaries.

Specific Features

A substantial amount of fluorite is associated with cancrinite and carbonate material. This is similar to sample ESY-8, except for the absence of veins.

ESY-10

General Information

Sample ESY-10 is an inequigranular, highly altered, nepheline syenite. The coarse grained material comprises 1 to 15 mm grains of 1) perthitic, euhedral alkali feldspar, 2) completely altered, subhedral nepheline, 3) anhedral apatite (Fig. 3.10), 4) irregular biotite, 5) prismatic titanite, and 6) subhedral, rounded to elongate aegirine. Subhedral, 0.1 to 0.5 mm felsic material (alkali feldspar and nepheline) as well as biotite exist between the coarse grains. The fine grains may form from magma quenching or from replacement of the surrounding phenocrysts. This fine grained material is also poikilitic, containing a number of alteration inclusions. In hand sample the weathered surface is very similar to samples ESY-9 and ESY-8. The surface is light to dark in colour and is covered by 5 mm pits and 0.5 to 2 cm dirty white phenocrysts (most likely alkali feldspar). Fresh surfaces contain a variety of phenocrysts which are: 1) 0.5 to 1 cm, prismatic, milky white feldspar, 2) 0.5 to 1.5 cm, prismatic, colourless alkali feldspar or nepheline, 3) 1 to 5 mm, red to pink grains (possibly feldspar), 4) light green, 1 to 3 mm, aggregate grains (biotite?), and 5) dark green to black, 1 to 3 mm anhedral grains.

Mineralogy

Coarse-Grained Material

- Pseudomorphed nepheline: Near prismatic, 1 to 6 mm, completely altered nepheline composes 25-30% of the mineral assemblage. The grains are now pseudomorphs composed of 0.05 to 0.1 mm cancrinite with associated fluorite giving a purple staining. This material is often adjacent to similarly sized felsic grains (most likely alkali feldspar or nepheline).
- Alkali feldspar: Large, 1 to 15 mm, perthitic, euhedral to subhedral alkali feldspar composes 30-35% of the mineral assemblage. Many internal inclusions are present but are most likely

alteration products of fine grained sericite. Many 0.5 mm wide veins are present and have been in-filled by sericite. Carlsbad and tartan twinning are commonly present, especially in the larger grains.

- Anhedral apatite: Two coarse grains of apatite are present and compose 2-3% of the mineral assemblage. These grains have an irregular grain boundary and are highly fractured. The higher relief and lack of alteration are used to distinguish these from nepheline and alkali feldspar.
- Anhedral biotite: Anhedral, 0.5 to 1.5 mm, altered biotite composes 10 to 15% of the mineral assemblage. Small, prismatic opaques as well as smaller grains of titanite are associated with the biotite.
- Prismatic titanite: Euhedral, 0.5 to 2 mm titanite composes 5-10% of the mineral assemblage. These grains are commonly fractured, which occasionally causes them to split into separate sections. Simple twins are common, especially among the larger grains (Fig. 3.10).
- Subhedral aegirine: Subhedral to anhedral, 0.5 to 3 mm, rounded grains and laths of aegirine compose 5-10% of the mineral assemblage. These grains often have a fresh core that is highly fractured, surrounded by very fine grained aggregate alteration products. The fractures within these grains occasionally cause the grains to split into separate sections, much like titanite.

Interstitial Material

A small percentage of the mineral assemblage (1-2%) is composed of 0.01 to 0.1 mm biotite, alkali feldspar, cancrinite, and possibly nepheline.

Specific Features

Felsic rich veins (most likely feldspar material) crosscut all the material within the section. Small fractions of biotite and aegirine appear to have been picked up and later deposited within these veins. Fluorite is again present in the alteration products (cancrinite) of nepheline.

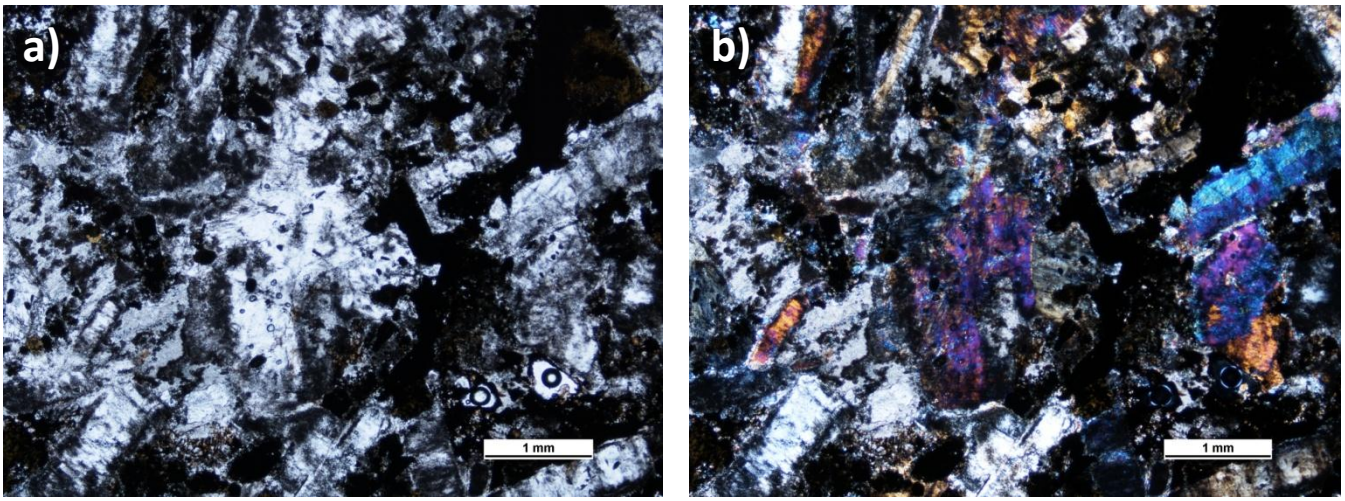

Figure 3.9: Microphotograph showing the overall mineralogy of sample ESY-9. Panel a) is taken in PPL and panel b) is taken in XPL. The overall mineralogy shows elongate, subhedral biotite, euhedral magnetite with hematite/ilmenite exsolution lamellae, and subhedral to anhedral leucocratic grains of alkali feldspar and nepheline.

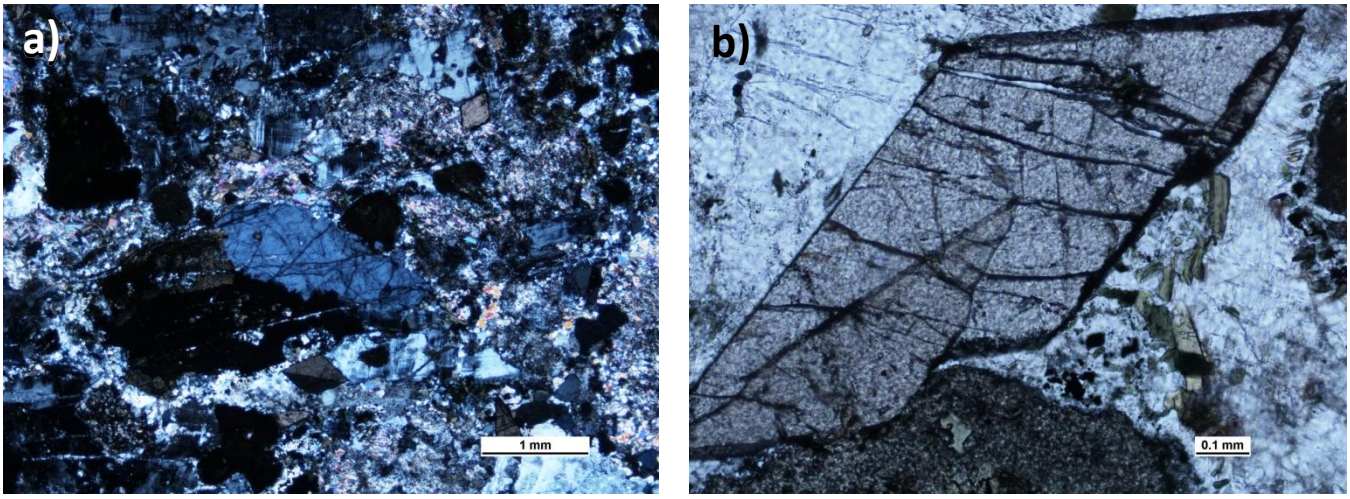

Figure 3.10: Microphotograph of sample ESY-10. **a)** XPL image of a subhedral, highly fractured prism of apatite within a fine-grained matrix. The fractures can be seen to contain small amounts of highly birefringent material (either carbonate or sericite). **b)** Prismatic titanite containing a simple twin in the bottom left corner. Both grains contain continuing fractures from one another. Toward the top of the photo the larger titanite is breaking into two pieces along a fracture.

ESY-11

General Information

Sample ESY-11 is an inequigranular, highly altered nepheline syenite. The coarse grained material ranges in size between 0.5 to 5 mm. This size fraction is composed of the following phenocrysts: 1) extremely anhedral alkali feldspar, 2) altered nepheline, 3) anhedral, altered aegirine, 4) glomerophyritic, aggregated biotite, and 5) subhedral titanite. Between these grains is a fine grained, subhedral, crystalline matrix. This matrix is dominantly formed of alkali feldspar with smaller amounts of nepheline, anhedral amphibole, biotite, sericite, and fluorite. In hand sample the weathered surface is light brown in colour and contains 3 to 5 mm pits as well as ~5 mm, dirty white, prismatic phenocrysts. On the fresh surface four phenocrysts are hosted within a fine grained crystalline matrix. These phenocrysts are: 1) prismatic, colourless, 3 to 15 mm feldspars, 2) prismatic, colourless to white, 3 to 15 mm grains (altered nepheline?), 3) green, vitreous mafic grains rimmed by black mafic aggregate material, and 4) anhedral, 1 to 2 mm grains.

Mineralogy

Coarse-Grained Material (75%)

- Altered nepheline: Highly altered, pseudomorphed, 2 to 5 mm nepheline constitutes 25-30% of the coarse grained mineral assemblage. The core remains as unaltered nepheline with alteration occurring dominantly around the rim. Much of the alteration, both within the core and along the rim, is an unknown leucocratic mineral with an abundance of intergrown fluorite; this intergrowth resembles a myrmekitic texture (Fig. 3.11).
- Anhedral alkali feldspar: Extremely anhedral, 1 to 3 mm alkali feldspar composes 25-30% of the coarse grained mineral assemblage. These grains are thoroughly altered from rim to core

producing a variety of fine grained leucocratic material as well as sericite. The remaining alkali feldspar is perthitic and/or contains abundant tartan twinning.

- Anhedral aegirine: Highly altered, 0.5 to 3 mm, laths to stubby grains of anhedral aegirine compose 10-15% of the coarse-grained mineral assemblage. Most grains are completely altered to a fine grained, low birefringence, high relief mineral aggregate. Aegirine is the commonly associated with biotite, creating a sub-glomerophyritic texture.
- Biotite: Glomerophyritic, subhedral, 0.1 to 1 mm, aggregated biotite composes 25-30% of the coarse-grained mineral assemblage. Low degrees of alteration can be seen in some grains. Most biotite grains contain inclusions of a high relief, low birefringent mineral (Fig. 3.11).
- Titanite: Subhedral, often fractured, 0.5 to 2 mm titanite composes ~5% of the coarse-grained mineral assemblage. These grains contain a number of inclusions including biotite, alkali feldspar, and alteration products of aegirine.

Interstitial Material (25%)

Grains ranging in size between 0.01 to 0.1 mm compose the interstitial mineral assemblage. Subhedral to anhedral alkali feldspar, plagioclase, and biotite are the dominant minerals with smaller amounts of anhedral amphibole and nepheline. Small inclusions, most likely sericite, can be found throughout the alkali feldspar and plagioclase grains.

Specific Features

A few 0.5 to 1 mm grains of apatite are present within the interstitial material. These grains are euhedral and elongate. Although much of the surrounding material is highly altered, these grains do not contain any alteration products. Fluorite is part of the alteration assemblage of nepheline.

ESY-12

General Information

Sample ESY-12 is an inequigranular, highly altered nepheline syenite. Altered, 0.5 to 4 mm phenocrysts sit in a 0.01 to 0.2 mm dominantly leucocratic matrix. The phenocrysts consist of the following minerals: 1) anhedral, altered, 0.5 to 3 mm alkali feldspar, 2) 1 to 5 mm pseudomorphs of nepheline, 3) anhedral, highly altered 0.5 to 2 mm biotite and biotite aggregates, and 4) anhedral, 0.5 to 2 mm plagioclase. The matrix material is dominantly composed of 0.01 to 0.05 alkali feldspar, plagioclase, prismatic opaques, and possibly nepheline. Microphenocrysts of alkali feldspar and biotite uncommonly occur within the matrix material. In hand sample the weathered surface is light-brown to gray in colour. Surface features include 0.1 to 10 mm prismatic, milky white phenocrysts hosted in a fine grained matrix. On fresh surfaces there is a dark-gray matrix playing host to an assortment of phenocrysts. These include 1) prismatic, pink to white feldspar, 2) prismatic, 5 mm aggregate (possibly nepheline alteration), and 3) subhedral mafics (possibly biotite).

Mineralogy

Coarse-Grained Material (30%)

- Altered nepheline: Completely altered, 1 to 5 mm, subhedral nepheline pseudomorphs compose 35-40% of the coarse-grained mineral assemblage. The nepheline has been completely replaced by 0.1 to 0.5 mm aggregated cancrinite with associated fluorite (Fig. 3.12). Fractures present within these pseudomorphs have been in-filled by an orange to brown mafic mineral. These in-filled fractures cause an orange staining in areas of the grain.
- Alkali feldspar: Anhedral, 0.5 to 3 mm alkali feldspar composes 30-35% of the coarse grained mineral assemblage. Abundant alteration-related inclusions are evident from the dirty-looking

colourless grains in PPL as well as small, high birefringence minerals in XPL. Alteration to calcite appears on the grain boundary. Both simple Carlsbad twins as well as tartan twinning are visible in these crystals.

- Anhedral biotite: Anhedral, 0.5 to 2 mm biotite is present as single crystals or glomerophenocrysts and composes 20-30% of the coarse grained mineral assemblage. Most grains contain alteration products of fine grained masses. An association between biotite and prismatic opaques is present in most glomerophyritic aggregates (Fig. 3.12).
- Anhedral plagioclase: Few anhedral, 1 to 3 mm plagioclase grains compose 3-5% of the coarse-grained mineral assemblage. Internal alteration products, most likely fine grained sericite, occur throughout these grains. Polysynthetic twinning occurs in all grains.

Matrix Material (70%)

The matrix material is leucocratic and comprises 0.01 to 0.05 alkali feldspar, plagioclase, prismatic opaques, and possibly nepheline as well as microphenocrysts of alkali feldspar and biotite. The alkali feldspar microphenocrysts have a number of internal alteration products, mostly fine grained sericite. Purple staining (fluorite representation) is present in 40-50% of the matrix material.

Specific Features

Calcite-rich veins, ~0.2 mm wide, cut through alkali feldspar phenocrysts. Within these veins are anhedral opaque minerals, composing 20% of the vein. Again, fluorite occupies the groundmass.

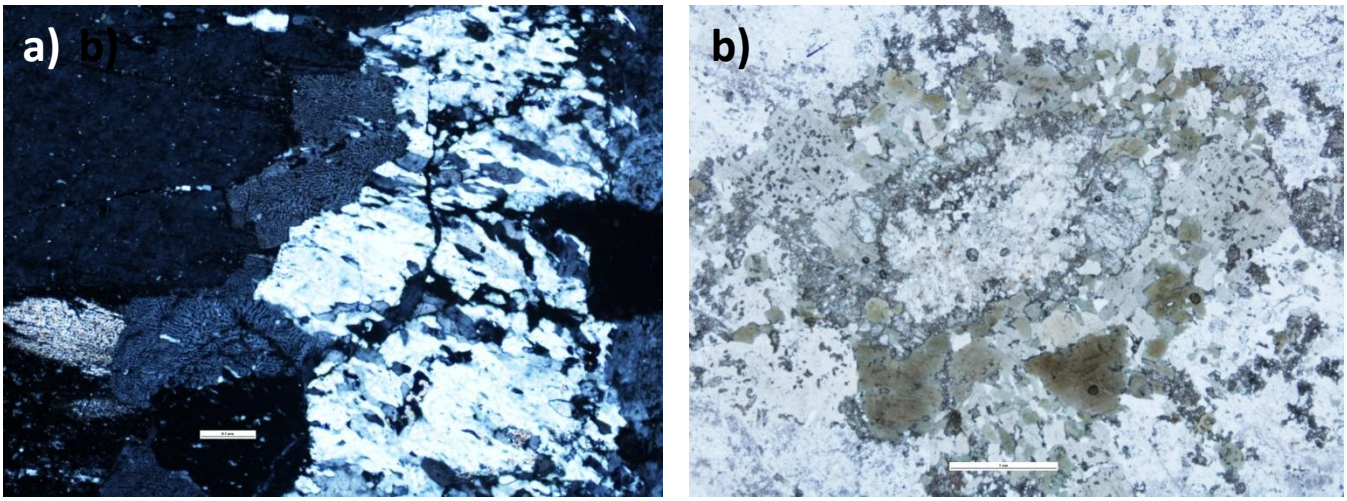

Figure 3.11: Microphotograph of sample ESY-11. **a)** A myrmekitic like texture found within the grain boundary of altering nepheline and the replacement product of cancrinite. The alteration is composed of an unknown felsic mineral and fluorite. **b)** Sub-glomophyritic biotite surrounding a completely altered aegirine pseudomorph which is now composed of a low birefringent, high relief mineral.

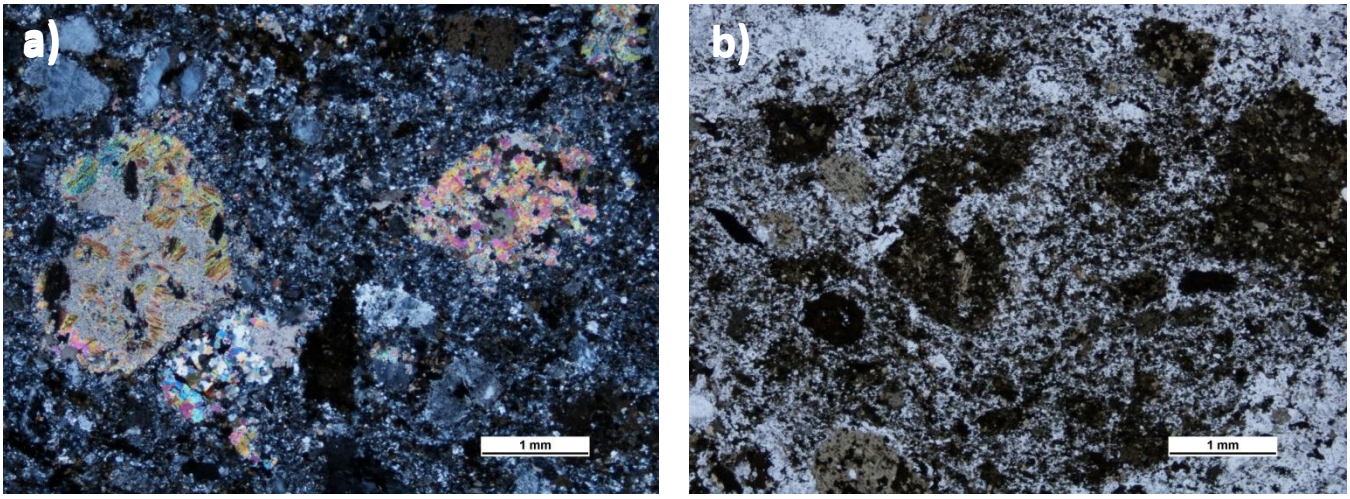

Figure 3.12: Microphotograph of sample ESY-12. **a)** Three pseudomorphs of nepheline now composed of cancrinite. A relationship between 0.25 mm grains of cancrinite and very fine-grained sericite/carbonate is shown within these grains. **b)** Glomerophyric aggregate biotite and very fine-grained amphibole form a cluster of mafic grains, creating an overall local cumulate texture.

ESY-13

General Information

Sample ESY-13 is a heavily altered, coarse-grained nepheline syenite. The grains in this sample range in size from 1 to 5 mm with minimal amounts of interstitial material between larger grains. The sample is dominated by nepheline pseudomorphs, now aggregated cancrinite, as well as perthitic alkali feldspar. Biotite appears as glomerophyritic masses, often associated with euhedral to subhedral, 1 mm magnetite. Plagioclase is present as ~0.5 mm grains that have extremely anhedral grain boundaries. The small amount of interstitial material appears to be fibrous, altered, highly anhedral feldspars with 0.01 to 0.05 mm, prismatic, fragmented biotite. In hand sample the weathered surface is light brown in colour. The surface contains pits which range in size due to the proximity of adjacent prismatic, protruding feldspar grains. These grains range in size from 5 to 20 mm. Similarly sized opaque grains, possibly biotite, are less abundant along this surface. Fresh surfaces show similar mineralogy but with three phenocrysts which are: 1) Prismatic milky-white (feldspar or nepheline), 2) subhedral, 1 to 5 mm, pink feldspars, and 3) black, subhedral aggregate grains (most likely biotite).

Mineralogy

Coarse-Grained Material (90%)

- Nepheline pseudomorphs: Anhedral, 1 to 5 mm, completely altered nepheline composes nearly 50% of the coarse-grained mineral assemblage. The nepheline has been completely replaced by 0.05 to 0.5 mm aggregated cancrinite and by anhedral sodalite.
- Alkali feldspar: Perthitic, 0.5 to 5 mm alkali feldspar composes 30-35% of the coarse-grained mineral assemblage within this sample. These crystals have highly irregular grain boundaries and

appear ‘dirty’ in PPL. These two features are due to alteration of the grains. Simple Carlsbad twins are present in most grains while tartan twinning appears in grains that are less perthitic.

- Aggregated biotite: Anhedral, 0.5 to 3 mm, glomerophyritic aggregates of biotite compose 15-20% of the coarse-grained mineral assemblage. These grains are highly irregular along grain boundaries. Small inclusions within the grains are composed of carbonate minerals and prismatic opaques. Many of the aggregates are associated with 1 to 2 mm opaque grains.
- Anhedral plagioclase: Anhedral, 0.5 to 1 mm grains of plagioclase compose 5-10% of the coarse-grained mineral assemblage. These grains contain are notably altered, containing carbonate and sericite alteration minerals concentrated both along the boundary and within the core. Polysynthetic twinning is prominent throughout these grains.

Interstitial Material (10%)

Minor amounts of interstitial material are present in this sample. The grains range in size from 0.01 to 0.5 mm. The material is dominantly composed (90%) of feldspar (which oddly looks fibrous) with minor amounts of anhedral amphibole, prismatic and fragmented biotite, and alteration products of fine-grained sericite. Small amounts of fluorite are present in some areas, evident as a purple colouration.

Specific Features

Aside from the fluorite, which is associated with the interstitial material, there are a number of calcite veins running through the alkali feldspar grains. The veins are composed of ~0.1 mm grains of aggregated calcite. They are carrot-shaped, being ~0.5 mm wide at the grain boundary and coming to a peak near the core of the host grain. Some of the veins persist completely through the grain, from boundary to boundary. The cancrinite material has an atypical texture in that it appears to have a

directional flow pattern, especially when surrounding coarse grained feldspar (Fig. 3.13). Associated with the cancrinite are areas of isotropic material, most likely alteration of nepheline to sodalite.

ESY-14

General Information

Sample ESY-14 is an extremely altered, poikilitic, carbonatized nepheline syenite. The sample is dominated by a fine grained, leucocratic groundmass (fine grained sericite, cancrinite, and carbonate) hosting highly altered alkali feldspar, plagioclase, completely altered nepheline, and subhedral titanite. The anhedral phenocrysts range in size from 1 to 10 mm. Most phenocrysts are clumped into groups, creating a glomerophyritic texture. In hand sample the weathered surface is light grey-yellow in colour. The surface comprises many different prismatic grains. The only distinguishing factor among these is that one group of phenocrysts is white while the other is dark-gray. Fresh surfaces have milky white, 1 to 10 mm phenocrysts that gradually alter to a dark brown material. These are hosted within a dark-green to gray matrix (Fig. 3.14).

Mineralogy

Coarse-Grained Material (20%)

- Nepheline: Anhedral, completely altered, ~0.5 mm nepheline composes 10-15% of the phenocryst assemblage. The grains are now composed of anhedral, 0.05 to 0.1 cancrinite with associated with fluorite.
- Alkali feldspar: Extremely altered, anhedral, 1 to 10 mm, glomerophyritic alkali feldspar composes 75-80% of the phenocryst assemblage. The grains contain a number of alteration inclusions which are most likely sericite and possibly carbonate. The perthitic texture is present throughout all grains. Both simple Carlsbad twins and tartan twins are found throughout the

grains. Alkali feldspars are associated with subhedral opaques and brown, extremely fine-grained unknown mafic minerals.

- Plagioclase: Anhedral, 0.5 to 3 mm plagioclase composes 10-15% of the phenocryst assemblage. These grains have irregular grain boundaries as well as a number of alteration inclusions. These inclusions are fine-grained sericite and possibly small amounts of carbonate. Polysynthetic twinning is common.
- Titanite: Anhedral, ~1 mm titanite composes ~5% of the total phenocryst assemblage. These grains contain many fractures that caused the grain to split into fragments. The fractures are in-filled by the surrounding matrix material.

Interstitial Material (80%)

The interstitial material dominantly consists of leucocratic minerals. The material is a mixture of fine grained sericite, carbonate, and cancrinite. Anhedral amphibole composes 5-10% of the matrix material. The remnants of almost completely altered feldspars appear as 0.05 mm grains within the matrix. Associated with these are 0.01 mm prismatic opaques.

Specific Features

Purple isotropic material (fluorite) surrounds the matrix minerals. Carrot shaped veins are again present within the alkali feldspar. However, these are not carbonate veins. They are made of the same brown alteration products that surround the alkali feldspar phenocrysts.

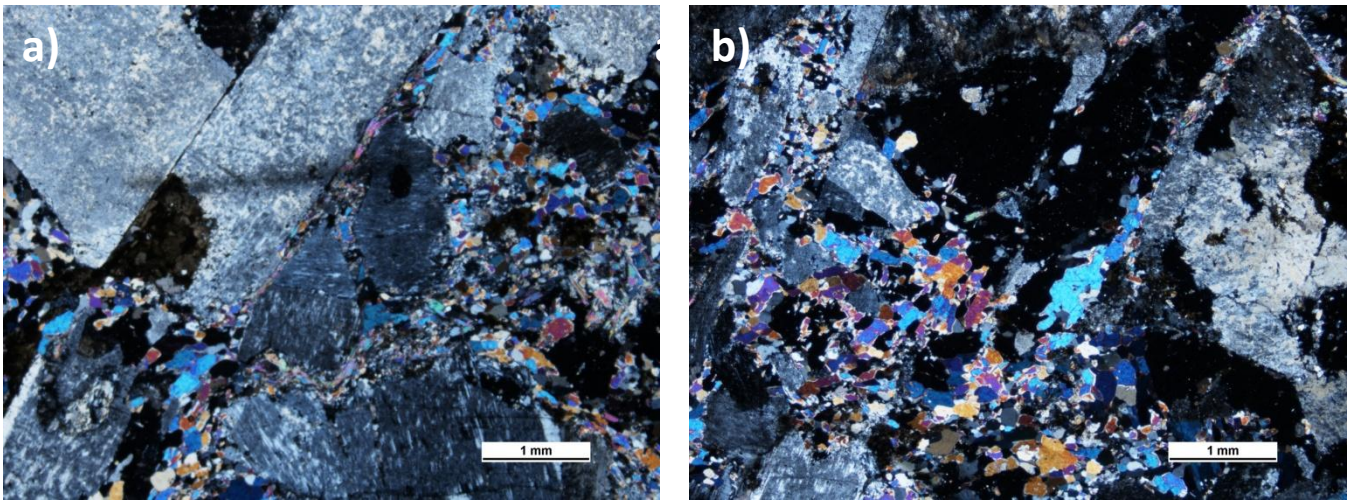

Figure 3.13: Microphotograph of sample ESY-13 show the relationships of cancrinite with surrounding coarse grained material. **a)** Cancrinite is smeared between coarse grained alkali feldspars. Both anhedral, elongate cancrinite and subhedral blocks of cancrinite are present. **b)** In the same section subhedral, blocks of cancrinite are present between coarse-grained alkali feldspar. No smearing of these grains is present. To the top of this panel are isotropic grains of sodalite.

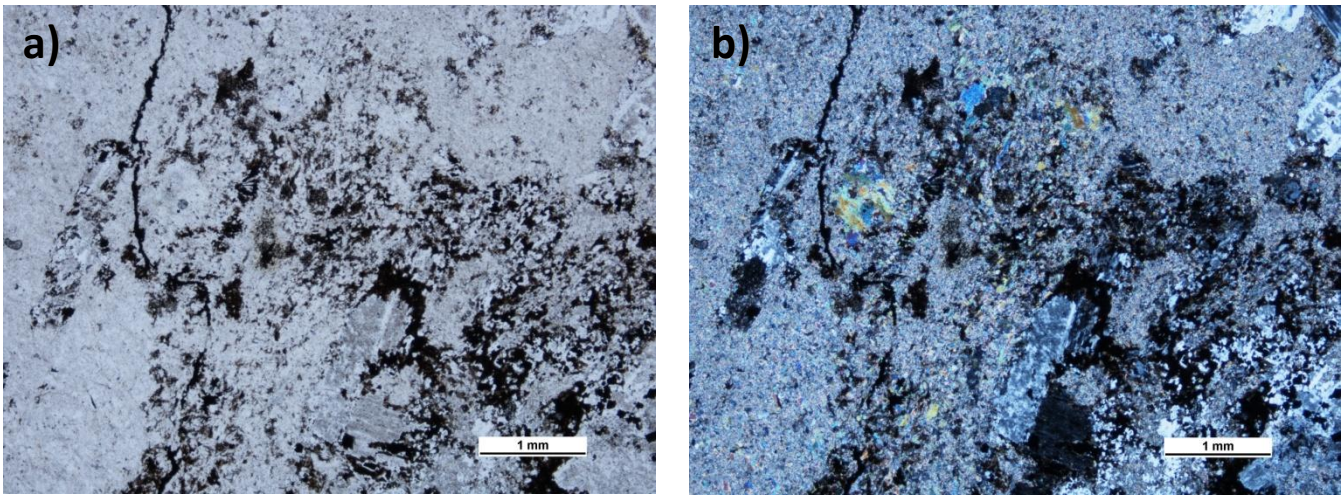

Figure 3.14: Microphotograph of sample ESY-14 show the overall mineralogy and relationships between grains. **a)** is taken in PPL and panel **b)** in XPL. Anhedral grains of alkali feldspar, biotite, cancrinite aggregates, and magnetite are found within a very fine-grained sericite and carbonate matrix. A single veins composed of opaque material (dominantly magnetite) partially runs through the sample and disperses to the bottom.

3.1.2 *Phonolites*

PH-1

General Information

Sample PH-1 is an altered aphanitic phonolite containing a variety of phenocrysts. Three types of phenocryst are present 1) large subhedral grains of plagioclase, 2) dark-green aggregates of secondary mica and amphiboles forming prismatic shapes, and 3) colourless, pseudomorphic aggregates of white mica, calcite, and an epidote mineral (?). Some phenocrysts appear as broken fragments. The matrix is fine grained with a grain size between 10 and 50 μm. It is dominated by granular felsic minerals (alkali feldspar, rare plagioclase, possibly some nepheline) (~70%) and prismatic and anhedral grains of mafic minerals (mica, possibly amphibole) making ~30% of the matrix. Calcite and sericite are also present in the matrix in minor amounts. The phenocryst and the matrix mineral assemblage are similar. In hand specimen a pitted, weathered, light gray to brown surface dominates. Within the centers of the weathered pits are mafic grains. Two sets of leucocratic veins cross cut each other at approximately 55°. One set protrudes from the surface while the other set is flush and composed of carbonates. On the fresh surfaces, mafic phenocrysts (0.5-5 mm in size) are enclosed by a matrix rim that is more leucocratic than the surrounding melanocratic matrix.

Mineralogy

Phenocrysts (15-20%)

- Plagioclase: Single 5 mm subhedral rounded grains of plagioclase compose 5-10% of the phenocryst assemblage. Alteration products include very fine-grained inclusions of carbonate and white mica. Polysynthetic twinning is only visible in the least altered regions.

- Mafic aggregates: Glomerophyritic grains of 0.5 to 3 mm dark green mafic aggregates make ~15% of the phenocryst assemblage. Secondary mica and amphibole form elongated prismatic shapes with highly altered grain boundaries. The alteration prevents the exact identification of these minerals as many optical properties are unusable (Fig. 3.15).
- Calcite-sericite aggregates: Approximately 80% of the phenocryst assemblage is composed of completely altered, 1 to 5 mm, prismatic pseudomorphs composed of calcite, sericite, and an epidote mineral (?). These grains contain many optical properties of t epidote group, which include birefringence and relief. However, not all the properties for any epidote mineral filled the requirements for exact identification (Fig. 3.15).

Matrix (80-85%)

The groundmass dominantly (70%) consists of granular aggregates of 0.1 mm leucocratic material (alkali feldspar with rare nepheline and plagioclase) with lesser amounts (30%) of similarly sized anhedral mafic material (mica and possibly amphibole). Minor amounts of calcite, sericite, and magnetite with ilmenite/hematite exsolution lamellae are also present. Adjacent to and surrounding the mafic aggregate glomerophenocrysts are 0.5 mm wide leucocratic rich groundmass rims. These rims are composed solely of alkali feldspar.

Specific Features

Two types of veins are present in thin section. The <0.5mm leucocratic veins (alkali feldspar, plagioclase, and nepheline) have two orientations which intersect each other at ~55°. A second vein type composed of calcite is ~1mm wide. These veins run parallel to one set of the leucocratic veins and cuts the second set.

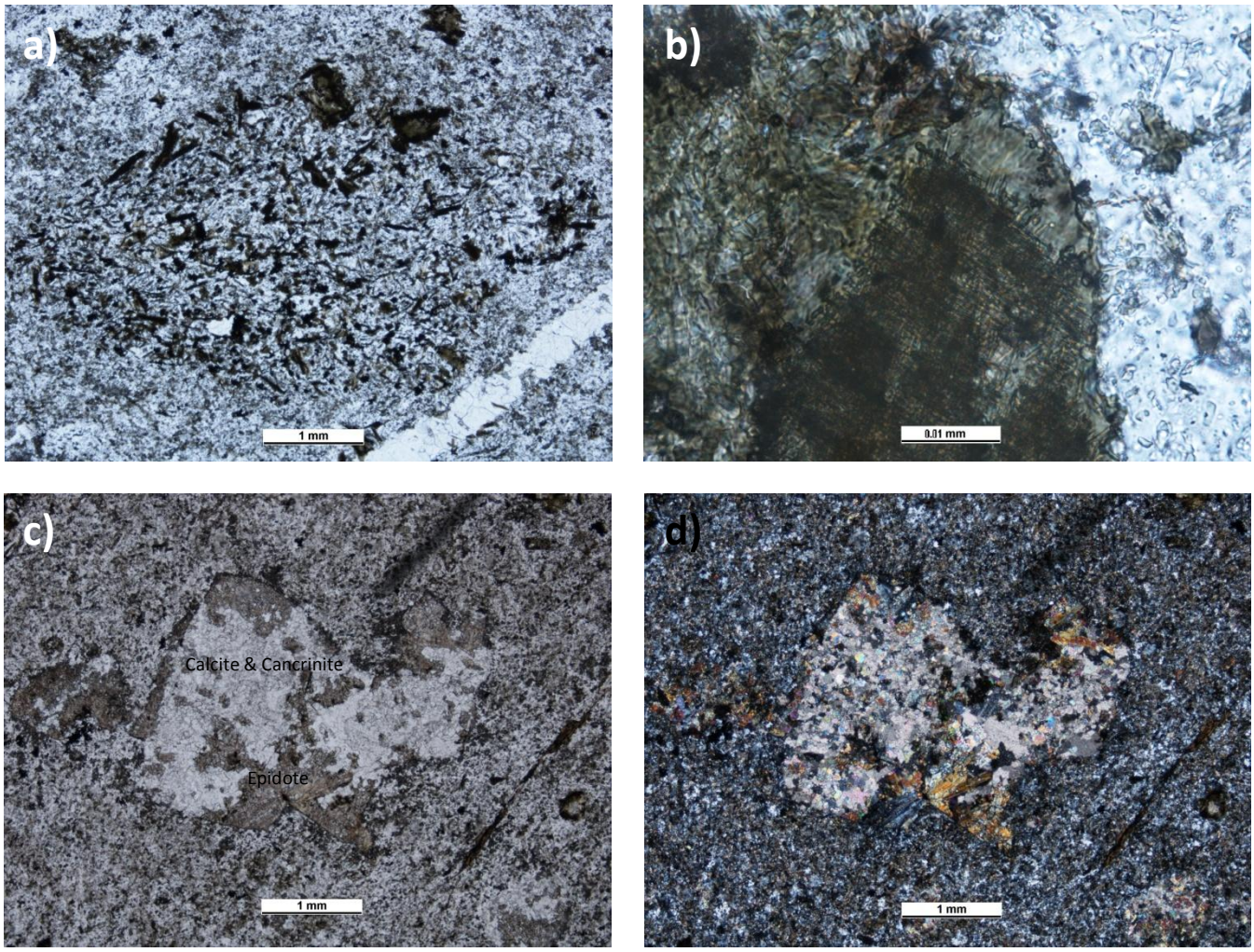

Figure 3.15: Microphotographs of sample PH-1. **a-b)** Diamond-shaped pseudomorph of dark-green mafic aggregates in PPL (a) and XPL (b). Some grains show cleavage at 120°-60° suggesting secondary amphibole (seen in panel **b)**). c-d) A pseudomorph composed of an aggregate of calcite (extremely high birefringent mineral), smaller cancrinite (medium birefringent mineral), and a high relief mineral resembling epidote (c – PPL, d – XPL).

PH-2

General Information

Sample PH-2 is an aphanitic phonolite bearing phenocrysts in a fine-grained matrix. The four phenocryst types include: 1) poikilitic prismatic subhedral grains of alkali feldspar, 2) prismatic apatite with anhedral grain boundaries (Fig. 3.16), 3) colourless pseudomorphic aggregates of both very fine-grained and fine-grained white mica with some cancrinite (?), and 4) rare relatively small phenocrysts of plagioclase. Nearly all colourless phenocrysts have a dirty appearance in plain polarized light. The matrix is fine-grained with a grain size between 0.5 to 0.01 mm. It is dominated by felsic (alkali feldspar, nepheline, and lesser plagioclase), anhedral microphenocrysts and aggregated white mica making 70% of the matrix, and contains laths of ilmenite with minor amounts of anhedral amphibole comprising the remainder. In hand sample the weathered surface is gray to light-brown in colour. Sparse white to light brown, phenocrysts 1 cm in length are present along this surface. On fresh surfaces a dark-gray matrix contains phenocrysts (0.1 to 10 mm). These phenocrysts are prismatic rose-pink, prismatic dark-gray, or prismatic with a glassy lustre.

Mineralogy

Phenocrysts (20-25%)

- Alkali Feldspar: Colourless, dirty looking, 1 to 2 mm sized alkali feldspar compose ~30% of the phenocryst assemblage. Aggregated white mica and rare, very fine-grained, hexagonal orange to brown unidentifiable grains appear as inclusions within the phenocryst. Carlsbad twinning is found in half of the phenocrysts. Alteration can be noted throughout the grain, from core to rim.

- Apatite: Dirty looking, ~1mm sized grains of apatite compose ~5% of the phenocryst assemblage. Inclusions consist of aggregated white mica and colourless grains too small to identify. Degree of alteration is similar to that found in alkali feldspar (Fig. 3.16).
- Colourless aggregate: Pseudomorphic aggregates of past nepheline are dominantly composed of very-fine grained white mica with minor amounts of anhedral sericite and cancrinite and compose ~65% of the phenocryst assemblage. All larger, identifiable material has parallel extinction. Thin, sub-parallel, mafic veins are found in one third of these phenocrysts and are often associated with yellow to brown staining of the juxtaposed material.
- Plagioclase: Rounded, prismatic, ~0.5 mm phenocrysts of plagioclase compose ~1-2% of the phenocryst assemblage. Colourless inclusions (white mica?) are spotted throughout the phenocrysts. Polysynthetic twinning sparsely appears while the remainder of the grain is highly altered.

Matrix (75-80%)

The groundmass is composed (60%) of 0.1 to 0.5 mm, prismatic microphenocrysts of twinned alkali feldspar, nepheline, and few plagioclase grains. Very fine-grained aggregated white mica, identical to the pseudomorphs, composes 15% of the matrix. Randomly oriented interstitial laths of ilmenite and very few anhedral amphibole grains form a framework around the leucocratic microphenocrysts and compose the remaining ~15% of the matrix.

Specific Features

A single, 0.5mm wide leucocratic vein runs continuously through the section. Poikilitic alkali feldspar, elongate white mica aggregates, and possibly nepheline are found in this vein. Also found in the sample are 5 to 20 μm, hexagonal, orange to brown grains (Fig. 3.16). These show no affinity with any other material as they appear in many phenocrysts and in the matrix.

PH-3

General Information

Sample PH-3 is a porphyritic phonolite containing four types of phenocrysts: 1) altered feldspar pseudomorphs, 2) prismatic to lens shaped pseudomorph aggregates of cancrinite and very fine grained white mica, 3) poikilitic, prismatic apatite, and 4) elongate aggregates of altered mafic (amphibole and biotite) material. The matrix is fine grained with a grain size between 30 to 60 μm. It is composed of ~60% anhedral white mica and alkali feldspar, ~40% amphibole laths, and ~1-5% prismatic magnetite. A subtle purple colour persists in much of the matrix material. The mafic material defines a trachytic texture in the sample. In hand sample the featureless weathered surface is gray to light brown. Fresh surfaces has a mild-gray colour which contains four phenocrysts: 1) 10 mm, rose pink coloured grains, 2) 10 mm, milky white anhedral grains, 3) 5 mm, colourless, prismatic grains, and 4) <0.1 mm mafics.

Mineralogy

Phenocrysts (25-30%)

- Altered feldspar pseudomorphs: A single 8 mm long, completely altered feldspar phenocryst consists of fine grained feldspar, 0.5mm cancrinite, and anhedral sodalite. This grain composes 10% of the phenocryst assemblage.
- Cancrinite and mica aggregates: Many 1 to 10 mm lenses and prismatic pseudomorphs composed of aggregated cancrinite and white mica compose 75% of the phenocryst assemblage. Some feldspar or nepheline is present as anhedral grains but identification is difficult due to complete alteration (Fig. 3.17).

- Apatite: Poikilitic, 2 to 3 mm elongate grains of apatite compose ~8% of the phenocryst assemblage. Inclusions consist of high birefringence grains which are too small for identification. These grains are also broken perpendicular to their length, creating a basal parting texture.
- Mafic aggregates: Fine grained, altered aggregated biotite and amphibole define 5 mm long by 0.5 mm wide lenses of mafic phenocrysts. These grains constitute ~7% of the phenocryst assemblage.

Matrix (70-75%)

The groundmass is composed of (60%) anhedral grains of alkali feldspar and aggregated white mica with (40%) laths of amphibole and minor prismatic polygons of magnetite. A trachytic texture in the groundmass is defined by the sub-parallel orientation of amphibole laths and prismatic, anhedral alkali feldspar. In addition to this flow structure, some of the pseudomorphed phenocrysts are apparently deformed parallel to the orientation of the groundmass.

Specific Features

Two sets of nearly perpendicular veins are present. The first consists of fine grained leucocratic (feldspar and calcite) material that cuts all matrix and phenocryst minerals. The second vein features a transition from aggregated carbonates to yellow fluorite. This vein truncates the first vein. Within the groundmass, single purple fluorite grains as well as an overall purple tinge of many areas of the matrix are present. An isotropic mineral within the feldspar, or possibly nepheline, contains an isotopic mineral (sodalite?) (Fig. 3.17). Again, 5 to 20 μm, hexagonal, orange to brown grains are randomly distributed in the groundmass.

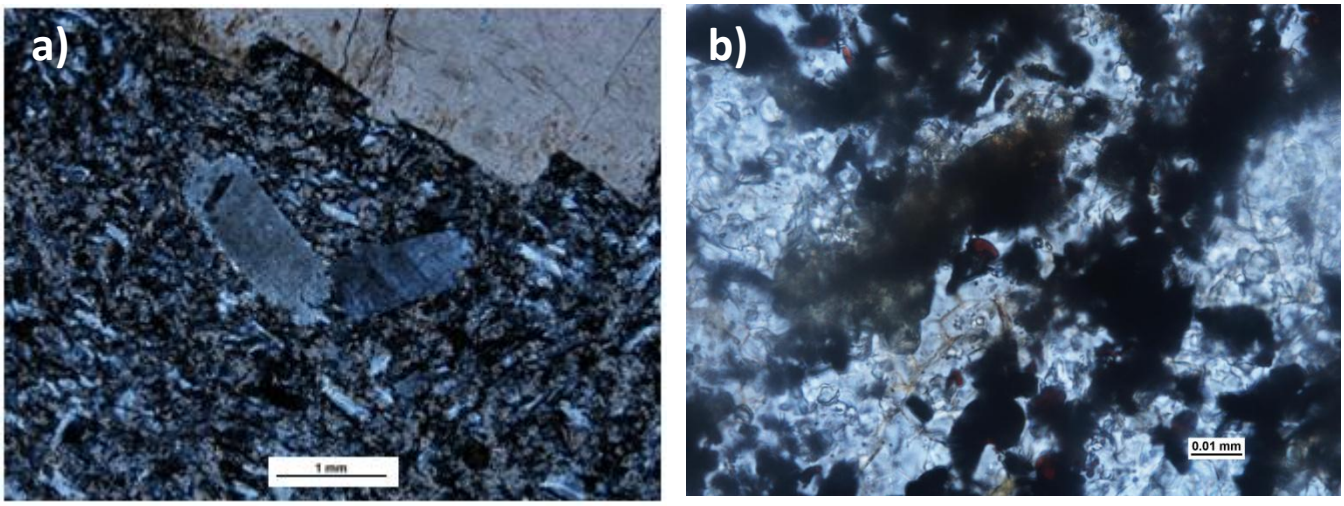

Figure 3.16: Microphotographs of sample PH-2. **a)** Two subhedral apatite micro-phenocrysts within the alkali feldspar-rich matrix (XPL). **b)** Near hexagonal, ~0.025 mm, orange to brown grains found within both the matrix and within the prismatic pseudomorphs (shown here in the matrix) (PPL).

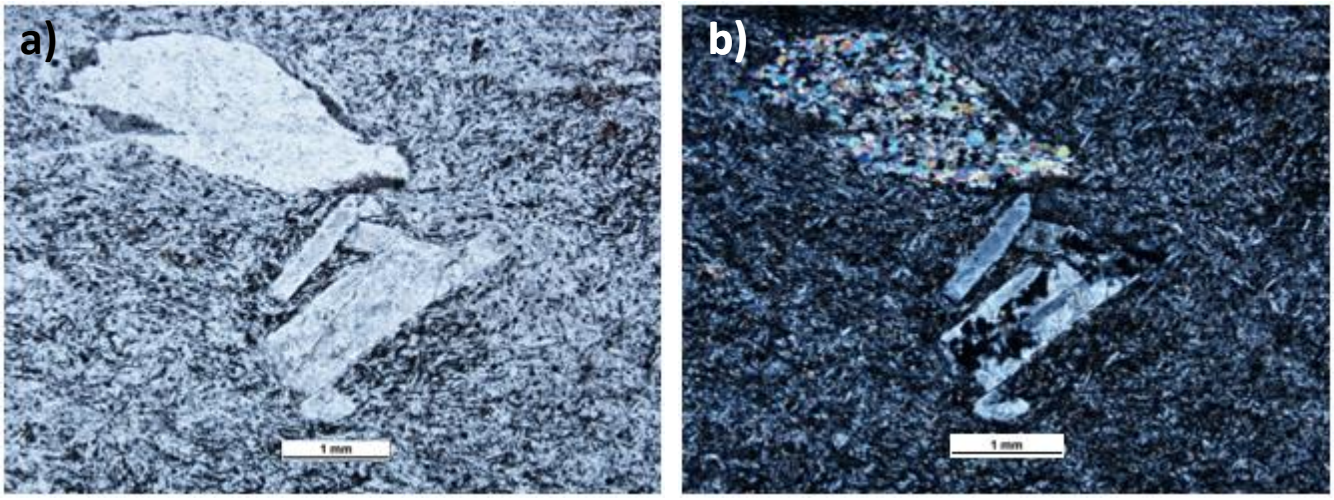

Figure 3.17: Microphotograph of sample PH-3 taken in PPL in panel **a)** and XPL in panel **b)**. **a)** Two colourless phenocrysts sitting in a trachytic matrix. The upper phenocryst has lens shap while the lower is near-prismatic. **b)** The upper phenocryst is formed of an aggregate of subhedral to anhedral cancrinite. The lower phenocryst is an alkali feldspar with an isotropic core (possibly sodalite).

PH-5

General Information

Sample PH-5 is a porphyritic phonolite. It contains four distinct phenocrysts: 1) prismatic, poikilitic alkali feldspar, 2) poikilitic anhedral apatite, 3) highly altered aegirine, and 4) massive lenses containing aggregated cancrinite ± alkali feldspar, fluorite, calcite, sericite, aggregated white mica, and titanite. The phenocrysts vary greatly in terms of structure. Some appear as prismatic polygons while others are smeared out lenses. The matrix consists of fine grained material between 30 to 60 μm. Laths of very fine grained amphibole compose ~55% of the matrix material while the remaining 45% is anhedral alkali feldspar, white mica, and possibly small amounts to nepheline. The mafic material in the matrix defines a trachytic flow texture within the sample. In hand sample the weathered surface is gray to light-brown. Covering the surface are elongate pits between 1 to 20 mm and protruding prismatic phenocrysts between 5 to 15 mm. Fresh surfaces have a gray to green matrix which host three phenocryst types: 1) 0.5-2 mm elongate, mafic grains, 2) parallel elongate light pink lenses, and 3) prismatic, milky-white grains.

Mineralogy

Phenocrysts (30%)

- Alkali feldspar: Prismatic grains of 1 to 3 mm alkali feldspar compose 10% of the phenocryst assemblage. The grains contain an abundance of high birefringence inclusions that appear to be small white micas. The circular centers of grains contain microcline twinning while the rims have no twinning. Overprinting Carlsbad twins are present in some of the alkali feldspar grains, in which the core and rim of the feldspar has a common twin (Fig 3.18).

- Apatite: Poikilitic, 0.5 to 2 mm elongate grains of apatite compose 5% of the phenocryst assemblage. Unidentifiable, high birefringence inclusions are distributed equally through the grains (Fig. 3.18).
- Aegirine: Highly altered 1 to 3 mm laths and 1 mm stubby, eight-sided aegirine grains compose 10% of the phenocryst assemblage. Some grains contain a fresh core used for identification while the exterior of the grains have been completely altered to a fine grained material.
- Massive lenses: A majority of the lenses are 2 to 3 mm in length and are composed of 0.1 mm cancrinite. The larger lenses are 3 to 15 mm in length and are composed of a cancrinite with or without the following minerals: alkali feldspar, fluorite, calcite, sericite, aggregated white mica, and titanite. The larger lenses are highly altered and contain a varying set of minerals. Together the lenses compose 75% of the phenocryst assemblage.

Matrix (70%)

The groundmass contains 55% mafic amphibole laths and 45% interstitial anhedral alkali feldspar, white mica, and possibly nepheline and calcite. Similarly to PH-3, a trachytic texture in the groundmass is defined by the sub-parallel orientation of the amphibole laths. Phenocryst lenses are also elongate in the flow direction of the matrix (Fig 3.18).

Special Features

In areas where the trachytic groundmass is protected behind a larger phenocryst, the dominant mafic minerals of the groundmass are overtaken by microphenocrysts of alkali feldspar. Large (1 mm) fluorite phenocrysts are found within the larger phenocryst lens.

PH-6

General Information

Sample PH-6 is a porphyritic phonolite. Three distinct phenocrysts are present in the sample: 1) aggregates of fine grained anhedral biotite with associated magnetite, 2) felsic aggregates of sericite, alkali feldspar, plagioclase, nepheline, calcite, and very fine-grained white mica, and 3) poikilitic alkali feldspar. The matrix is composed of both felsic and mafic minerals which are between 20 and 80 μm in size. The leucocratic grains consist of poikilitic, elongate grains of alkali feldspar and anhedral prismatic nepheline and compose ~75% of the matrix. The other 25% is anhedral biotite, amphibole, and euhedral magnetite with exsolution lamellae of ilmenite/hematite. In hand sample the weathered surface is brown. It contains 1 cm wide pits and 0.1 to 10 mm elongate mafic phenocrysts. Fresh surfaces show a gray matrix with red staining. Three phenocrysts are present: 1) 1 to 20 mm white prisms, 2) 1 to 20 mm white anhedral elongates, and 3) 0.1 to 10 mm mafic elongates.

Mineralogy

Phenocryst (10-15%)

- Mafic aggregates: Consisting of 0.05 mm aggregated grains of biotite and 0.05 to 0.5 mm grains of magnetite, the mafic aggregates are 1 to 3 mm in size and compose ~30% of the phenocryst assemblage. The biotite aggregate is highly altered, often showing anhedral grain boundaries.
- Felsic aggregates: Composing ~65% of the phenocryst assemblage the felsic aggregates appear as drawn-out phenocryst, 2 to 20 mm in length and 2 to 3 mm in width (Fig 3.19). The felsic minerals that make up these phenocrysts are listed in order of most to least abundant: fine-grained and altered white mica, sericite, alkali feldspar, plagioclase, nepheline, and calcite.
- Alkali Feldspar: Composing the final 5% of the phenocryst assemblage, the poikilitic, anhedral alkali feldspar is between 0.5 to 2 mm in size. Inclusions within the grain include fine grained white mica and possibly some carbonate along the grain boundary.

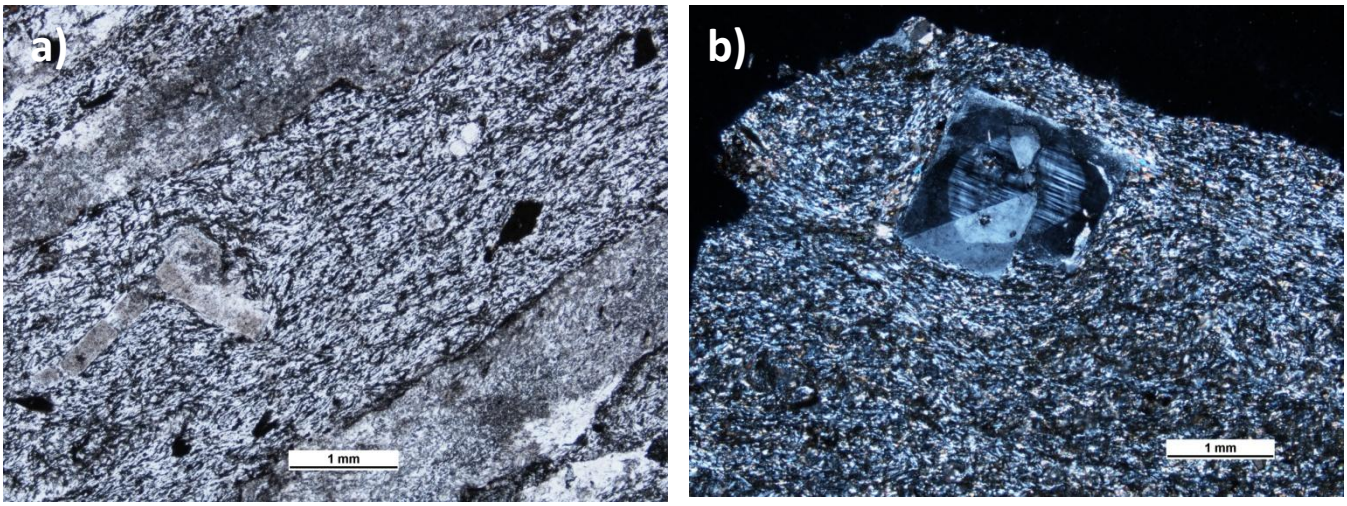

Figure 3.18: Microphotograph from sample PH-5. Panel **a)** is taken in PPL and panel **b)** is taken in XPL. **a)** Two anhedral prismatic apatite phenocrysts are enclosed by a trachytic groundmass. The apatite grains are 'dirty' as they contain a number of alteration inclusions. Two other colourless, hexagonal, 0.25 mm grains are present to the upper-right of the photos center. These are also apatite shown along the basal edge. **b)** A zoned alkali feldspar surrounded by a trachytic groundmass. A simple twin is shown with the grain.

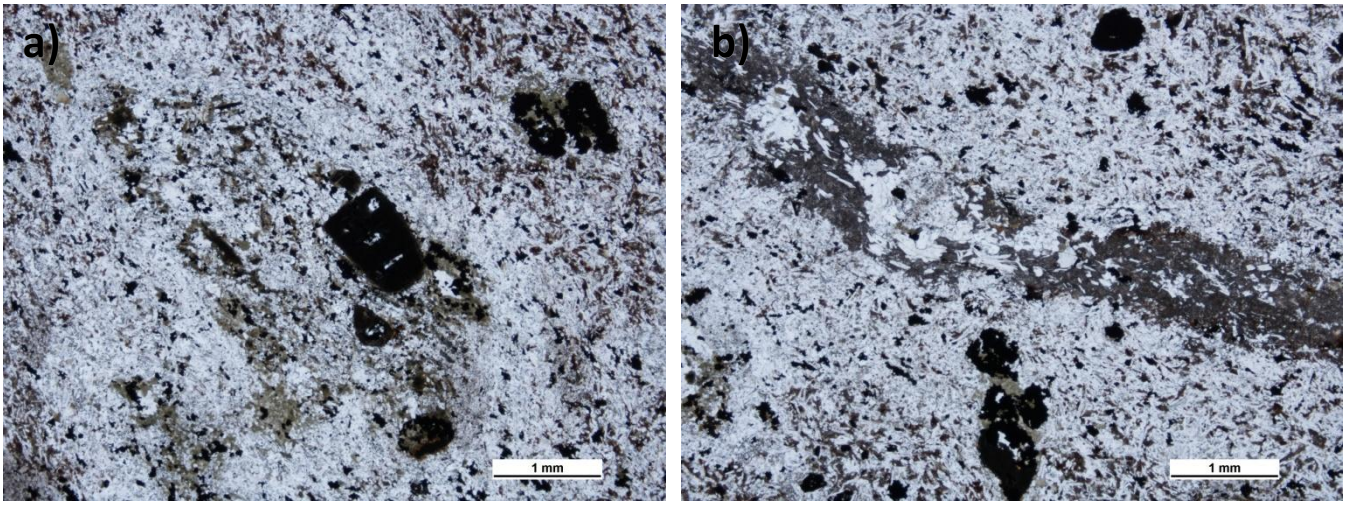

Figure 3.19: Microphotograph from sample PH-6. Both panels have been taken in PPL. **a)** Glomeroporphyritic, anhedral, fragmented biotite grains form clusteres within the groundmass. Surrounding these clusteres are mafic poor rims within the groundmass. **b)** Altered, felsic phenocrysts are elongated from left to right in this photo. The phenocryst has been stretched and now forms an irregular shape with a poor grain boundary. The phenocryst is composed of fine-grained sericite, cancrinite, fragmented biotite, magnetite, and fragmented feldspar. Near the bottom of the figure biotite and anhedral mafics are again forming into a mineral cluster.

Matrix (85-90%)

The groundmass consists of laths of alkali feldspar, anhedral nepheline, and fine grained white mica (75%), and anhedral biotite, elongate amphibole, and euhedral magnetite (25%). The grains range in size from 20 to 80 µm. Around all phenocrysts, especially mafic aggregates, are felsic rims of matrix material composed of relatively larger microphenocrysts of alkali feldspar with no mafic material (Fig 3.19). A sub-trachytic texture, defined by the mafic groundmass material, can be seen around the edge of some phenocrysts.

PH-7

General Information

Sample PH-7 is a porphyritic phonolite containing coarse-grained, highly altered, leucocratic phenocrysts within a fine-grained matrix. The four phenocrysts present in this sample are: 1) highly altered alkali feldspar, 2) complete pseudomorphs composed of calcite and fine-grained white mica, 3) rounded, anhedral grains of aegirine, and 4) coarse, anhedral magnetite/ilmenite. All phenocrysts appear highly altered with little to no remaining fresh surfaces. The matrix is fine grained with a grain size between 0.05 to 0.2 mm. It is dominated by aggregates of white mica and alkali feldspar (possibly some plagioclase) (70%) and anhedral amphibole with prismatic magnetite/ilmenite making up the remaining 30%. Small amounts of calcite and rare unidentifiable orange grains are sparsely present within the sample. In hand sample the weathered surface is stained light brown. Sharp exposures of dirty white 5 to 20 mm prisms are present along this surface. The fresh surface has an orange to brown aphanitic matrix. The phenocrysts seen on the weathered surface are also visible on fresh surfaces in addition to <1mm mafic, high lustre phenocrysts. Thin veins that are approximately 0.5 mm in width run sub-parallel to one another through both the hand sample and thin section. A single 2 cm wide, mafic

vein runs perpendicular and cuts through the thinner veins. Moving toward the large vein, the matrix material progressively becomes finer and develops a deeper orange to brown colour.

Mineralogy

Phenocrysts (5-8%)

- Alkali feldspar: Two 2 to 3 mm grains of highly altered alkali feldspar compose ~30% of the phenocryst assemblage. Although both grains are alkali feldspar their appearance varies. One grain contains an assortment of nearly parallel mafic veins with orange staining. The other grain contains a circular core with polysynthetic twinning (plagioclase) with a featureless rim. A large Carlsbad twin, forming a triangular pattern, is present in the other alkali feldspar grain.
- Calcite and mica pseudomorphs: The calcite and white mica pseudomorphs appear identical to those from other phonolite samples with this pseudomorph type. The sole difference appears to be the lack of any medium- to coarse-grained material. These pseudomorphs compose 40% of the phenocryst assemblage.
- Anhedral aegirine: The aegirine forms rounded medium-sized grains between 0.5 and 1.5 mm. These compose 10% of the phenocryst assemblage.
- Magnetite/ilmenite: Anhedral and euhedral grains of 0.5 to 2 mm magnetite compose the remaining 20% of the phenocryst assemblage. Under reflected light the grains have an exsolution texture in which ilmenite/hematite grow within magnetite.

Matrix (92-95%)

The groundmass is composed of 70% white mica and alkali feldspar and 30% anhedral amphibole and magnetite/ilmenite. The white mica and alkali feldspar form an immense mass of grains that are often indistinguishable from one another. Adjacent to some phenocrysts and to a thick vein are

changes within the groundmass, including an overall decrease in grain size, an intensification of orange to brown discolouration, and enrichment in felsic minerals.

Specific Features

Two sets of veins running perpendicular to one another are present. Both sets are mafic in composition. The thin 0.5 mm wide veins contain a massive infill of unidentifiable mafic material and associated magnetite/ilmenite. These are cut by a perpendicular 2 cm wide mafic vein. This vein is composed of a variety of minerals that include aegirine, biotite, magnetite, and calcite. A rare purple tint from fluorite in the groundmass is present along the edge of the slide, farthest away from the larger vein.

3.2 *Accessory Minerals*

Accessory minerals are minerals which compose less than 5% of the rock. In this study all accessory minerals were found using energy dispersive spectroscopy (EDS) when interesting or highly reflective minerals appeared adjacent to grains selected for EMP.

The dominant accessory mineral is apatite ($Ca_5(PO_4)_3(F,Cl,OH)$). It was identified using optical properties and EDS spectra (Fig. 3.20). This mineral was found as single 0.1 to 1 mm grains, both basal and elongate sections, as well as aggregate masses of 0.05 to 0.1 mm grains. Although found in nepheline syenites, it is dominantly seen and easier to identify within the fine grained matrix of the phonolite (Fig. 3.20). No REEs are present within the EDS spectra of apatite.

Fluorite (CaF_2) was found in most of the samples of nepheline syenite and phonolite. The fluorite appeared as part of the late stage groundmass assemblage and as a mineral filling up 0.01 mm wide veins within the groundmass. Abundant REE concentrations are throughout the fluorite as shown by the EDS spectra (Fig. 3.21).

Pyrochlore ($(Na,Ca)_2Nb_2O_6(OH,F)$) is found as 1 to 10 µm globules within larger titanite grains (Fig. 3.22). Titanite grains that host pyrochlore are always found within fluorite-rich veins. In contrast, titanite found within the remainder of the mineral assemblage (not found in fluorite-rich veins) does not contain pyrochlore.

Strontianite ($SrCO_3$) is also found within the veins of fluorite as 50 µm grains. These grains form monomineralic aggregates within central parts of the fluorite veins with crystals of anhedral to subhedral shape. Strontianite is enriched in REEs as can be seen on the EDS spectrum (Fig. 3.23).

Zircon ($ZrSiO_4$) and barite ($BaSO_4$) are two accessory minerals found within weathered feldspar grains. Both were identified using EDS spectra (Fig. 3.24). The zircons form angular grains with size 100 µm within highly weathered alkali feldspar grains. Barite appears as both 10 µm globules and as 1 to 2 µm veins, often adjacent to one another, within highly weathered alkali feldspar and plagioclase grains in both nepheline syenite and phonolite samples (Fig. 3.25). Both zircon and barite show no enrichment of REEs within their EDS spectra.

Rare earth element minerals were identified using EDS. REE-minerals are found in two settings: in fluorite veins and as grains near or enclosed in apatite. The grains in both are 10 to 30 µm in size and are often subhedral to anhedral. The REE-minerals associated with apatite are either enclosed in apatite or are adjacent to larger apatite grains (Fig. 3.26). REE-minerals associated with fluorite are largest when found within the fluorite veins and become progressively smaller as you move away from the vein boundary and into the surrounding matrix (Fig. 3.27). The EDS spectrum show that REE-minerals also contain F, C, and Ca most likely relating them to the Ca-bearing members of the bastnasite group.

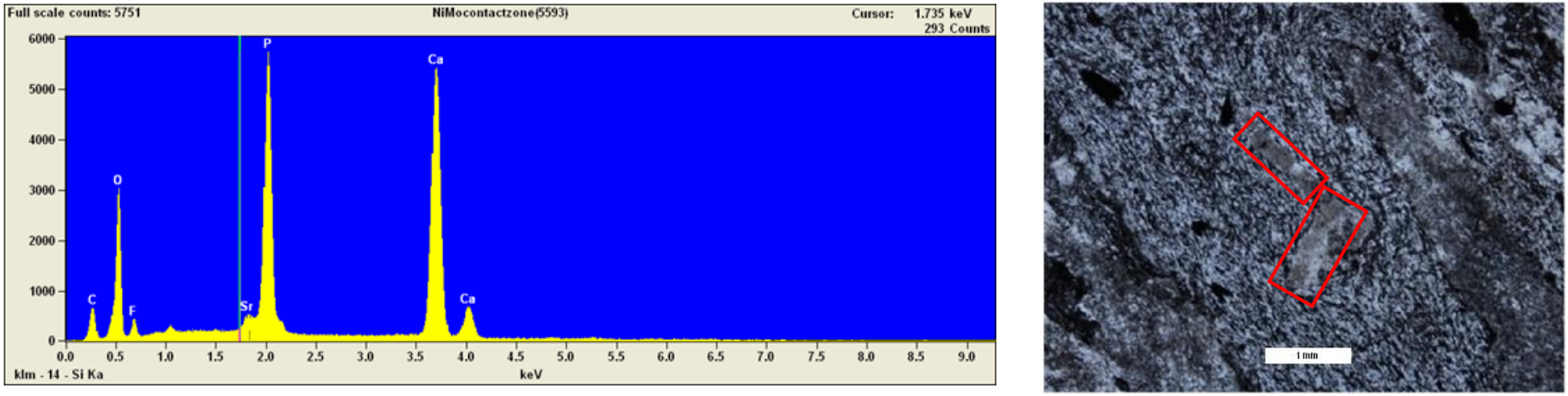

Figure 3.20: EDS spectrum and XPL optical image used to identify apatite. (left panel) EDS spectrum created during microprobe analysis of sample PH-3. Relatively large peaks of oxygen (O), phosphate (P), and calcium (Ca) show their relative abundance and are used for identification of apatite. (right panel) Two apatite grains within the trachytic matrix of sample PH-3.

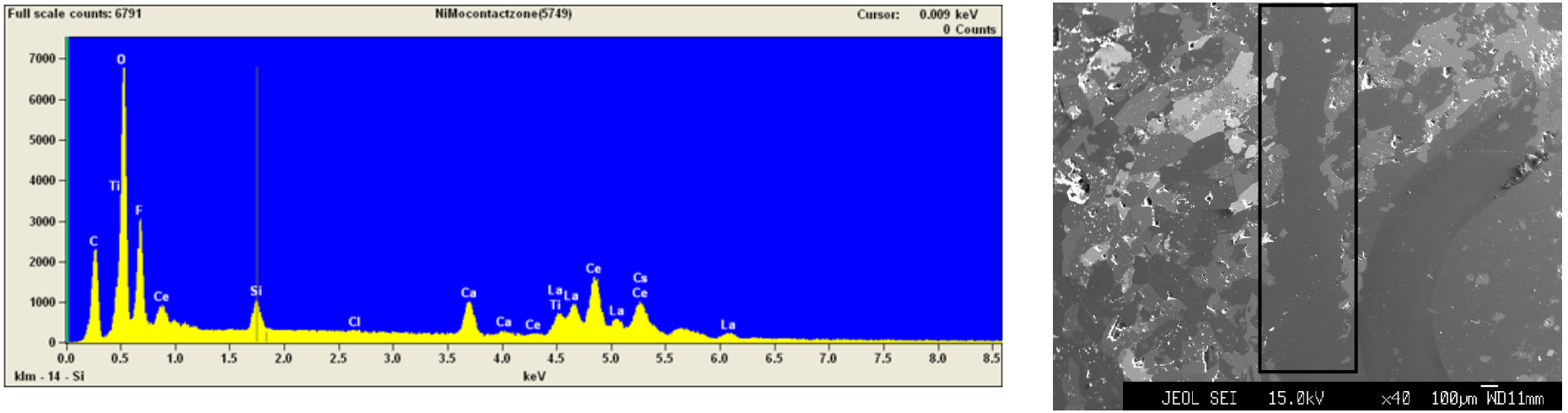

Figure 3.21: EDS spectrum and electron microprobe backscatter image used to identify fluorite. (left panel) EDS spectrum created during EMP analysis of sample ESY-7 showing relatively high peaks of fluorine (F), oxygen (O), and carbon (C). (right panel) A single fluorite vein runs from top to bottom of the image and is darker-gray relative to most surrounding material. This is highlighted within the enclosed black rectangle.

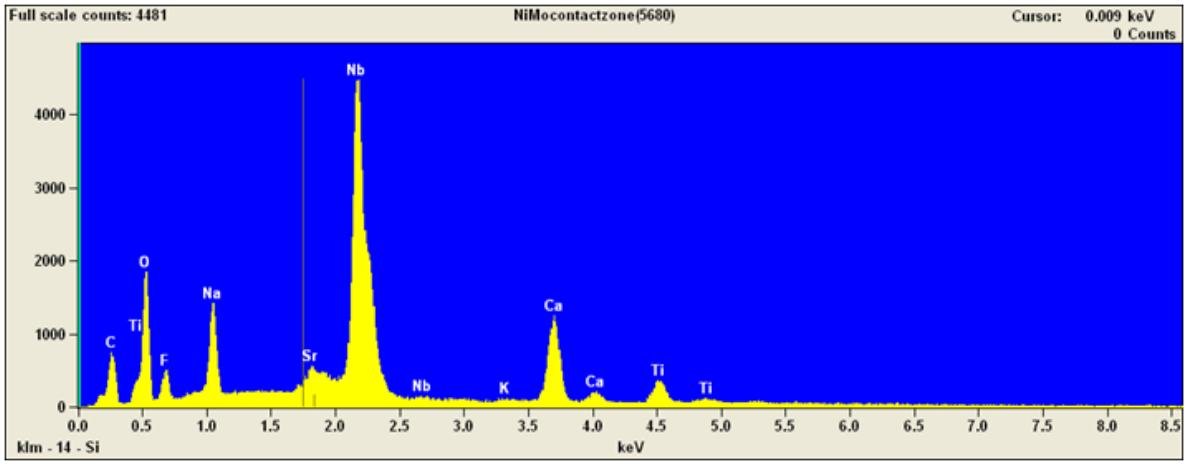

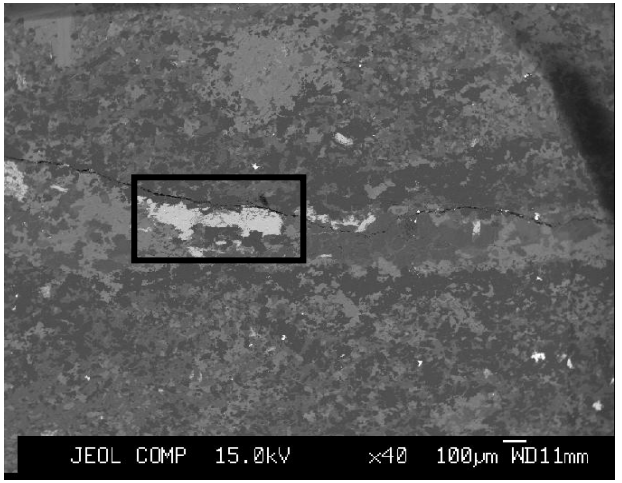

Figure 3.22: EDS spectrum and EMP backscatter image used to identify pyrochlore. (left panel) EDS spectrum created during microprobe analysis of sample PH-1. Peaks of niobium (Nb) and calcium (Ca) show greater relative abundance and are used for identification of pyrochlore. (right panel). An EMP backscatter image showing single 500 µm grain of titanite is enclosed in a fluorite vein and shown within the black rectangle. Pyrochlore exists as ~1 µm globule inclusions within these titanite grains

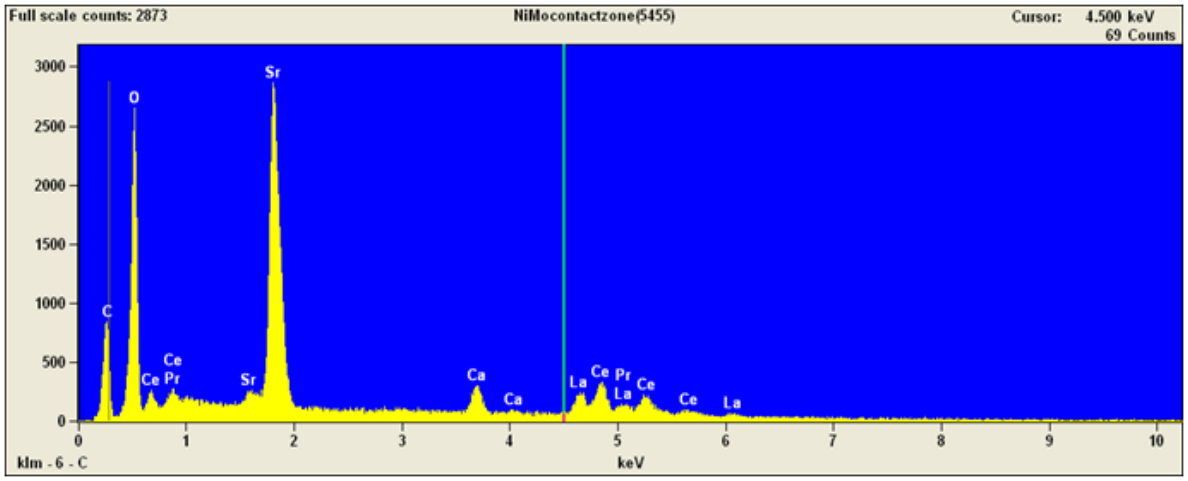

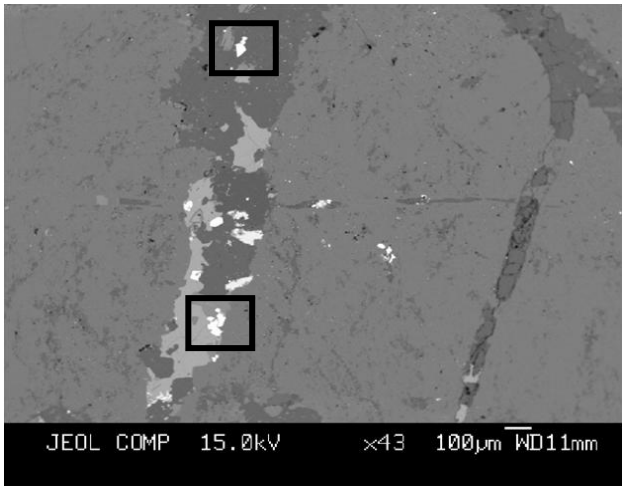

Figure 3.23: EDS spectrum and EMP backscatter image used to identify strontianite. (left panel) EDS spectrum created during microprobe analysis of sample ESY-1. Relatively large peaks in carbon (C), oxygen (O), and strontium (Sr) are used for identification of strontianite. (right panel) An EMP backscatter image of sample ESY-1. Two dark gray veins of fluorite are running near-parallel to one another. Enclosed in two black rectangles within these veins are 50 µm strontianite grains.

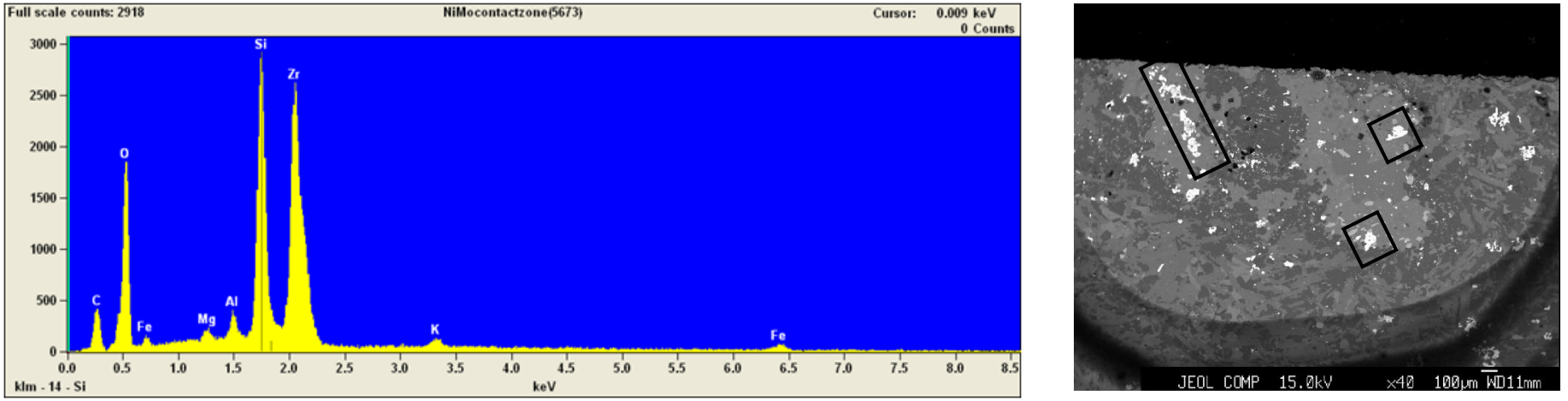

Figure 3.24: EDS spectrum and an EMP backscatter image used to identify zircon. (left panel) An EDS image created during EMP analysis of sample PH-6. Relative large peaks in oxygen (O), silicon (Si), and zirconium (Zr) are used for identification of zircon. (right panel) An EMP backscatter image showing 100 µm zircon grains found in and adjacent to feldspar and indicated enclosed within the black rectangular boxes.

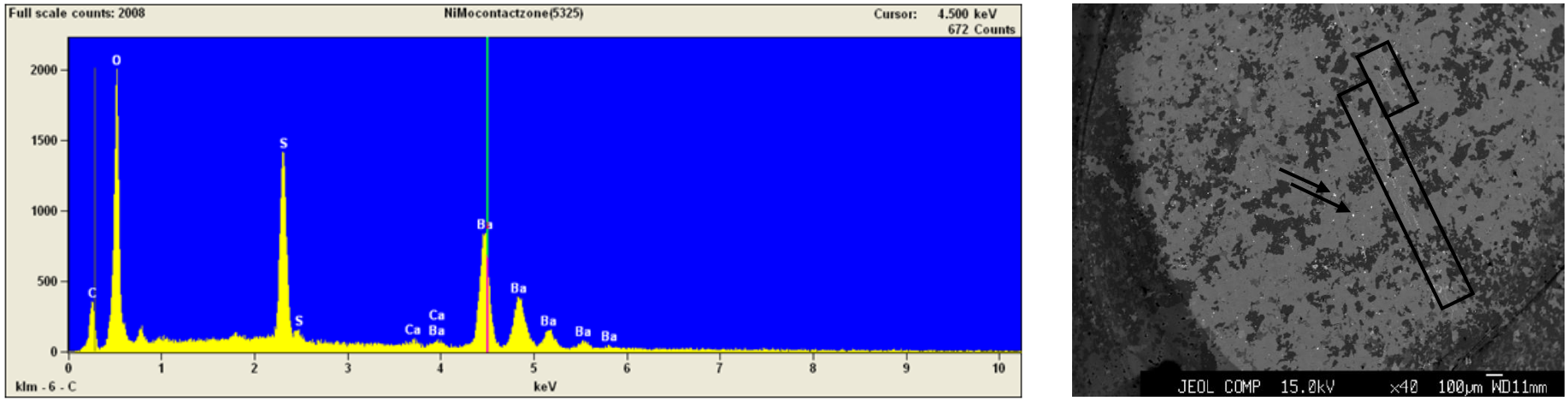

Figure 3.25: EDS spectrum and an EMP backscatter image used to identify barite. (left panel) An EDS image created during EMP analysis of sample ESY-12. Relatively large peaks in oxygen (O), sulphur (S), and barium (Ba) are used for identification of barite. (right panel) An EMP backscatter image showing parallel veins and ~10 µm inclusions of barite enclosed in a larger alkali feldspar grain. The veins are shown by the black rectangular boxes while inclusions are indicated by black arrows.

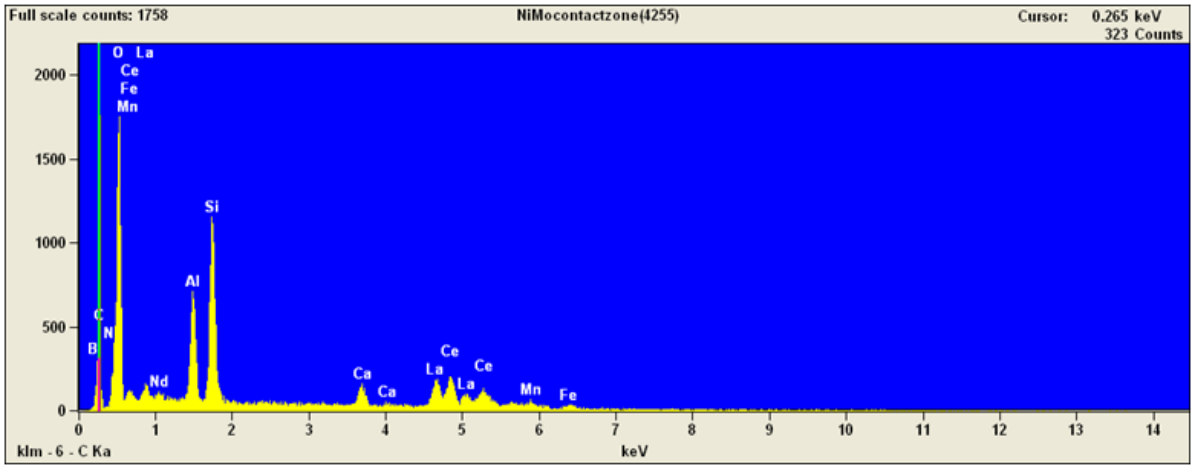

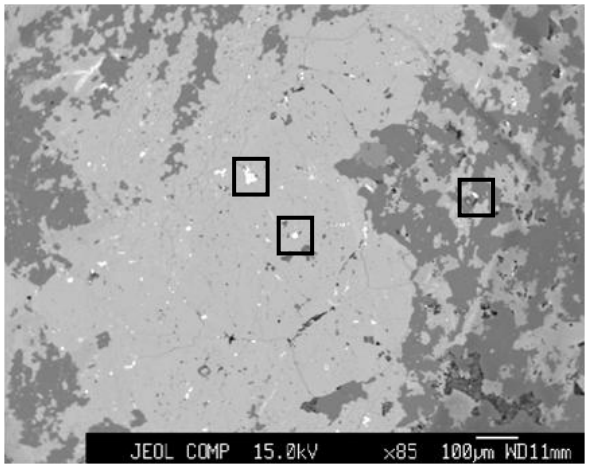

Figure 3.26: EDS spectrum and an EMP backscatter image used to identify REE-minerals associated with apatite. (left panel) An EDS image created during EMP analysis of sample PH-2. Minor peaks in cerium (Ce) and lanthanum (La) show the presence of REE-minerals. The peaks on the left of the spectrum are contamination of surrounding material. (right panel) An EMP backscatter image showing 5-30 µm REE-minerals found in and adjacent to aggregate apatite (light gray). The RRE-minerals are indicated by the black, square boxes.

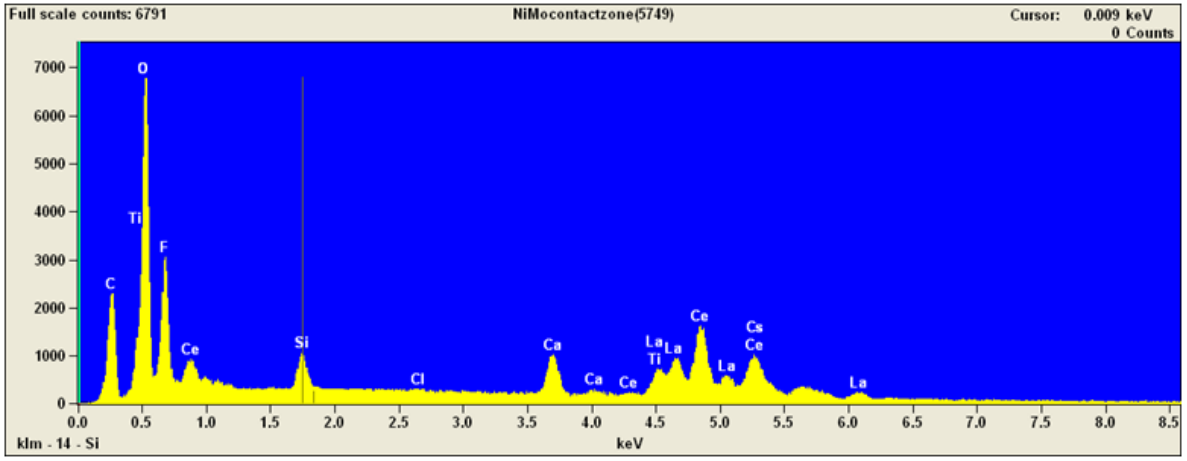

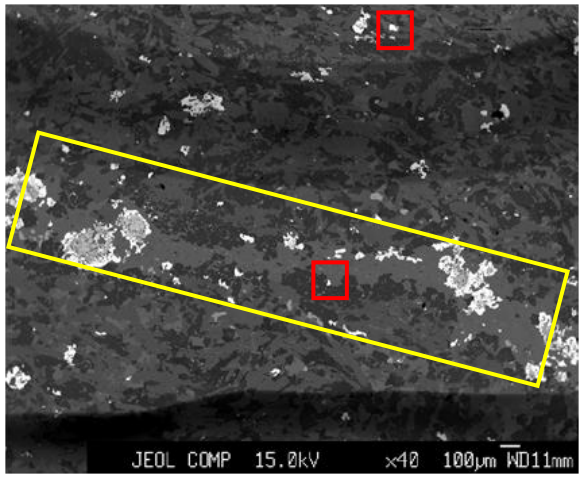

Figure 3.27: EDS spectrum and an EMP backscatter image used to identify REE-minerals associated with fluorite. (left panel) An EDS image created during EMP analysis of sample PH-6 Minor peaks in cerium (Ce) and lanthanum (La) show the presence of REE-minerals. Fluorite contamination occurs as indicated by its presence in the EDS spectrum. (right panel) An EMP backscatter image showing a fluorite vein (yellow rectangle) with associated REE-minerals (red boxes).

3.3 *Mineral Chemistry*

The chemical composition of main rock forming minerals in fourteen nepheline syenite samples and six phonolite samples was determined using EMP. All tabulated results are in Appendix A. The analysis focused on alkali feldspar, plagioclase, and biotite.

3.3.1 *Feldspars*

Feldspar is a dominant major rock forming mineral of the coarse grained nepheline syenites and a common phenocryst in the phonolites. Using EMP, the mineral chemistry was determined for both alkali feldspar and plagioclase (Fig 3.28). In all the studied rocks plagioclase is albite with the composition varying from $Ab_2An_0Or_{98}$ to $Ab_{19}An_1Or_{80.}$ Little to no compositional variation occurs between the plagioclase for nepheline syenite and phonolite as many of the compositional points plot in the same area on the triangular graph (Fig 3.29 a). There is also no confident variation seen between the groundmass and phenocrysts assemblage in these samples (Fig 3.30 a). The alkali feldspare has a composition from $AbAn_0Or_1$ to $Ab_{62}An_1Or_{37.}$ There is no systematic variation between alkali feldspar in the nepheline syenite and phonolite plots as they also plot in an overall large group within the triangular compositional graph (Fig 3.29 b). However, phenocrysts show a trend from less K-rich to more K-rich compositions, whereas groundmass alkali feldspar has similar compositions to the K-rich phenocrysts (Fig 3.0 b).

3.3.2 *Biotite*

Biotite is a major rock-forming mineral and is found as both phenocrysts and groundmass in phonolites and as coarse grained and interstitial material in nepheline syenites. A relationship between nepheline syenite and phonolite biotites is evident using EMP analyses. At relatively high Mg and high Al/low Si concentrations, the nepheline syenite and phonolite biotite samples plot together. Only

nepheline syenite biotites show relatively low Mg and low Al/high Si concentrations (Fig 3.3.4). Using the tabulated EMP analyses, plots using oxides versus (MgO/(MgO+FeO)) cations were created to indicate trends and variations within nepheline syenite and phonolite samples (Fig 3.3.5). Samples of phonolite plot in the enriched MgO area of the graphs but vary laterally depending on the oxide plotted. Samples of nepheline syenite plot dominantly in the depleted MgO area of the graph with some samples plotting in the enriched MgO area. A similarity exists between the phonolite biotites and the high-Mg nepheline syenite biotites

In general, two distinct groupings form in the graphs; one with relatively high MgO, low FeO values and one with relatively low MgO, high FeO values. Three oxide patterns occur in association with these groups. The first is an enrichment of oxide with depletion in MgO which occurs in three oxides being TiO_2, Al_2O_3, and MnO (Fig 3.3.5 a,b,&c). The second is a depletion in oxide with depletion in MgO which occurs in two oxides, SiO_2 and CaO (Fig 3.3.5 d&e). The final is one in which little to no oxide variation occurs from MgO enrichment to MgO depletion which occurs in two oxides being Na_2O and K_2O (Fig 3.3.5 f&g). All analyses of biotite in phonolite plot in the high-MgO part of the diagram and have very similar composition to biotites of similar MgO composition from nepheline syenite.

The groundmass and phenocryst assemblages of biotite show distinct trends when plotted as oxides versus MgO/(MgO+FeO) cations (Fig 3.3.6). Phenocryst and coarse grained biotite assemblages have a large variety in the plots from enriched to depleted values of MgO. Only three samples of groundmass biotite were collected during EMP analysis. Two of these samples plot in the MgO depleted area of the graphs. The final groundmass sample plots in the MgO enrich area of the graphs. Oxide variation occur in all three samples, although the MgO depleted samples tend to have similar values.

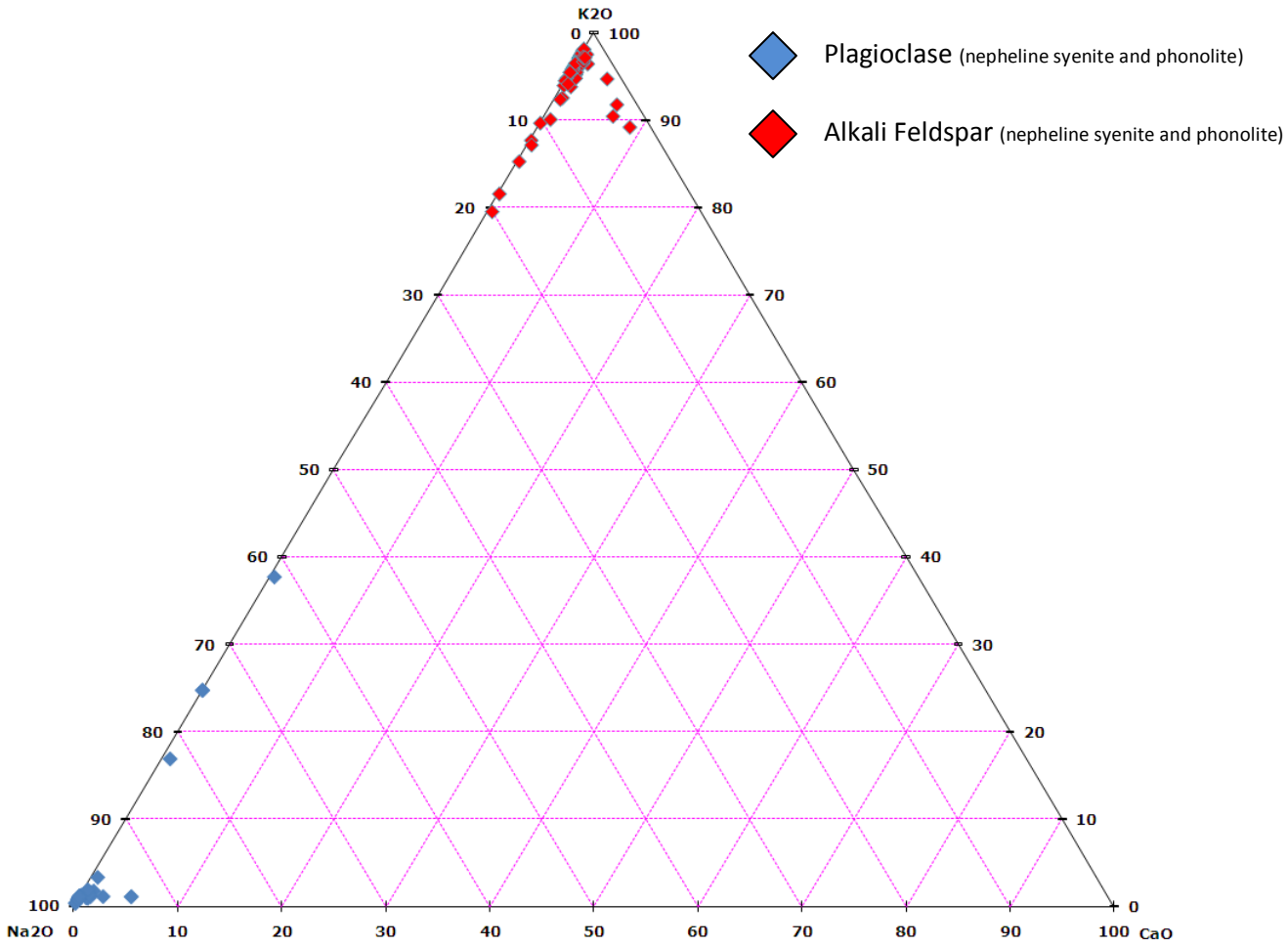

Figure 3.28: EMP analysis for alkali feldspar and plagioclase plotted on a compositional triangular diagram of Na_2O-CaO-K_2O. Nepheline syenite and phonolite samples have been combined for each of alkali feldspar and plagioclase. Seen at the top of the triangle are the plot markers for alkali feldspar (red diamonds). These fall into the K_2O (sanidine) end of the composition diagram. Seen at the bottom left of the triangle are the plot markers for plagioclase (blue diamonds). These fall into the Na_2O (albite) end of the compositional diagram.

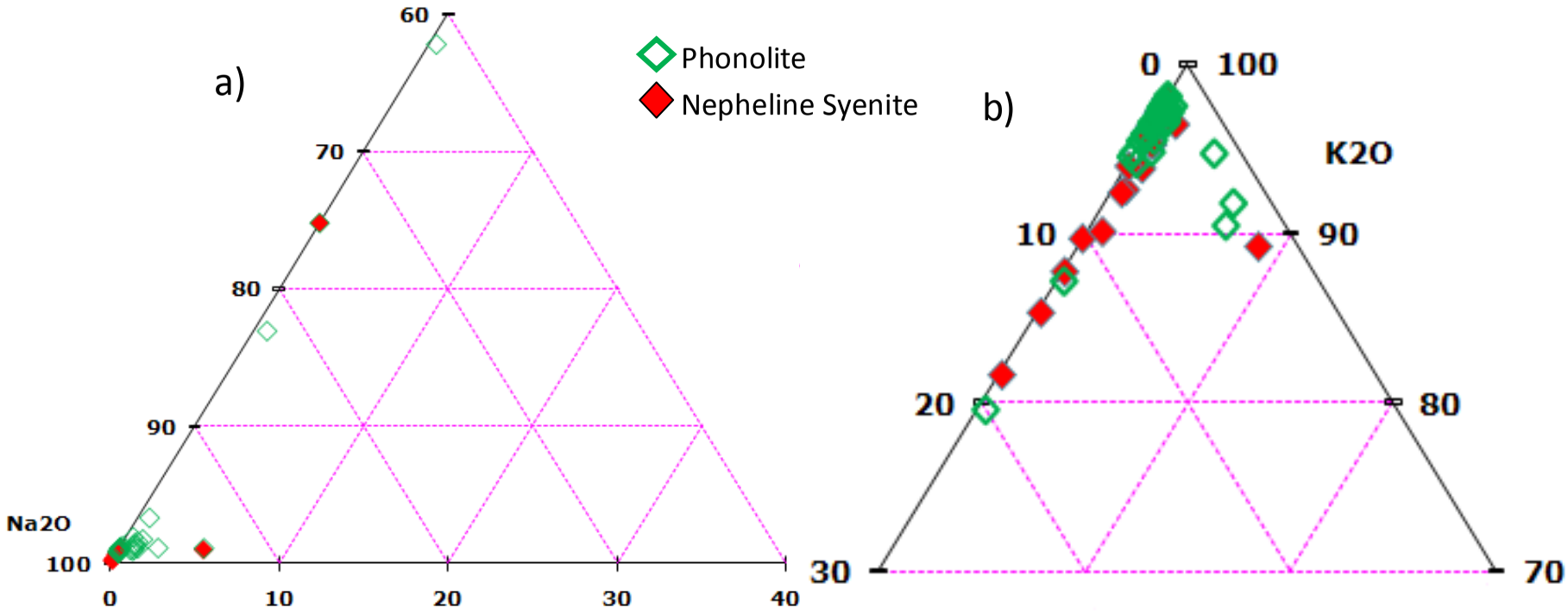

Figure 3.29: Triangular compositional diagrams comparing alkali feldspar and plagioclase from phonolites and nepheline syenites.

(a) An enlarged end (Na_2O) of the triangular compositional diagram. Plagioclase is plotted as phonolite samples and nepheline syenite samples. There is little variation is the plotting area of the two markers suggesting no compositional difference between plagioclase of phonolites and alkali feldspar

b) An enlarged end (K_2O) of the triangular compositional diagram. Alkali feldspar is plotted as phonolite samples (green diamond) and as nepheline syenite samples (red diamond). The variation between the two markers for alkali feldspar is little, showing no compositional difference between alkali feldspar of phonolites and nepheline syenites

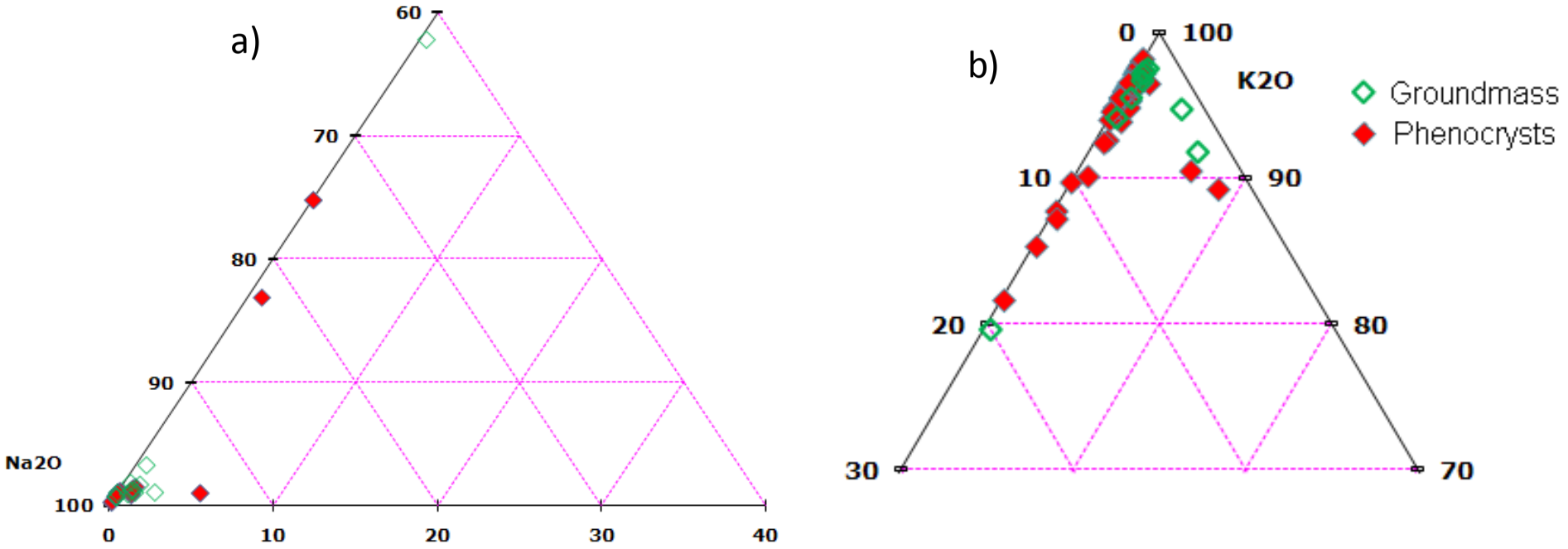

Figure 3.30: Triangular compositional diagrams comparing the groundmass and phenocrysts of alkali feldspar and plagioclase.

(a) An enlarged end (Na_2O) of the triangular compositional diagram. Plagioclase is plotted as groundmass material and phenocryst material. There is little variation is the plotting area of the two markers suggesting no compositional difference between the groundmass and phenocrysts assemblage in these samples.

(b) An enlarged end (K_2O) of the triangular compositional diagram. Alkali feldspar is plotted as groundmass material and as phenocryst material. The variation between the two markers for alkali feldspar is little, showing no compositional difference between the groundmass and phenocryst assemblage in these samples.

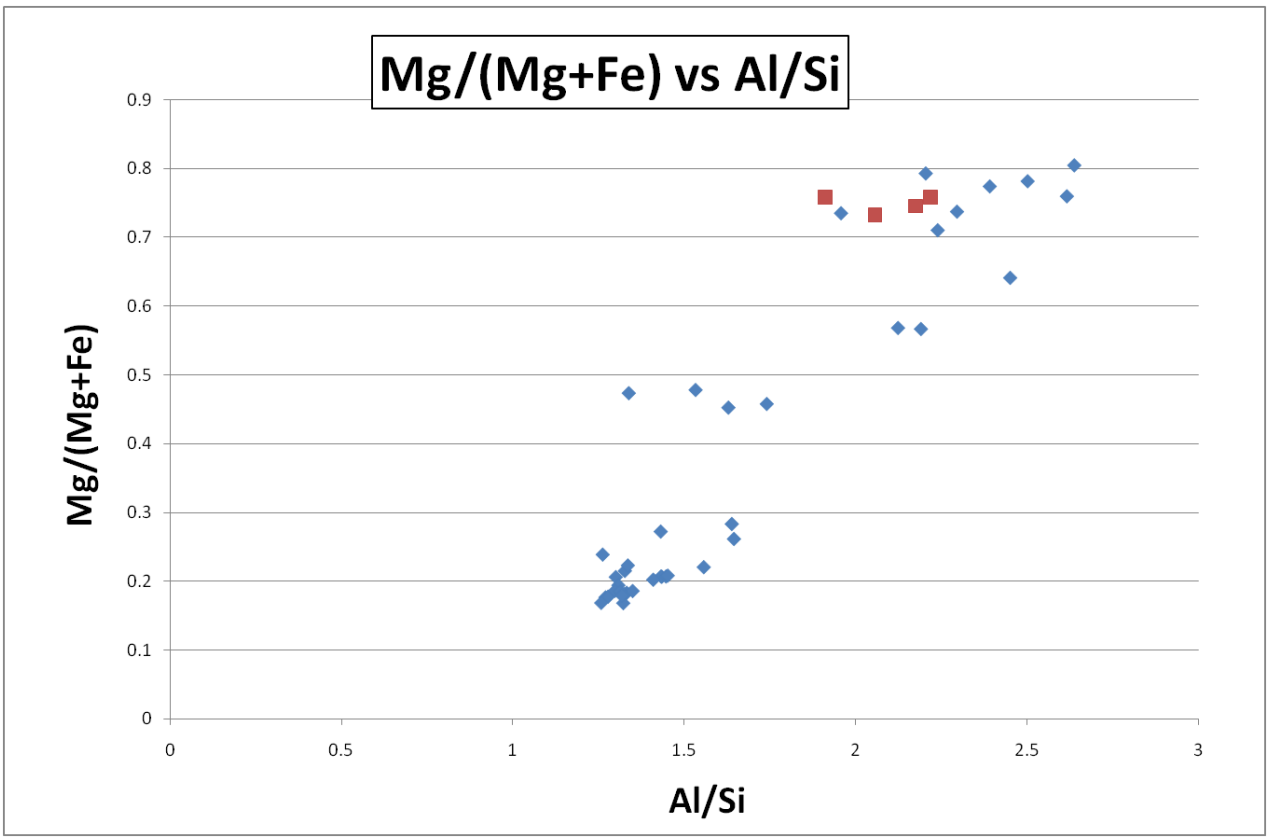

Figure 3.31: Scatter plot of EMP analysis cations of biotite. A tightly clustered group of analyses of nepheline syenite biotites are found in the Mg-poor area. A dispersed group of analyses of both nepheline syenite and of phonolite biotites are found in the Mg-rich area.

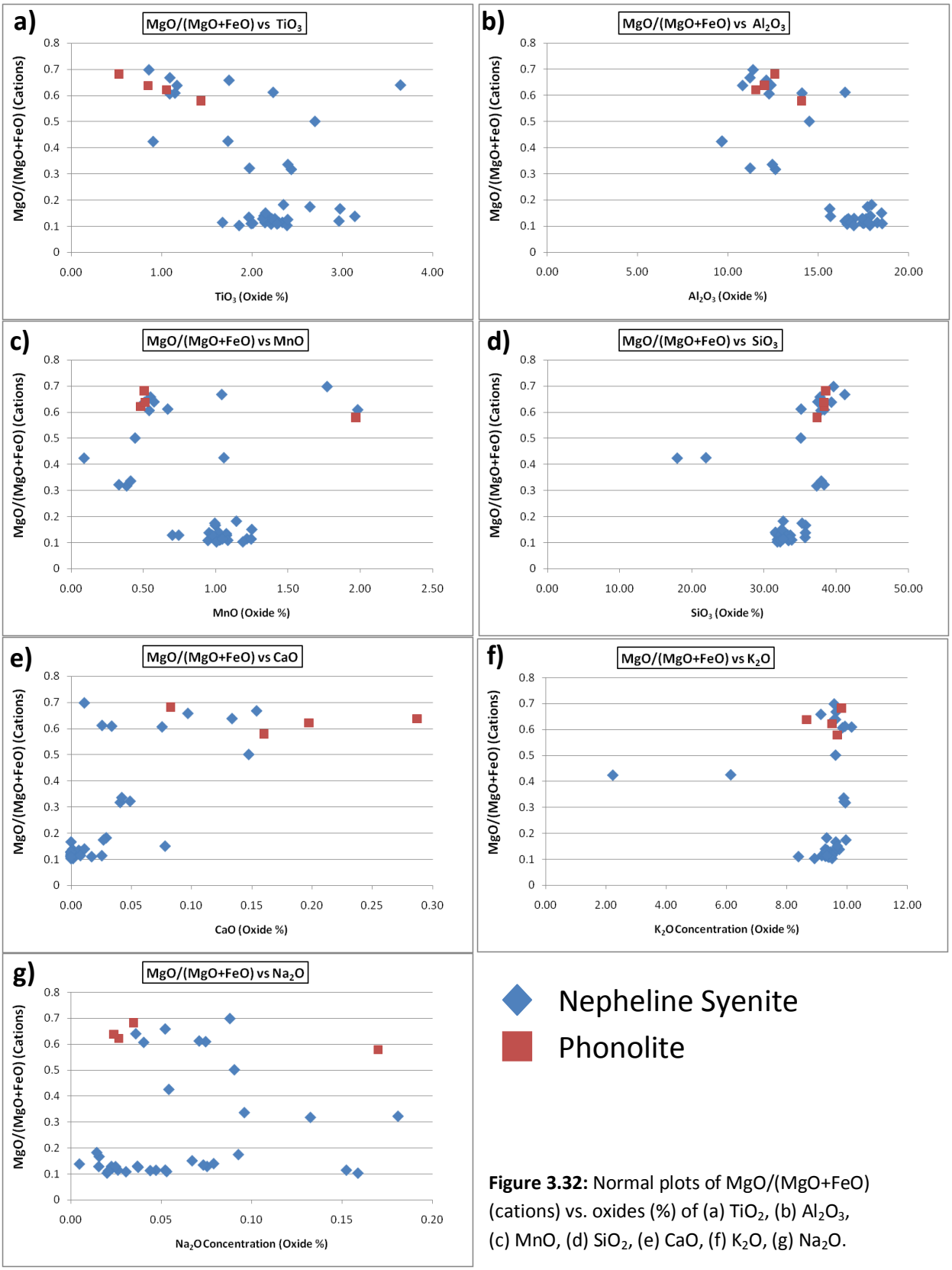

Figure 3.32: Normal plots of MgO/(MgO+FeO) (cations) vs. oxides (%) of (a) TiO_2, (b) Al_2O_3, (c) MnO, (d) SiO_2, (e) CaO, (f) K_2O, (g) Na_2O.

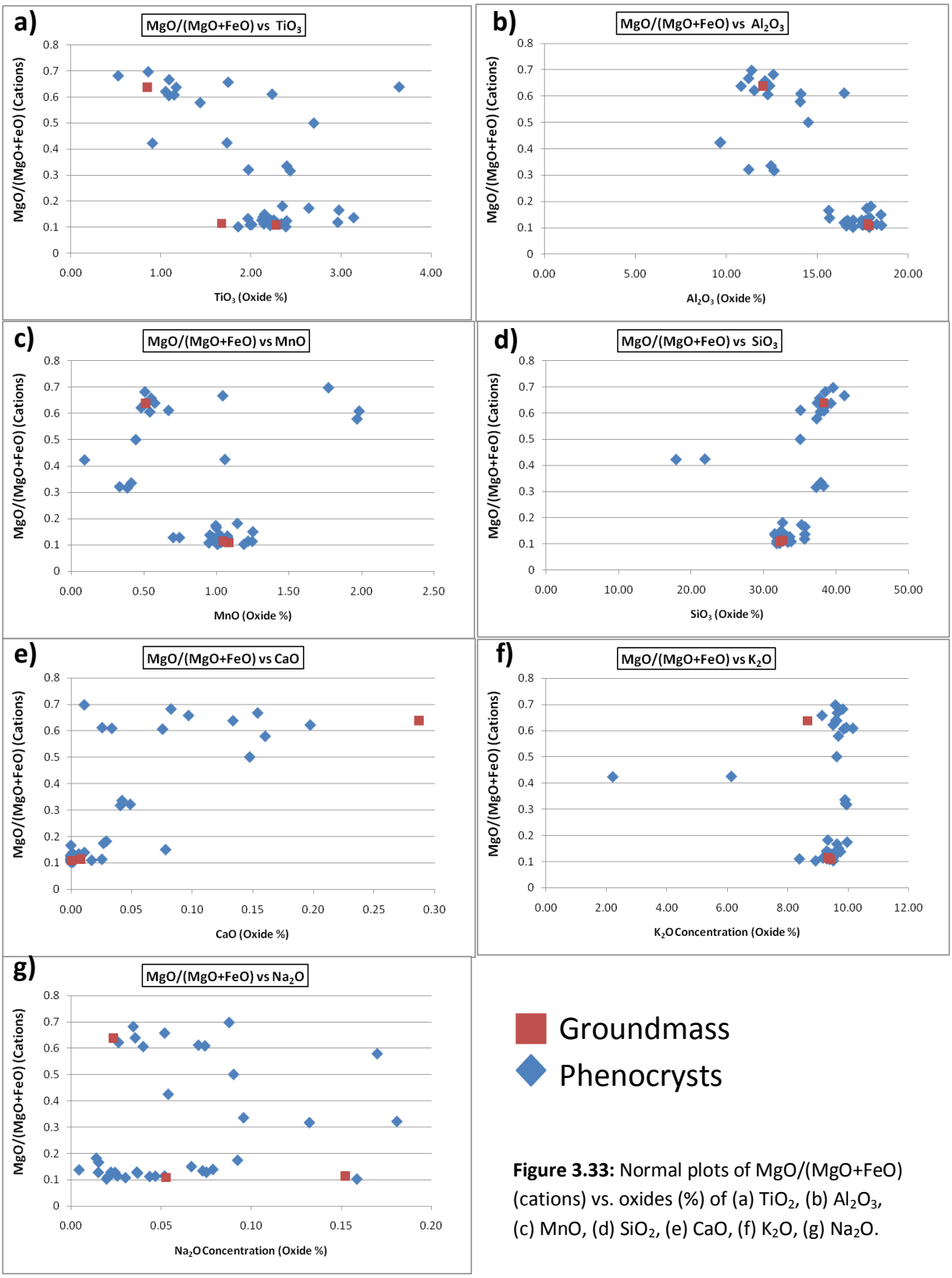

Figure 3.33: Normal plots of MgO/(MgO+FeO) (cations) vs. oxides (%) of (a) TiO_2, (b) Al_2O_3, (c) MnO, (d) SiO_2, (e) CaO, (f) K_2O, (g) Na_2O.

Chapter 4: Discussion

Previous investigations of the Lofdal intrusive complex of northern Namibia have largely focused on the carbonatite dykes and their association with REE mineralization (Kaul, 2010; Ndalulilwa, 2009). This study is one of the first to investigate the petrogenesis of the nepheline syenite plugs and phonolite dykes, and their association with REE mineralization, from the Lofdal intrusive complex. The following paragraphs will use the petrographic descriptions to compare the nepheline syenites and phonolites, to describe the associations of accessory minerals with the remaining rock, and to give the results context to a carbonatite-syenite complex.

4.1 *Description Overview*

Petrographic descriptions and EMP analyses were used to explain the mineral assemblage, the mineral chemistry, and the crystallization history of the nepheline syenites and phonolites. The following is a comparison review of the mineralogy and mineral chemistry present in these rocks.

4.1.1 *Nepheline Syenite and Phonolite Comparison*

The nepheline syenites from the Lofdal intrusive complex are dominantly composed of coarse-grained minerals of: alkali feldspar, plagioclase, cancrinite (partially or completely replacing nepheline), sericite, and biotite. All of these minerals are also found as interstitial matrix. Variations in the mineral assemblage from sample to sample consist of the presence or lack of: apatite, aegirine, titanite, magnetite, sodalite, fluorite, amphibole, and carbonate minerals.

Phonolites are mineralogically similar to nepheline syenites (Fig 4.1). They are composed of 1-15 mm in length phenocrysts set in a very fine-grained groundmass. The major rock-forming phenocrysts consist of: alkali feldspar, plagioclase, nepheline, cancrinite, and sericite. Variations in the mineral assemblage from sample to sample consist of the presence of lack of: aegirine, biotite, magnetite,

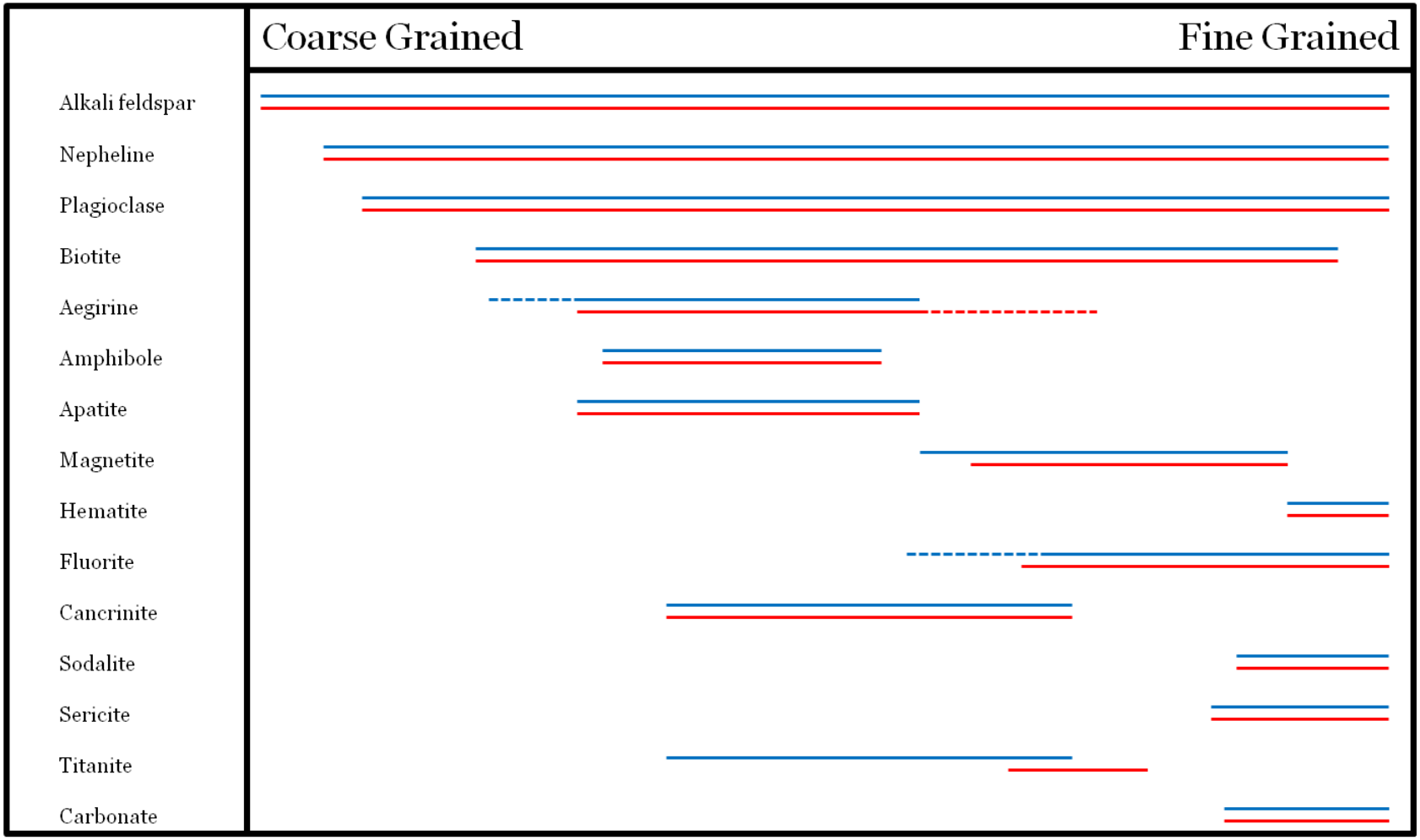

Figure 4.1: Crystallization sequence of nepheline syenite and phonolite mineral assemblages.

apatite, sodalite, fluorite, amphibole, and carbonate minerals. The groundmass of the phonolites is dominantly composed of the same major rock-forming phenocryst assemblage minerals.

The alteration mineral cancrinite gives indication of a volatile-rich magma. Cancrinite ($Na_6Ca_2[(CO_3)_2|Al_6Si_6O_{24}]\cdot 2H_2O$) is a common constituent of nepheline syenite magmas and often forms between the reaction of nepheline ($(Na,K)AlSiO_4$) with a CO_2 residual liquid. The phonolite groundmass in many samples shows indication of a fluorite-purple colouration. This is indication that the magmas also had a fluorite volatile chemical component.

The EMP analyses and resulting graphs for feldspar (Fig 3.28, 3.29, 3.30) indicate a high similarity between the albite mineral chemistry of nepheline syenites to phonolites and of groundmass to phenocrysts as well as the alkali feldspar mineral chemistry of the same parameters. The indication that albite and alkali feldspar share similar chemical composition trends in nepheline syenites and phonolites would suggest a parental magma association between the two rock types. The similarity in groundmass and phenocryst chemical compositional trends furthers the concept that the two rock types were from a similar parental magma. These trends may uphold the long believed relationship of carbonatite-syenite relationships in which the extrusive phonolites originate from the same of magmatic body as the intrusive nepheline syenites (Winter, 2010; Woolley, 2003; Woolley, 2008). However, the case may be that the magmatic bodies are not the same but very similar. This will be explored with the biotite analyses and graphs.

Unlike the feldspar analyses, biotite EMP analyses and resulting graphs (Fig 3.31, 3.32, 3.33) indicate a range of crystallization resulting possibly due to more than one magmatic event leading to the emplacement of the nepheline syenites and phonolites. The graphs appear to have two overall clusters of groups occurring at relatively high magnesium (Mg) values and relatively low Mg values. Nepheline syenite biotites are diverse and occur in both of these groups, with the larger and tighter cluster occurring at relatively low Mg values. Phonolite biotites are restricted to relatively high Mg values of the

graphs, overlapping with the group of nepheline syenite biotites in the same area, and are dispersed through a greater range of values. This relationship occurs in all Mg plots and indicates two magmatic events; one in which earlier nepheline syenites were emplaced and a second co-magmatic emplacement of nepheline syenite with phonolites. The possibilities that lead to these relationships are: 1) the two magmas are related through fractional crystallization, 2) a magma contamination or some inhomogeneity occurred in the original parental magma, 3) the two magmatic emplacements have separate but similar parental magmas.

A fractional crystallization trend is not occurring as can be interpreted from the oxide vs Mg trends. Samples relatively high in Mg contain higher values of SiO_2 and lower values of TiO_2 and Al_2O_3. This is opposite of what would be expected from a simple fractionation trend. The viability that a contamination occurred in the original magma is plausible but there is not sufficicent evidence to make such an interpretation. The association between the nepheline syenite and phonolite biotites at high Mg values is interpreted as being from a separate magma source than the nepheline syenite biotites at low Mg values.

Interestingly, a similarity between the phenocrysts and groundmass biotites occurs at both high and low Mg values. The samples at low Mg values are those from interstitial material of nepheline syenite. The sample at high Mg values is form the groundmass of a phonolite. Because the groundmass and phenocryst/coarse grained assemblages similar values of Mg, the magmatic chemistry was relatively constant from beginning to end of crystallization.

4.2 *Accessory Minerals – REE Associations*

The accessory minerals were identified using optical microscopy and EDS spectra. This resulted in the identification of six minerals: apatite, fluorite, pyrochlore, strontianite, zircon, and barite. Each of these minerals formed either through magmatic events, hydrothermal events, or both.

Apatite and zircon are the only accessory minerals to form solely during magmatic crystallization. Apatite is found as phenocrysts and micro-phenocrysts aggregate assemblages within both nepheline syenite and phonolite. Most apatite grains are associated with REE-minerals. The REE-minerals form both within and along the grain boundaries of apatite. This formation (both within and along the exterior of apatite) suggests that the REE-minerals formed magmatically, following formation of apatite. Zircon is only found enclosed within feldspars. Their lack of REE-minerals and anhedral fractured shape suggests that they formed prior to magmatic crystallization of feldspar and much earlier than most minerals in the rocks.

Pyrochlore, strontianite, and barite are all late forming accessory minerals, often associated with hydrothermal activity. Pyrochlore only occurs as globules in titanite grains which are found in late forming veins. No REE-minerals are associated with pyrochlore. Together this suggests that the pyrochlore formed through exsolution grains due to reaction with the surrounding vein material with titanite. Strontianite is also found in late forming veins and does not have any REE-mineral association. Barite is found as small globules and as vein filling material in feldspars. The feldspars which do have barite formation are often found relatively closer to late forming veins, possibly causing exsolution of barite within the feldspars. Again, no REE-mineral association occurs.

Magmatic fluorite is present within the groundmass of phonolite and in interstitial material of nepheline syenite. Late forming veins, rich in fluorite, are found in both samples again. Often near the veins are REE-minerals. These REE-minerals are present either within or adjacent to the fluorite-rich veins and are interpreted as occurring during late stage hydrothermal activity. Ca, C, and F are relatively more concentrated in these REE-minerals leading to the relation that these REE-minerals belong to the Ca-bearing members of the bastnasite group.

There are two REE-mineral formations within these rocks. Magmatic forming REE-minerals are found in association within and along the exterior of apatite. Late stage hydrothermal forming REE-minerals are found in association with fluorite-rich veins. The two are chemically different as the REE-minerals forming in association with fluorite being of the CA-bearing member of the bastnasite group.

4.3 *Context - Early Intrusive History of the Lofdal Complex*

The Lofdal intrusive complex is a ~750 Ma intrusive system composed of syenites, nepheline syenites, phonolite, diatreme breccias, and carbonatites. The complex is under current investigation for its potential host of REEs. At present the carbonatites are most essential in this investigation as they are well known to host REEs. However, through this projects investigation REEs are heavily found to be associated with earlier forming and surrounding nepheline syenites and phonolites.

The Lofdal nepheline syenite plugs and phonolite dykes intruded the highly metamorphosed HMC basement rock approximately 750 Ma. These rock units are rift-related to regional fracturing of an intra-continental plate setting. The nepheline syenite plugs represent the main intrusive body while the phonolite dykes are a later stage, SW – NE striking intrusive unit. A suite of carbonatites dykes followed in the still active fracture system, resulting in carbonatites dykes being emplaced within or adjacent to earlier phonolite dykes. Occurring parallel in time, brecciation and alteration of the surrounding syenites and metamorphic basement rock occurred. An end product of this was an enrichment of REEs within the silicate and carbonate magmatically emplaced rocks (Swinden & Siegfried, 2011).

The early forming nepheline syenites are found in three main bodies with many satellite intrusions locally occurring. The later phonolites are found a SW – NE striking dykes intruding through the HMC and the nepheline syenite plugs. The two rock units have a similar mineralogical assemblage and both contain magmatic apatite, in association with REE-mineralization, and fluorite-rich veins, in association with the Ca-member of the bastnasite REE group. The magmatic REE-minerals related to

apatite show enrichment in cesium (Ce) and lanthanum (La) and formed during late stage crystallization. Following complete crystallization of the magmatic bodies a hydrothermal fluid persisted through the open fractures within the nepheline syenites and phonolites. This fluorite-rich hydrothermal fluid allowed for the formation of late stage Ca-bearing REE-minerals.

The formation of REE-minerals in the nepheline syenites and phonolites are known to occur in two events. The magmatic phase occurs at the end of crystallization of the nepheline syenites and phonolites. The hydrothermal phase REE-minerals occur following complete crystallization of the nepheline syenites and phonolites. However, it is unknown if the fluids are pre-, syn-, or post-intrusive of the carbonatites. Further work should explore the relation of nepheline syenites and phonolites to carbonatites to aide in the complete understanding of the REE-mineralization.

Chapter 5 Conclusion

5.1 *Conclusions*

1. The petrography of the nepheline syenites and phonolites show a similar mineralogical assemblage. This great abundance of common minerals, both primary and secondary, suggests that the two magmatic units have originated from the same parental magma or from parental magmas which have similar chemical characteristics.

2. Feldspar EMP analyses show nepheline syenite and phonolite similarities indicating a related parental magma or two very similar parental magmas. The biotite EMP analyses show two groups of biotite suggesting two different magma sources. One group (Mg-poor) is composed solely of nepheline syenite and the other (Mg-rich) is a mixture of nepheline syenite and phonolite, indicating that there was a co-magmatic relationship between the (Mg-rich) phonolites and nepheline syenites.

3. Two REE-mineralization events occur in the nepheline syenites and phonolites. The first and older is a magmatic crystallization phase. The magmatic REE-minerals are Ce and La rich and are found in association with apatite. The second and younger REE-mineralization event is related to late stage hydrothermal activity. The hydrothermal REE-minerals are (Ce) and (La) rich and also contain (F), (Ca), and (C), making them part of the Ca-bearing member of the bastnasite group. These are found in association with fluorite-rich veins.

5.2 *Recommendations*

Now knowing that enrichment in REE-minerals occurs beyond the carbonatites of the Lofdal intrusive complex, further exploration of the nepheline syenites and phonolites may reveal further enrichment REE-minerals. If not, the knowledge gained by understanding the nepheline syenites and phonolites will further the understanding of the carbonatites and their REE-mineralization occurrence.

References

BBC. (2010, October 30). *BBC News, Asia-Pacific*. Retrieved November 1, 2010, from British Broadcasting Corporation: http://www.bbc.co.uk/news/world-asia-pacific-11657982

Bell, K. (1989). *Carbonatites Genesis and Evolution.* London, England: Unwin Hyman Ltd.

Bradsher, K. (2010, October 19). *China Said to Widen Its Embargo of Minerals*. Retrieved October 21, 2010, from The New York Times: http://www.nytimes.com/2010/10/20/business/global/20rare.html?_r=3&ref=global-home

Coulson, I.M., Chambers, A.D. (1996). Patterns of zonation in rare-earth-bearing minerals in nepheline syenites of the North Qoroq Center, South Greenland. *The Canadian Mineralogist.* 34, 1163-1178.

Deer, W.A., Howie, R.A., Zussman, J. (1992). *The Rock Forming Minerals* (2nd Edition). London, England. Pearson Education Limited.

Frets, D. C. (1969). *Geology and structure of the Huab-Welwitchia area.* South West Africa, Chamber of Mines, Precambrian Research Unit: University of Cape Town Libraries.

Jones, A. P., Wall, F., & Williams, C. T. (1996). *Rare Earth Minerals: chemistry, origin and ore deposits.* Bodmin, Cornwall, Great Britain: The Mineralogical Society.

Kaul, A. (2010). *A petrological study of REE-Rich carbonatite intrusions from the Lofdal Farm area, Namibia, Africa.* Wolfville, Nova Scotia, Canada: Acadia University.

Lang, O. (2010, October 21). *BBC News, Asia-Pacific*. Retrieved October 22, 2010, from British Broadcasting Corporation: http://www.bbc.co.uk/news/world-asia-pacific-11584229

Le Maitre, R. W. (2002). *Igneous rocks - a classification and gloassary of terms* (2nd Edition ed.). Great Britain: Cambridge University Press.

Lee, W., & Wyllie, P. J. (1998). Processes of Crustal Carbonatite Formation by Liquid Immiscibility and Differentiation, Elucidated by Model Systems. *Journal of Petrology, 39*, 2005-2013.

MacKenzie, W. S., Donaldson, C. H., & Guilford, C. (1982). *Atlas of igneous rocks and their textures.* Essex, England: Longman Scientific & Technical.

Miller, R. M. (2008). *The Geology of Namibia* (Vol. II). Windhoek, Namibia: Geological Survey of Namibia.

Mitchell, R. H., & Jambor, J. L. (Eds.). (1996). *Minerological Association of canada Short Course Series. Undersaturated Alakaline Rocks: Mineralogy, Petrogenesis, and Economic Potential* (Vol. 24). Winnipeg, Manitoba, Canada.

Molycorp Minerals. (2009). *About Us: History: Molycorp Minerals*. Retrieved March 10, 2011, from Molycorp Minerals: The Rare Earths Company: http://www.molycorp.com/history.asp

Ndalulilwa, K. D. (2009). *The semi-quantative petrographic, mineralogical and geochemical characterization of mineralisation of carbonatites from the Lofdal area in Namibia.* Windhoek, Namibia: University of Free State (UFS).

Swinden, H. S., & Siegfried, P. (2011). *43-101 Technical Report on the Rare Earth Element Occurrences in the Lofdal.* Halifax, Nova Scotia: Namibia Rare Earths Inc.

Wall, F., & Mariano, A. N. (1996). *Rare earth minerals in carbonatites: a discussion centered on the Kangankunde Carbonatite, Malawi.* (A. P. Jones, F. Wall, & C. T. Williams, Eds.) London, UK: Chapman & Hall.

Wall, F., Niku-Paavola, V. N., Storey, C., Muller, A., & Jeffries, T. (2008). Xenotime-(Y) from carbonatite dykes at Lofdal, Namibia: unusually low LREE:HREE ratio in carbonatite, and the first dating of xenotime overgrowths on zircon. *The Canadian Mineralogist*, 861-877.

Watson, E.B. (1980) Apatite and phosphorus in mantle source regions: An experimental study of apatite/melt equilibria at pressures to 25 kbar. *Earth and Planetary Science Letters*, 51 (2), 322-335.

Winter, J. D. (2010). *Principles of Igneous and Metamorphic Petrology* (2nd Edition ed.). Upper Saddle River, New Jersey: Peason Education Inc.

Woolley, A. R. (2003). Igneous silicate rocks associated with carbonatites: their diversity, relative abundances and implications for carbonatite genesis. *Periodico di Mineralogia*, 9-17.

Woolley, A. R., & Kjarsgaard, B. A. (2008). Paragenetic types of carbonatite as indicated by the diversity and relative abundance of associated silicate rocks: evidence from a global database. *The Canadian Mineralogist, 46*, 741-752.

.

Appendix A: Electron Microprobe Analysis

The following tables are the values for alkali-feldspar collected from the Electron Microprobe analysis of the rock samples of the nepheline syenites and phonolites

Sample	SiO2	TiO2	Al2O3	FeO	MnO	MgO	CaO	Na2O	K2O	Cr2O3	BaO	SrO	Cl	F	Total	Comment
ESY-1	62.30	0.00	18.42	0.42	0.00	0.02	1.49	0.33	14.96	0.00	-	0.02	-	0.00	97.93	Phenocryst_Core
ESY-2	66.61	0.00	19.21	0.10	0.00	0.00	0.00	0.52	13.47	0.00	0.49	0.00	0.00	0.00	100.41	Phenocryst
ESY-2	67.59	0.00	19.16	0.08	0.00	0.00	0.00	0.26	12.35	0.00	0.32	0.00	0.00	0.00	99.75	Phenocryst
ESY-2	63.73	0.05	18.39	0.18	0.02	0.00	0.02	0.61	15.72	0.03	-	0.00	-	0.03	98.76	Phenocryst
ESY-2	65.41	0.06	18.62	0.24	0.01	0.00	0.02	1.94	13.99	0.02	-	0.00	-	0.02	100.31	Phenocryst
ESY-2	65.80	0.03	18.79	0.23	0.00	0.00	0.03	2.28	13.38	0.04	-	0.00	-	0.04	100.58	Phenocryst
ESY-2	62.96	0.13	18.55	0.11	0.02	0.00	0.02	0.44	15.80	0.07	-	0.00	-	0.07	98.09	Phenocryst
ESY-2	64.98	0.02	18.35	0.24	0.00	0.00	0.01	1.62	14.10	0.03	-	0.00	-	0.03	99.34	Phenocryst
ESY-2	63.11	0.14	18.28	0.27	0.02	0.00	0.01	0.53	15.40	0.08	-	0.00	-	0.08	97.84	Phenocryst_Core
ESY-2	63.38	0.00	18.15	0.18	0.02	0.00	0.00	0.46	16.01	0.00	0.22	0.00	0.00	0.00	98.43	Phenocryst_Rim
ESY-3	63.22	0.00	18.17	0.00	0.00	0.00	0.00	0.33	15.80	0.00	-	0.00	-	0.00	97.52	Phenocryst
ESY-11	62.64	0.02	17.99	0.26	0.00	0.00	0.00	0.46	15.35	0.00	-	0.00	-	0.00	96.73	Phenocryst_Core
ESY-11	63.55	0.01	17.97	0.29	0.00	0.00	0.00	0.63	15.37	0.00	-	0.00	-	0.00	97.82	Phenocryst_Rim
ESY-12	63.57	0.29	18.62	0.35	0.10	0.02	0.12	1.10	15.11	0.09	0.66	0.02	0.00	0.09	100.07	Phenocryst
ESY-12	63.02	0.33	18.88	0.24	0.11	0.02	0.07	0.53	15.89	0.09	1.10	0.02	0.02	0.09	100.35	Phenocryst
ESY-12	62.67	0.36	18.99	0.31	0.11	0.02	0.14	0.86	15.21	0.07	1.69	0.02	0.00	0.07	100.45	Phenocryst
ESY-12	63.36	0.34	18.58	0.36	0.11	0.02	0.08	0.48	16.22	0.07	0.88	0.02	0.00	0.07	100.56	Phenocryst
ESY-12	63.36	0.32	18.54	0.38	0.09	0.03	0.06	0.44	16.14	0.08	1.12	0.03	0.00	0.08	100.61	Phenocryst
ESY-12	62.84	0.41	18.92	0.36	0.09	0.02	0.10	1.13	14.80	0.09	1.71	0.02	0.00	0.09	100.50	Phenocryst
ESY-12	62.81	0.40	19.05	0.32	0.11	0.02	0.13	1.44	14.18	0.08	1.93	0.02	0.00	0.08	100.51	Phenocryst
ESY-12	62.68	0.38	19.07	0.33	0.12	0.01	0.11	0.66	15.52	0.08	1.69	0.01	0.00	0.08	100.70	Phenocryst
ESY-12	62.97	0.33	18.70	0.34	0.12	0.02	0.10	0.67	15.48	0.09	1.10	0.02	0.00	0.09	99.97	Phenocryst
ESY-12	61.21	0.40	18.41	0.28	0.10	0.03	0.19	0.38	15.46	0.08	1.80	0.03	0.00	0.08	98.41	Phenocryst
ESY-12	63.42	0.04	18.64	0.26	0.00	0.00	0.03	0.95	15.16	0.00	0.60	0.00	0.00	0.00	99.12	Phenocryst
ESY-12	64.02	0.08	18.97	0.26	0.02	0.00	0.02	2.70	12.07	0.00	0.83	0.00	0.00	0.00	98.98	Phenocryst_Core
ESY-12	62.86	0.09	18.65	0.24	0.00	0.00	0.02	0.66	15.66	0.00	0.78	0.00	0.00	0.00	98.99	Phenocryst_Rim
ESY-12	62.83	0.07	18.55	0.21	0.00	0.00	0.01	0.60	15.84	0.01	0.81	0.00	0.00	0.01	98.93	Phenocryst_Rim
PH-2	65.39	0.14	18.62	0.22	0.11	0.06	0.10	0.64	15.70	0.24	-	0.06	-	0.24	101.22	Groundmass
PH-2	64.22	0.00	17.87	0.06	0.00	0.00	0.03	0.42	16.27	0.00	-	0.00	-	0.00	98.86	Phenocryst
PH-2	64.67	0.01	18.19	0.04	0.00	0.00	0.01	0.45	16.27	0.00	-	0.00	-	0.00	99.65	Phenocryst
PH-2	64.44	0.00	18.29	0.06	0.00	0.00	0.02	0.48	16.17	0.00	-	0.00	-	0.00	99.45	Phenocryst
PH-2	64.54	0.00	18.07	0.08	0.00	0.00	0.02	0.54	16.12	0.00	-	0.00	-	0.00	99.36	Phenocryst
PH-2	65.64	0.16	18.49	0.16	0.11	0.06	0.12	0.46	16.10	0.21	-	0.06	-	0.21	101.50	Phenocryst
PH-2	63.83	0.02	18.11	0.08	0.00	0.00	0.00	0.37	16.10	0.01	-	0.00	-	0.01	98.52	Phenocryst

Appendix A: Electron Microprobe Analysis

The following tables are the values for alkali-feldspar collected from the Electron Microprobe analysis of the rock samples of the nepheline syenites and phonolites

Sample	SiO2	TiO2	Al2O3	FeO	MnO	MgO	CaO	Na2O	K2O	Cr2O3	BaO	SrO	Cl	F	Total	Comment
PH-2	64.89	0.15	18.44	0.15	0.11	0.07	0.15	0.73	16.01	0.22	-	0.07	-	0.22	100.92	Phenocryst
PH-2	65.72	0.00	18.42	0.06	0.03	0.00	0.01	0.56	16.00	0.01	-	0.00	-	0.01	100.81	Phenocryst
PH-2	64.08	0.01	18.19	0.04	0.04	0.00	0.10	0.48	16.00	0.00	-	0.00	-	0.00	98.95	Phenocryst
PH-2	64.30	0.03	18.23	0.04	0.00	0.00	0.00	0.43	15.97	0.01	-	0.00	-	0.01	99.02	Phenocryst
PH-2	65.84	0.00	18.63	0.07	0.01	0.00	0.01	0.40	15.96	0.00	-	0.00	-	0.00	100.93	Phenocryst
PH-2	64.65	0.00	18.37	0.08	0.00	0.01	0.01	0.67	15.65	0.01	-	0.01	-	0.01	99.45	Phenocryst
PH-2	62.82	0.04	18.18	0.09	0.03	0.00	1.14	0.50	15.54	0.00	-	0.00	-	0.00	98.35	Phenocryst
PH-2	65.18	0.00	18.29	0.03	0.01	0.00	0.02	0.45	16.17	0.01	-	0.00	-	0.01	100.15	Phenocryst
PH-2	64.59	0.00	18.18	0.04	0.00	0.00	0.03	0.49	16.00	0.00	-	0.00	-	0.00	99.32	Phenocryst
PH-3	63.26	0.01	17.91	0.26	0.02	0.00	1.10	0.33	16.00	0.00	-	0.00	-	0.00	98.89	Groundmass
PH-3	63.68	0.00	17.85	0.03	0.01	0.00	0.02	0.45	16.16	0.00	-	0.00	-	0.00	98.21	Phenocryst
PH-3	64.04	0.00	18.27	0.03	0.03	0.00	0.00	0.90	16.31	0.00	-	0.00	-	0.00	99.57	Phenocryst_Core
PH-3	64.86	0.00	18.18	0.04	0.01	0.00	0.00	0.31	16.15	0.00	-	0.00	-	0.00	99.56	Phenocryst_Rim
PH-5	61.97	0.03	18.18	0.04	0.00	0.00	0.00	0.40	15.46	0.00	-	0.00	-	0.00	96.08	Phenocryst
PH-5	62.21	0.20	18.03	0.19	0.03	0.00	0.00	0.54	14.95	0.00	-	0.00	-	0.00	96.14	Phenocryst
PH-5	61.90	0.13	18.21	0.12	0.00	0.00	0.01	0.55	14.89	0.00	-	0.00	-	0.00	95.81	Phenocryst
PH-5	61.94	0.15	18.11	0.23	0.00	0.00	0.03	0.65	14.77	0.00	-	0.00	-	0.00	95.89	Phenocryst
PH-5	62.13	0.09	18.20	0.15	0.00	0.00	0.00	0.64	14.77	0.00	-	0.00	-	0.00	95.97	Phenocryst
PH-5	61.86	0.07	18.08	0.13	0.00	0.00	0.00	0.55	15.11	0.00	-	0.00	-	0.00	95.81	Phenocryst_Core
PH-5	61.96	0.06	17.66	0.90	0.00	0.00	0.00	0.88	15.09	0.00	-	0.00	-	0.00	96.54	Phenocryst_Core
PH-5	61.09	0.08	18.16	0.16	0.00	0.00	0.00	0.70	14.60	0.00	-	0.00	-	0.00	94.79	Phenocryst_Core
PH-5	62.34	0.00	18.19	0.05	0.00	0.00	0.00	0.38	15.67	0.00	-	0.00	-	0.00	96.63	Phenocryst_Rim
PH-5	59.43	0.05	18.46	0.07	0.00	0.00	0.00	0.67	14.13	0.00	-	0.00	-	0.00	92.81	Phenocryst_Rim
PH-6	63.63	0.28	18.57	0.18	0.11	0.01	0.08	0.37	16.48	0.11	0.71	0.01	0.00	0.11	100.57	Groundmass
PH-7	64.25	0.00	18.08	0.06	0.00	0.01	0.67	0.23	16.17	0.00	0.09	0.01	0.00	0.00	99.74	Groundmass
PH-7	65.91	0.13	18.32	0.19	0.12	0.05	0.11	0.45	16.37	0.21	-	0.05	-	0.21	101.86	Groundmass
PH-7	66.25	0.13	18.65	0.18	0.10	0.06	0.08	0.41	16.26	0.19	-	0.06	-	0.19	102.32	Groundmass
PH-7	66.59	0.15	18.54	0.40	0.11	0.09	0.10	0.31	16.11	0.22	-	0.09	-	0.22	102.64	Groundmass
PH-7	66.19	0.13	18.65	0.17	0.11	0.06	0.08	0.89	15.42	0.23	-	0.06	-	0.23	101.93	Groundmass
PH-7	67.13	0.12	19.22	0.17	0.10	0.08	0.08	3.26	12.98	0.23	-	0.08	-	0.23	103.37	Groundmass
PH-7	63.56	0.00	18.27	0.00	0.00	0.00	0.00	0.33	16.35	0.00	0.09	0.00	0.00	0.00	98.61	Phenocryst
PH-7	63.49	0.00	18.29	0.18	0.01	0.00	0.00	0.32	16.53	0.00	0.00	0.00	0.00	0.00	98.85	Phenocryst
PH-7	65.91	0.15	18.46	0.17	0.12	0.06	0.06	0.41	16.29	0.21	-	0.06	-	0.21	101.83	Phenocryst
PH-7	67.61	0.12	18.74	0.16	0.12	0.06	0.08	2.07	14.59	0.23	-	0.06	-	0.23	103.77	Phenocryst
PH-7	66.18	0.15	18.38	0.18	0.11	0.07	0.10	0.38	16.18	0.19	-	0.07	-	0.19	101.92	Phenocryst_Rim

Appendix A: Electron Microprobe Analysis

The following tables are the values for plagioclase collected from the Electron Microprobe analysis of the rock samples of the nepheline syenites and phonolites

Sample	SiO2	TiO2	Al2O3	FeO	MnO	MgO	CaO	Na2O	K2O	Cr2O3	BaO	SrO	Cl	F	Total	Comment
ESY-1	67.77	0.00	19.48	0.11	0.00	0.00	0.00	11.14	0.12	0.00	-	-	-	-	98.63	Phenocryst_Rim
ESY-2	72.11	0.00	20.29	0.03	0.00	0.00	0.00	12.29	0.14	0.00	-	-	-	-	104.87	Phenocryst
ESY-2	71.20	0.02	20.35	0.05	0.00	0.00	0.00	9.74	3.20	0.00	-	-	-	-	104.56	Phenocryst
ESY-2	71.61	0.00	19.90	0.28	0.00	0.00	0.62	11.65	0.13	0.00	-	-	-	-	104.19	Phenocryst_Rim
ESY-4	67.77	0.00	18.89	0.04	0.00	0.00	0.00	11.82	0.03	0.00	-	-	-	-	98.55	Phenocryst
ESY-4	69.00	0.00	19.85	0.08	0.00	0.00	0.00	11.75	0.05	0.00	-	-	-	-	100.72	Phenocryst
ESY-7	71.23	0.00	20.21	0.13	0.01	0.00	0.00	11.64	0.11	0.02	-	-	-	-	103.36	Phenocryst
ESY-7	74.46	0.00	21.29	0.07	0.01	0.00	0.01	11.38	0.14	0.01	-	-	-	-	107.38	Phenocryst
ESY-7	69.93	0.00	19.65	0.13	0.00	0.00	0.00	12.48	0.09	0.00	-	-	-	-	102.27	Phenocryst
ESY-7	68.48	0.00	19.38	0.07	0.01	0.00	0.00	12.37	0.14	0.01	-	-	-	-	100.47	Phenocryst
ESY-7	71.57	0.00	20.24	0.05	0.00	0.00	0.00	12.32	0.11	0.01	-	-	-	-	104.29	Phenocryst
ESY-7	71.68	0.00	20.20	0.05	0.00	0.00	0.01	12.23	0.11	0.00	-	-	-	-	104.29	Phenocryst
ESY-7	69.92	0.00	19.98	0.04	0.00	0.00	0.00	12.15	0.13	0.00	-	-	-	-	102.22	Phenocryst
ESY-7	71.43	0.00	20.18	0.16	0.00	0.00	0.00	12.02	0.10	0.00	-	-	-	-	103.89	Phenocryst_Rim
ESY-7	73.32	0.00	20.52	0.05	0.00	0.00	0.00	12.45	0.12	0.00	-	-	-	-	106.45	Phenocryst_Core
PH-6	67.86	0.23	19.20	0.13	0.10	0.01	0.07	7.90	0.12	0.06	0.45	0.00	0.04	0.00	96.16	Phenocryst
PH-6	67.79	0.23	19.37	0.16	0.10	0.01	0.06	8.65	0.11	0.08	0.42	0.00	0.04	0.00	97.00	Groundmass
PH-6	68.69	0.25	19.33	0.10	0.08	0.02	0.08	6.89	0.12	0.07	0.49	0.00	0.05	0.00	96.14	Groundmass
PH-7	68.71	0.00	18.82	0.00	0.00	0.00	0.01	6.53	0.06	0.00	0.00	0.00	0.00	0.00	94.13	Phenocryst
PH-7	71.23	0.00	20.21	0.13	0.01	0.00	0.00	11.64	0.11	0.02	-	-	-	-	103.36	Phenocryst
PH-7	74.46	0.00	21.29	0.07	0.01	0.00	0.01	11.38	0.14	0.01	-	-	-	-	107.38	Phenocryst
PH-7	71.39	0.11	20.13	0.12	0.07	0.04	0.11	10.84	2.22	0.18	-	-	-	-	105.20	Phenocryst
PH-7	71.20	0.02	20.35	0.05	0.00	0.00	0.00	9.74	3.20	0.00	-	-	-	-	104.56	Phenocryst
PH-7	71.57	0.00	20.24	0.05	0.00	0.00	0.00	12.32	0.11	0.01	-	-	-	-	104.29	Phenocryst
PH-7	72.11	0.00	20.29	0.03	0.00	0.00	0.00	12.29	0.14	0.00	-	-	-	-	104.87	Phenocryst
PH-7	71.68	0.00	20.20	0.05	0.00	0.00	0.01	12.23	0.11	0.00	-	-	-	-	104.29	Phenocryst
PH-7	69.92	0.00	19.98	0.04	0.00	0.00	0.00	12.15	0.13	0.00	-	-	-	-	102.22	Phenocryst
PH-7	72.37	0.08	20.18	0.59	0.09	0.05	0.11	12.08	0.11	0.17	-	-	-	-	105.82	Phenocryst
PH-7	69.84	0.11	20.32	0.16	0.08	0.04	0.11	12.03	0.12	0.17	-	-	-	-	102.99	Phenocryst
PH-7	74.21	0.11	20.07	0.11	0.08	0.05	0.09	11.77	0.17	0.18	-	-	-	-	106.85	Phenocryst
PH-7	71.43	0.00	20.18	0.16	0.00	0.00	0.00	12.02	0.10	0.00	-	-	-	-	103.89	Phenocryst_Rim
PH-7	71.61	0.00	19.90	0.28	0.00	0.00	0.62	11.65	0.13	0.00	-	-	-	-	104.19	Phenocryst_Rim
PH-7	71.66	0.12	20.37	0.11	0.10	0.05	0.14	12.34	0.13	0.17	-	-	-	-	105.20	Groundmass

Appendix A: Electron Microprobe Analysis

The following tables are the values for plagioclase collected from the Electron Microprobe analysis of the rock samples of the nepheline syenites and phonolites

Sample	SiO2	TiO2	Al2O3	FeO	MnO	MgO	CaO	Na2O	K2O	Cr2O3	BaO	SrO	Cl	F	Total	Comment
PH-7	71.42	0.12	20.18	0.17	0.09	0.05	0.09	12.29	0.12	0.16	-	-	-	-	104.69	Groundmass
PH-7	70.24	0.12	20.15	0.29	0.10	0.04	0.29	12.22	0.14	0.16	-	-	-	-	103.75	Groundmass
PH-7	72.47	0.11	20.46	0.13	0.10	0.05	0.08	11.88	0.40	0.16	-	-	-	-	105.83	Groundmass
PH-7	72.99	0.08	20.59	0.14	0.10	0.04	0.11	11.81	0.15	0.20	-	-	-	-	106.21	Groundmass
PH-7	68.20	0.00	18.85	0.02	0.00	0.00	0.01	6.42	0.05	0.00	0.00	0.00	0.00	0.01	93.55	Groundmass
PH-7	67.70	0.00	18.88	0.07	0.00	0.00	0.01	6.54	0.05	0.00	0.00	0.00	0.00	0.00	93.25	Groundmass
PH-7	67.68	0.00	19.07	0.00	0.00	0.00	0.00	9.43	0.10	0.00	0.00	0.00	0.00	0.02	96.30	Groundmass
PH-7	68.93	0.00	19.31	0.01	0.00	0.00	0.03	6.69	0.13	0.00	0.00	0.00	0.00	0.00	95.09	Groundmass
PH-7	70.01	0.13	19.87	0.13	0.09	0.05	0.07	9.11	5.56	0.22	-	-	-	-	105.23	Groundmass

Appendix A: Electron Microprobe Analysis

The following tables are the values for biotite collected from the Electron Microprobe analysis of the rock samples of the nepheline syenites and phonolites

Sample	SiO2	TiO2	Al2O3	FeO	MnO	MgO	CaO	Na2O	K2O	Cr2O3	BaO	SrO	Cl	F	Total	Comment
ESY_1	35.74	2.98	15.64	27.23	1.00	3.04	0.00	0.02	9.63	0.00	-	-	-	-	**95.26**	Phenocryst_Core
ESY_1	32.64	2.35	17.95	28.74	1.14	2.18	0.03	0.01	9.33	0.00	-	-	-	-	**94.38**	Phenocryst_Core
ESY_1	35.67	2.96	16.49	26.42	1.01	2.36	0.00	0.02	9.53	0.00	-	-	-	-	**94.48**	Phenocryst_Core
ESY_1	32.17	2.34	17.56	29.76	1.22	2.06	0.00	0.05	9.48	0.00	-	-	-	-	**94.65**	Phenocryst_Core
ESY_1	35.72	3.14	15.68	26.77	0.95	3.34	0.00	0.00	9.74	0.00	-	-	-	-	**95.35**	Phenocryst_Rim
ESY_1	32.22	2.39	17.87	29.30	1.19	2.11	0.00	0.02	9.50	0.00	-	-	-	-	**94.60**	Phenocryst_Rim
ESY_1	31.93	2.14	18.27	29.71	1.25	1.91	0.03	0.05	9.16	0.00	-	-	-	-	**94.45**	Phenocryst_Rim
ESY_1	33.83	1.99	18.54	26.80	1.03	1.92	0.02	1.03	8.39	0.00	-	-	-	-	**93.54**	Phenocryst_Rim
ESY_2	38.36	1.15	14.10	15.67	1.98	13.68	0.03	0.07	10.15	0.11	-	-	-	-	**95.31**	Phenocryst_Core
ESY_2	41.17	1.09	11.23	12.68	1.04	16.43	0.15	0.69	9.64	0.09	-	-	-	-	**94.24**	Phenocryst_Core
ESY_2	39.62	0.86	11.40	13.21	1.77	14.88	0.01	0.09	9.58	0.07	-	-	-	-	**91.48**	Phenocryst_Rim
ESY_4	32.32	2.29	17.46	29.56	0.99	2.10	0.00	0.04	9.34	0.00	-	-	-	-	**94.10**	Phenocryst_Core
ESY_4	33.37	2.21	16.60	28.46	0.95	2.35	0.00	0.03	9.38	0.00	-	-	-	-	**93.36**	Phenocryst_Core
ESY_4	33.64	2.21	16.67	29.08	1.02	2.42	0.00	0.02	9.46	0.00	-	-	-	-	**94.51**	Phenocryst_Core
ESY_4	32.15	2.25	17.43	28.86	0.70	2.50	0.00	0.08	9.38	0.00	-	-	-	-	**93.34**	Phenocryst_Core
ESY_4	32.74	2.22	17.65	28.93	0.74	2.62	0.01	0.02	9.53	0.00	-	-	-	-	**94.47**	Phenocryst_Core
ESY_4	33.27	2.14	16.98	29.57	0.97	2.37	0.00	0.04	9.29	0.00	-	-	-	-	**94.64**	Phenocryst_Core
ESY_4	31.64	1.97	17.82	30.00	1.07	2.05	0.01	0.07	9.35	0.00	-	-	-	-	**93.98**	Phenocryst_Core
ESY_4	31.56	2.13	17.88	29.47	1.02	2.00	0.01	0.08	9.28	0.00	-	-	-	-	**93.45**	Phenocryst_Rim
ESY_4	33.08	2.40	16.60	29.29	0.98	2.41	0.00	0.04	9.40	0.00	-	-	-	-	**94.20**	Phenocryst_Rim
ESY_4	33.48	2.30	16.81	28.82	1.05	2.38	0.00	0.03	9.51	0.00	-	-	-	-	**94.36**	Phenocryst_Rim
ESY_4	31.86	2.01	17.52	30.26	1.03	2.19	0.00	0.02	9.28	0.00	-	-	-	-	**94.18**	Phenocryst_Rim
ESY_4	32.19	2.12	17.47	30.28	1.08	2.12	0.00	0.02	9.32	0.00	-	-	-	-	**94.60**	Phenocryst_Rim
ESY_4	31.83	1.86	16.97	28.23	1.01	2.04	0.00	0.16	8.92	0.00	-	-	-	-	**91.01**	Phenocryst_Rim
ESY_4	32.27	2.28	17.86	29.55	1.08	2.42	0.00	0.05	9.41	0.00	-	-	-	-	**94.92**	Groundmass
ESY_4	32.64	1.68	17.77	28.91	1.05	1.85	0.01	0.15	9.33	0.00	-	-	-	-	**93.38**	Groundmass
ESY_7	21.93	1.74	9.69	17.23	1.06	4.49	19.70	0.05	6.14	0.08	-	-	-	-	**82.10**	Phenocryst_Core
ESY_7	17.95	0.91	9.66	4.87	0.09	1.38	38.15	0.44	2.22	0.07	-	-	-	-	**75.74**	Phenocryst_Core
ESY_7	35.09	2.70	14.51	26.57	0.44	7.07	0.15	0.09	9.62	0.15	-	-	-	-	**96.39**	Phenocryst_Core
ESY_7	37.29	2.44	12.64	23.40	0.38	9.70	0.04	0.13	9.95	0.10	-	-	-	-	**96.07**	Phenocryst_Rim

Appendix A: Electron Microprobe Analysis

The following tables are the values for biotite collected from the Electron Microprobe analysis of the rock samples of the nepheline syenites and phonolites

Sample	SiO2	TiO2	Al2O3	FeO	MnO	MgO	CaO	Na2O	K2O	Cr2O3	BaO	SrO	Cl	F	Total	Comment
ESY_7	37.92	2.40	12.47	23.56	0.41	9.71	0.04	0.10	9.89	0.10	-	-	-	-	**96.60**	Phenocryst_Rim
ESY_7	38.31	1.97	11.24	20.60	0.33	11.59	0.05	0.18	9.91	0.07	-	-	-	-	**94.25**	Phenocryst_Rim
ESY_9	35.26	2.64	17.72	26.50	0.99	3.13	0.03	0.09	9.96	0.04	-	-	-	-	**96.89**	Phenocryst_Core
ESY_9	32.46	2.15	18.50	29.12	1.25	2.88	0.08	0.07	9.68	0.03	-	-	-	-	**96.58**	Phenocryst_Core
ESY_11	37.87	1.09	12.29	15.94	0.54	15.75	0.08	0.04	9.85	0.00	-	-	-	-	**93.44**	Phenocryst_Core
ESY_11	39.33	1.17	10.82	15.92	0.51	15.83	0.13	0.29	9.62	0.00	-	-	-	-	**93.62**	Phenocryst_Core
ESY_11	37.75	1.75	12.13	17.97	0.55	13.86	0.10	0.05	9.13	0.00	-	-	-	-	**93.29**	Phenocryst_Core
ESY_11	37.44	3.64	12.39	15.52	0.57	14.31	0.86	0.04	9.59	0.00	-	-	-	-	**94.36**	Phenocryst_Core
ESY_12	35.12	2.24	16.49	24.24	0.67	7.00	0.03	0.07	9.93	0.04	-	-	-	-	**96.57**	Phenocryst_Core
PH_3	37.36	1.44	14.07	14.47	1.97	14.31	0.16	0.17	9.67	0.02	-	-	-	-	**93.65**	Phenocryst_Core
PH_3	38.36	1.05	11.54	15.04	0.48	16.21	0.20	0.03	9.50	0.00	-	-	-	-	**92.41**	Phenocryst_Rim
PH_3	38.55	0.53	12.59	14.34	0.51	17.27	0.08	0.03	9.82	0.00	-	-	-	-	**93.72**	Phenocryst_Rim
PH_3	38.31	0.85	12.01	17.12	0.51	15.12	0.29	0.02	8.66	0.00	-	-	-	-	**92.88**	Groundmass

The following tables are the values for titanite collected from the Electron Microprobe analysis of the rock samples of the nepheline syenites and phonolites

Sample	SiO2	TiO2	Al2O3	FeO	MnO	MgO	CaO	Na2O	K2O	Cr2O3	BaO	SrO	Cl	F	Total	Comment
ESY_11	30.17	34.36	1.76	1.19	0.03	0.03	26.66	0.40	0.01	0.00	-	-	-	-	**94.62**	Phenocryst
ESY_11	29.19	35.73	0.92	1.30	0.04	0.06	27.84	0.11	0.02	0.01	-	-	-	-	**95.22**	Phenocryst

Appendix A: Electron Microprobe Analysis

The following tables are the values for muscovite collected from the Electron Microprobe analysis of the rock samples of the nepheline syenites and phonolites

Sample	SiO2	TiO2	Al2O3	FeO	MnO	MgO	CaO	Na2O	K2O	Cr2O3	BaO	SrO	Cl	F	Total	Comment
ESY_3	45.52	0.06	36.63	2.18	0.01	0.12	0.00	0.25	11.00	0.00	-	-	-	-	**95.79**	Groundmass
ESY_3	45.29	0.04	35.59	2.14	0.00	0.10	0.00	0.28	10.53	0.00	-	-	-	-	**93.96**	Groundmass
ESY_3	44.95	0.00	34.25	2.91	0.00	0.25	0.00	0.22	10.39	0.00	-	-	-	-	**92.97**	Groundmass
ESY_3	45.32	0.08	34.22	2.68	0.01	0.19	0.00	0.24	10.25	0.00	-	-	-	-	**92.98**	Phenocryst
ESY_3	44.84	0.00	34.60	3.18	0.00	0.30	0.00	0.17	10.03	0.00	-	-	-	-	**93.11**	Groundmass
PH_7	49.39	0.62	30.46	5.91	0.15	1.75	0.14	0.20	10.47	0.21	-	-	-	-	**99.30**	Phenocryst
PH_7	46.95	0.40	33.83	5.56	0.11	0.56	0.08	0.23	10.39	0.23	-	-	-	-	**98.34**	Groundmass

The following tables are the values for nepheline collected from the Electron Microprobe analysis of the rock samples of the nepheline syenites and phonolites

Sample	SiO2	TiO2	Al2O3	FeO	MnO	MgO	CaO	Na2O	K2O	Cr2O3	BaO	SrO	Cl	F	Total	Comment
ESY_2	40.92	0.00	32.57	0.76	0.01	0.00	0.06	21.76	0.05	0.00	-	-	-	-	96.14	Groundmass
ESY_2	46.14	0.00	34.18	0.09	0.00	0.01	0.07	17.16	5.86	0.00	-	-	-	-	103.49	Phenocryst
ESY_2	45.34	0.00	33.20	0.14	0.00	0.00	0.08	16.99	5.80	0.00	-	-	-	-	101.54	Phenocryst
ESY_2	43.65	0.00	33.20	0.00	0.00	0.00	0.14	16.78	5.92	0.00	0.00	0.00	0.00	0.02	99.70	Groundmass
PH_3	44.10	0.00	34.15	0.19	0.00	0.00	0.31	16.89	6.34	0.00	-	-	-	-	101.97	Phenocryst

Appendix A: Electron Microprobe Analysis

The following tables are the values for apatite collected from the Electron Microprobe analysis of the rock samples of the nepheline syenites and phonolites

Sample	SiO2	TiO2	Al2O3	FeO	MnO	MgO	CaO	Na2O	K2O	Cr2O3	BaO	SrO	Cl	F	Total	Comment
PH_2	0.73	0.02	0.32	0.15	0.05	0.01	52.72	0.14	0.06	0.07	-	-	-	-	54.27	Phenocryst
PH_2	0.35	0.03	0.00	0.13	0.09	0.02	53.59	0.17	0.03	0.05	-	-	-	-	54.47	Phenocryst
PH_2	0.20	0.03	0.00	0.07	0.03	0.00	55.61	0.04	0.03	0.10	-	-	-	-	56.11	Phenocryst
PH_2	0.04	0.01	0.00	0.10	0.06	0.00	55.64	0.06	0.02	0.06	-	-	-	-	56.01	Phenocryst
PH_3	0.31	0.06	0.00	0.15	0.12	0.03	52.12	0.67	0.02	0.13	-	-	-	-	53.61	Phenocryst
PH_3	0.63	0.04	0.00	0.22	0.08	0.09	55.37	0.31	0.03	0.04	-	-	-	-	56.80	Phenocryst

The following tables are the values for cancrinite collected from the Electron Microprobe analysis of the rock samples of the nepheline syenites and phonolites

Sample	SiO2	TiO2	Al2O3	FeO	MnO	MgO	CaO	Na2O	K2O	Cr2O3	BaO	SrO	Cl	F	Total	Comment
PH_3	42.66	0.00	34.02	0.07	0.00	0.01	6.94	7.76	0.01	0.00	-	-	-	-	91.46	Vein
PH_3	41.59	0.00	33.70	0.00	0.00	0.01	6.97	7.55	0.02	0.00	-	-	-	-	89.84	Phenocryst

Appendix A: Electron Microprobe Analysis

The following tables are the values for carbonates collected from the Electron Microprobe analysis of the rock samples of the nepheline syenites and phonolites

Sample	SiO2	TiO2	Al2O3	FeO	MnO	MgO	CaO	Na2O	K2O	Cr2O3	BaO	SrO	Cl	F	Total	Comment
ESY_7	0.13	0.13	0.11	0.82	1.40	0.16	59.32	0.07	0.06	0.21	-	-	-	-	62.40	Phenocryst
ESY_9	0.00	0.00	0.00	0.31	1.20	0.00	58.62	0.00	0.02	0.00	0.00	0.83	0.01	0.00	60.98	Groundmass
PH_7	0.12	0.14	0.05	0.53	2.15	0.15	60.61	0.06	0.05	0.24	-	-	-	-	64.11	Phenocryst
PH_7	0.00	0.00	0.00	1.91	2.34	0.14	58.42	0.02	0.03	0.06	-	-	-	-	62.92	Phenocryst